In presenting the dissertation as a partial fulfillment of the requirements for an advanced degree from the Georgia Institute of Technology, I agree that the Library of the Institute shall make it available for inspection and circulation in accordance with its regulations governing materials of this type. I agree that permission to copy from, or to publish from, this dissertation may be granted by the professor under whose direction it was written, or, in his absence, by the Dean of the Graduate Division when such copying or publication is solely for scholarly purposes and does not involve potential financial gain. It is understood that any copying from, or publication of, this dissertation which involves potential financial gain will not be allowed without written permission.

_____

7/25/68

# A STUDY OF THE PRE-IGNITION BEHAVIOR OF SELECTED GARMENT FABRICS AND CONSEQUENT BURN INJURY PROBABILITY

A THESIS

Presented to

The Faculty of the Division of Graduate

Studies and Research

by

Carroll Stone Kirkpatrick

In Partial Fulfillment

of the Requirements for the Degree

Master of Science in Mechanical Engineering

Georgia Institute of Technology

June, 1972

A STUDY OF THE PRE-IGNITION BEHAVIOR OF SELECTED GARMENT FABRICS AND CONSEQUENT BURN INJURY PROBABILITY

Approved:

_____

_____

_____

_____

Date approved by Chairman: June 1, 1972

# ACKNOWLEDGMENTS

Every phase of my work at the Georgia Institute of Technology has been an educational process of great personal benefit. I express gratitude to every professor, instructor, and administrator with whom I have had the honor of association.

Dr. A. E. Bergles must be singled out first to receive my sincerest expression of appreciation. Dr. Bergles has been my academic and thesis advisor, a source of guidance and help in every area of need, and a true personal friend. Without his help, preparation of this thesis might have seemed impossible.

The Fabric Flammability Project, School of Mechanical Engineering, under direction of Dr. W. Wulff and Dr. N. Zuber, the Principal Investigators, funded development of the Ignition Time Apparatus and provided me a salary during the experimental phases of the work. Additionally, Dr. Wulff was a source of assistance, whenever requested, during equipment design. He then served on my thesis reading committee. I owe both men and the Project a debt of gratitude.

Dr. A. Alkidas and Mr. R. W. Hess, graduate assistants in the Fabric Flammability Project, willingly provided assistance and advice.

An expression of appreciation is owed to the other readers on my thesis committee. Both Dr. W. D. McLeod, School of Mechanical Engineering, and Professor W. C. Boteler, School of Textile Engineer-

ing, contributed many suggestions which corrected this thesis to final form.

Dr. S. P. Kezios, Dr. P. Durbetaki, and Dr. S. L. Dickerson arranged the NASA Traineeship funds which I received. Without this assistance, full-time attendance at Georgia Tech would have been impossible.

I must recognize the technicians of the School of Mechanical Engineering for their contributions. Mr. B. L. Wallace was the primary machinist for the Ignition Time Apparatus, and Mr. H. J. Carr also helped frequently when needed. Mr. T. E. Clopton gathered the electronic equipment needed for the experiment. He then helped assemble the system rapidly into a working order, occasionally, even on his own time.

Finally, I must thank my wife, Jackie. She contributed a great share in the work. During the experimental period, she gave advice on setting up the monitoring equipment. Finally, she proofread this entire thesis and was able to remain an understanding mate.

TABLE OF CONTENTS

TABLE OF CONTENTS (Concluded)

# LIST OF TABLES

# LIST OF ILLUSTRATIONS

LIST OF ILLUSTRATIONS (Concluded)

# NOMENCLATURE

| | |
|---|---|
| $a$ | property subscript indicating air |
| $Bi$ | Biot number = $(h\delta/k)$ |
| $C_p$ | specific heat of fabric, [Btu/hr-ft$^2$] |
| $F$ | Fourier number = $(\alpha t/\delta^2)$ |
| $h$ | convective heat transfer coefficient, [Btu/hr-ft$^2$-$^oF$] |
| $H_o$ | convective heat loss from skin, [cal/cm$^2$-sec] |
| $I$ | radiant energy inside fabric thickness, [Btu/hr-ft$^2$] |
| $I_o^*$ | non-dimensional heat flux ratio = $[q_i'' (1-\rho_o)\delta/kT_o]$ |
| $k$ | thermal conductivity of fabric, [Btu/hr-ft-oF] |
| $p$ | constant of proportionality in the tissue damage rate function, [1/sec]. |
| $q_i''$ | incident heat flux, [Btu/hr-ft$^2$] |
| $R$ | universal gas constant, 1.986 [cal/mole - $^oC$] |
| $s$ | property subscript indicating skin |
| $t$ | time, sec |
| $T$ | temperature, $^oC$, $^oF$ |
| $T_i$ | fabric ignition temperature, $^oF$ |
| $T_m$ | fabric melting temperature, $^oF$ |
| $T_o$ | initial temperature of a system, $^oF$ |
| $T_s$ | skin tissue temperature, $^oC$ |
| $T_{so}$ | initial skin surface temperature, $^oC$ |
| $T_t$ | skin tissue temperature at some time, t, $^oC$ |

NOMENCLATURE (Continued)

| | |
|---|---|
| $x$ | distance, ft |
| $X^*$ | relative position = $(x/\delta)$ |
| $\alpha$ | thermal diffusivity = $[k/\rho C_p]$ |
| $\alpha_o$ | fabric absorptivity |
| $\gamma$ | skin temperature gradient = $\frac{\partial T}{\partial x}$, $[^oC/mm]$ |
| $\delta$ | fabric thickness, ft |
| $\Delta E$ | activation energy for the chemical reactions occurring during thermally induced tissue destruction, [cal/mole] |
| $\epsilon$ | skin emissivity |
| $\theta$ | normalized temperature = $[T - T_o/T_o]$ |
| $\kappa$ | fabric extinction coefficient, [1/ft] |
| $\kappa^*$ | fabric optical thickness = $\kappa\delta$ |
| $\lambda$ | wavelength of radiant energy, microns |
| $\rho$ | fabric density, $[lbm/ft^3]$ |
| $\rho_o$ | fabric reflectivity |
| $\tau_o$ | fabric transmittance |
| $\Omega$ | a dimensionless epidermal damage rate function evaluated at the skin depth where tissue temperature is $T_t$ |

# SUMMARY

This study originated from equipment design work and preliminary test work in the Fabric Flammability program at the Georgia Institute of Technology. The objectives were to develop a device with which to measure the ignition times of fabrics subjected to a step input of radiant energy and obtain the first set of data. The thesis objectives were expanded later to include ignition time data analysis in general, including transmittance, selection of some analytical technique for describing the heat flux-time to ignition relationship, description of human response to heat, and a coupling of the test data with human response data to evaluate possible modification of exposure incidents by human efforts for personal safety.

The Ignition Time Apparatus was designed, constructed, and instrumented. A total of 56 tests was conducted with 10 different fabrics over an incident heat flux range of 23,900 (Btu/hr-ft$^2$) to 72,700 (Btu/hr-ft$^2$). Ignition times for the tests varied between three and 90 seconds. A diathermanous model of the fabrics was found to give an ignition time estimate which was less than the observed times by about a factor of two. The skin was analyzed as a semi-infinite conducting body, and time to pain estimates by the analytical method were conservative as compared to data from the literature by a factor of two or less. The ignition time data finally were coupled with the physiological information in an initial

effort to describe the total system of man plus garment.

The primary conclusion is that a normal person, clothed by a layer of one of the tested fabrics, probably could escape injury from a household heat source. The time to pain plus a probable time of human reaction is less than the probable time to garment ignition.

This limited treatment of the so very complex total problem is restricted to a brief consideration of only 10 different fabrics, to single layers of fabric, to "normal" persons, and only to radiative heating sources. With clothing thicker than tested, likelihood that the fabric might become a hazard to the wearer is greater. Along with these facts, it was noted that persons who expose bare skin to radiant heat sources of household intensity might escape burn injury even though they would suffer pain.

# CHAPTER I

## INTRODUCTION AND OBJECTIVES

In 1954, Congress passed the Flammable Fabrics Act, subsequently amended in 1966, to protect the public from highly flammable apparel. As amended, the act directs the Department of Commerce to define criteria or standard tests, applicable to fabrics, in order to reduce the hazard. The responsibility for developing test methods by which to define fabric flammability was delegated to the National Bureau of Standards. The Government-Industry Research Committee on Fabric Flammability (GIRCFF) was formed and organized in the Office of Flammable Fabrics of the National Bureau of Standards, to formulate and administer an appropriate research program. Program results are to provide factual information on hazards associated with apparel fabric fires, and ultimately provide the necessary technical and scientific foundation for legislation.

The School of Mechanical Engineering at Georgia Institute of Technology earned a research grant from GIRCFF. Under the direction of Dr. W. Wulff and Dr. N. Zuber, a program of analysis and experimentation relevant to fabric ignition was undertaken. This program continues under sponsorship of the Committee. The present study was originated as part of the School of Mechanical Engineering fabric flammability program.

The original objectives of this thesis were to:

(1) Develop an ignition time apparatus

(2) Obtain the first set of data for ignition time of a number of fabrics subjected to a range of incident heat fluxes. The data from those preliminary experiments are included in this report, and form the basis from which this study has evolved. The additional objectives of this latter phase of the study were to:

(3) Analyze and present the data in general, and evaluate fabric transmittances.

(4) Select a simple analytical technique for describing ignition time as a function of incident heat flux.

(5) Describe human response to heat exposure, including pain sensation, burn injury, and protective reaction to avoid hurt.

(6) Couple the fabric ignition time test data with human response analyses to evaluate possible modification of garment exposure incidents by the efforts of an individual to protect himself.

# CHAPTER II

# IGNITION TIME TEST EQUIPMENT

## 2.1 Introduction

The Ignition Time Apparatus was developed in order that the characteristic time to ignition could be measured precisely. At the initiation of test equipment development, a characteristic ignition time definition was designated. The ignition time for any fabric was defined to be that time elapse from sudden exposure of a specimen of that fabric to uniform test flux until appearance of flame at the fabric front face [1]. This definition helped dictate initial equipment specifications, and provided guiding criteria throughout all phases of device development.

## 2.2 Design Development

Preliminary analyses of the flammable fabric ignition process by a simple conduction model, coupled with the definition of ignition time, generated the following initial specifications and requirements for the device [2]:

(a) Specimen heating by a radiative source capable of producing any heat flux up to about 50,000 Btu/hr-ft$^2$ incident on the fabric surface,

(b) exposures of as low as 20 milliseconds,

(c) remote flame detection.

These specifications suggested installation of a high density radiant heater, mounted close to a heat-tolerant opaque shield which would shade fabric samples from radiant heat flux, except at such time intervals when exposure was desired. Figure 1 describes this initial concept.

From basic equipment requirements, two concepts of exposure mechanism were analyzed. A rotating disk arrangement and a mobile shutter design were considered. The shutter system, shown in Figure 2, was selected and constructed. The design was devised such that subsequent incorporation of a second shutter to terminate the exposure periods would be possible with minimum manufacturing or assembly difficulty. The present test program, however, involved only single shutter operations.

## 2.3 Equipment Description

The major components of the Ignition Time Apparatus are:

(1) mechanical shutter system,

(2) heating source

(3) sample support assembly, and

(4) instrumentation.

As shown in Figures 2 and 3, the first three major components are bolted directly onto a 1 in. x 12 in. x 66 in. base plate cut from 6061 T651 aluminum tool plate. A slot, 1.500 in. wide and 0.125 in. deep, was milled lengthwise along the base plate centerline to establish alignment of all subassemblies.

2.3.1 Shutter System

The shutter system consists of the shutter plate and spring assembly, the release and catch system, and the cock/uncock system. An identical second system is required to incorporate a second shutter. Most details of the assembly can be seen in Figures 3 and 4.

The shutter plate (made of 0.032 in. thick annealed sheet steel) is held vertically in plate guides and connected to a heavy helical spring by a slender operating rod. The operating rod engages catch and release mechanisms at necked-down rod sections. After the shutter is cocked (with spring in extension) and released, spring contraction accelerates the shutter plate and operating rod. When, for the first time, the plate reaches that instant of zero velocity and extreme spring compression (opposite to starting position), a catch mechanism engages the operating rod to prohibit further motion. While the exposing edge is sweeping across the fabric sample center, the shutter plate attains maximum velocity.

The plate travels in a slotted brass guide assembly bolted to aluminum "T" extrusions (6061 T651). The bottom "T" was fitted into the milled base plate slot. The other was mounted to the top protrusions on the spring housing support blocks as shown in Figures 2 and 3. The operating rod, attached to one side of the shutter plate by a stainless steel swivel, was cut from 0.375 in. diameter drill rod (oil hardening) heat-treated to full hardness. The rod travels in a linear ball bearing press-fitted into a machined cylindrical block bolted radially into the spring housing assembly

at the inner or shutter plate side.

The operating rod is connected to a heavy helical primary spring by a spring terminal (hot-rolled steel) screwed snugly into the spring end. A similar terminal is screwed into the opposite end of the spring and bolted radially to the outer or jack side of the spring housing. These parts were sized to assure low stress levels [13,14] during operation of the device in order that premature fatigue failure is avoided.

The primary spring, 8.50 in. long at neutral, was wound on order by Newcomb Springs of Atlanta. Twenty turns of 0.250 in. diameter wire were wound on a 1.75 in. helix diameter. The design spring rate was 100 lbf/in. deflection, with maximum deformation of 3.0 in. allowable in compression or extension. By static dead load tests, actual spring rates were found to be 72 lbf/in. tension and 115 lbf/in. compression. The spring mass of approximately 1.20 lbm comprises approximately half of the effective translating mass. Design computations determining the required spring rate, as well as calculated and measured shutter speeds, are included in Appendix C.

The primary spring and spring terminals are enclosed within a 16 in. long section of hot rolled steel tube. A circular flange was welded onto the tube near the outer (jack side) end while a cylindrical sleeve was welded near the inner end. These attached pieces were turned on concentric centers to fit into the spring housing support blocks. Windows were cut into the tube between support blocks for visual access to the mobile spring terminal. Two other windows were cut into the tube forward of the shutter end support

blocks to accommodate the release mechanism.

Shutter release and catch mechanisms restrict shutter motion to desired shield/exposure actions. Both mechanisms are similar and are bolted to the base plate as well as to the inner (shutter side) spring housing support block. Both mechanisms consist of a steel yoke, with replaceable brass inserts which contact the operating rod, carried by a pair of steel rods. The release mechanism rod pair is attached to a Model 446-1, A. C. type, push-pull solenoid of 608 oz capacity manufactured by Dormeyer Industries. The catch mechanism yoke rides pressed against the operating rod by two compression springs. When the necked-down section of the operating rod near the shutter plate passes the catch yoke, compression spring action moves the yoke to engage the operating rod and immobilize the system. The steel rods for both catch and release slide through bronze bushings pressed into aluminum (6061-T651) blocks, which support the catch and release mechanisms. The catch yoke is relieved from primary spring load by the cocking jack.

The cock/uncock system is applied to extend or to compress the primary spring for cocking the shutter or returning the spring to neutral. The system consists of a heavy duty automotive screw jack, purchased from Sears, Roebuck Company, and a steel rod which locks into the mobile spring terminal. The jack is mounted onto the base plate with a steel angle as can be seen in the upper right hand side of Figure 3.

2.3.2 Heating Source

The radiant heat source selected to produce the desired fabric sample irradiation is a Model 5208-5 High Density Radiant Heater purchased from Research, Inc. The heater is designed for six tubular tungsten filament quartz lamps (Model 1200 T3/CL) purchased from General Electric Company. The lamps have an active length of 6.0 in., produce 1.2 KW each, and are air cooled. The highly reflective lamp housing is water cooled. Radiant heat flux is emitted through a 6 in. x 3 in. quartz window at maximum steady fluxes of 120,000 Btu/ $hr\text{-}ft^2$.

As shown in Figure 5, the heating source is mounted to the base plate with two aluminum blocks, thermally insulated by transite shields, such that the quartz window can be positioned various distances from the fabric sample. When the heater window has been located 0.25 in. from the shutter plate, the distance between fabric sample front face plane and heater window is approximately 1 in.

A variable transformer (A.C.) suitable to adjust power to the heater from zero to full power (7.2 KW) was obtained from School laboratories. Cooling air and water were supplied from building services.

2.3.3 Sample Support

Fabric specimens were positioned parallel to the heater window plane and held in place by the sample holder. The support permitted exposure of a 1 in. diameter circle of fabric 1.18 in. from the heater window. A thermoelectric flux meter was mounted in the sample

holder 0.40 in. behind the fabric free back face. Figures 5 and 6 illustrate the basic shutter and flux sensor arrangement.

2.3.4 Timing and Sensing Instrumentation

Instrumentation for the Ignition Time Device consisted of five different components.

(a) Microswitch - available from School laboratories. The microswitch was activated by the shutter plate to indicate onset of specimen exposure.

(b) Thermoelectric Flux Meter - Model C-1301-A purchased from Hy-Cal Engineering. This meter was mounted 0.40 in. behind the sample free back face to sense that heat flux transmitted through the fabric specimens, and also to indicate fabric ignition or melting.

(c) Infrascope - Mark I Infrascope purchased from Barnes Engineering. The Infrascope was intended to sense fabric front face ignition.*

(d) Oscilloscopes - two Tektronix Type 564 Dual Beam Storage oscilloscopes were available in School laboratories. The oscilloscopes recorded signals from the first three components. The oscilloscope traces were photographed for record by a Polaroid camera.

(e) Stopwatch - a Compass 1 Jewel Stopwatch available from School laboratories. The stop watch was used in conjunction with visual observation of irradiated specimens to help identify

* Application of the Infrascope proved disappointing in determining front face ignition in the present experiments since the irradiance reflected from the fabric front-face completely overwhelmed infrared flame emission.

ignition time. In cases of exposure longer than 45 seconds, the stopwatch was the only means of measuring time to ignition.

## 2.4 Equipment Operation

In this principal experiment, fabric specimens were exposed to radiant heat flux until ignition or melting occurred. After the exposing shutter was positioned to shade the fabric sample, the heat source was powered to desired intensity. Shutter release exposed the sample and triggered the recording instrumentation. Fabric ignition (or melting) was detected by flux meter or visually.* After fabric ignition, the heat source was turned off, the shutter was uncocked, and the spring was relieved to neutral. The next fabric sample was then mounted for testing.

---

* Visual detection of ignition was employed to verify flux meter indications as well as to determine extended exposure ignition times. The process is difficult in that the irradiated area was extremely bright from heater glow [5]. As the experiments continued, however, the observer became progressively more proficient in defining and recording the instant of first flame.

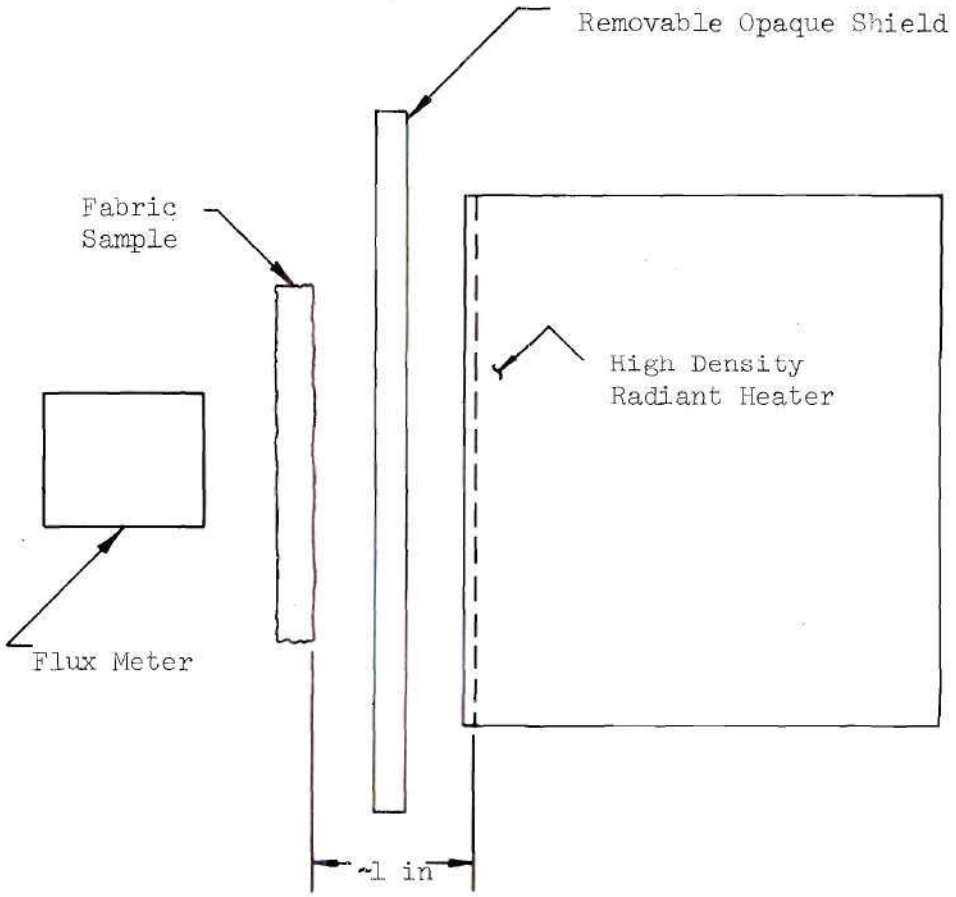


Figure 1. Ignition Time Apparatus - Initial Concept.

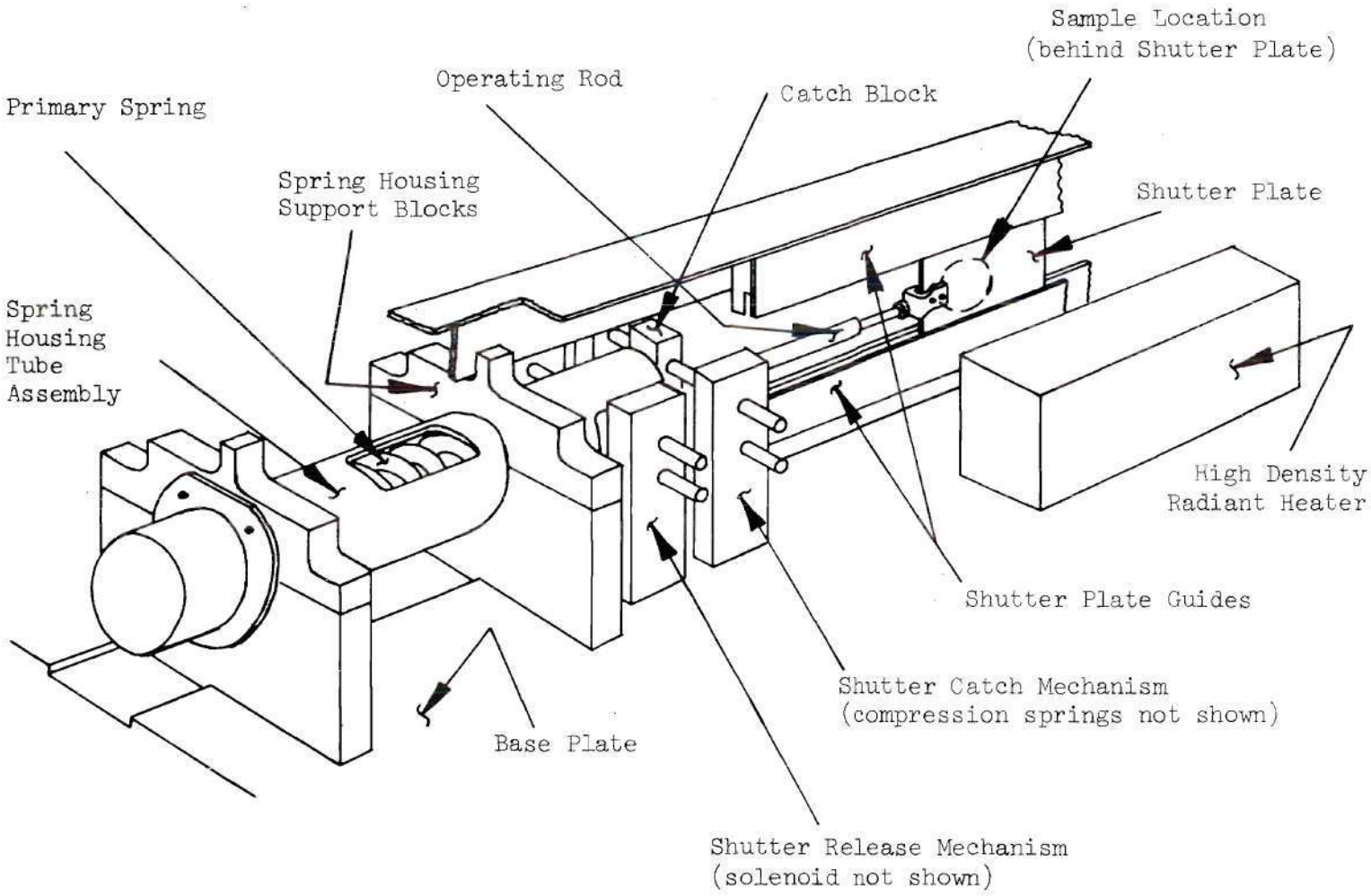


Figure 2. Schematic of Ignition Time Apparatus Reproduced from Reference [2].

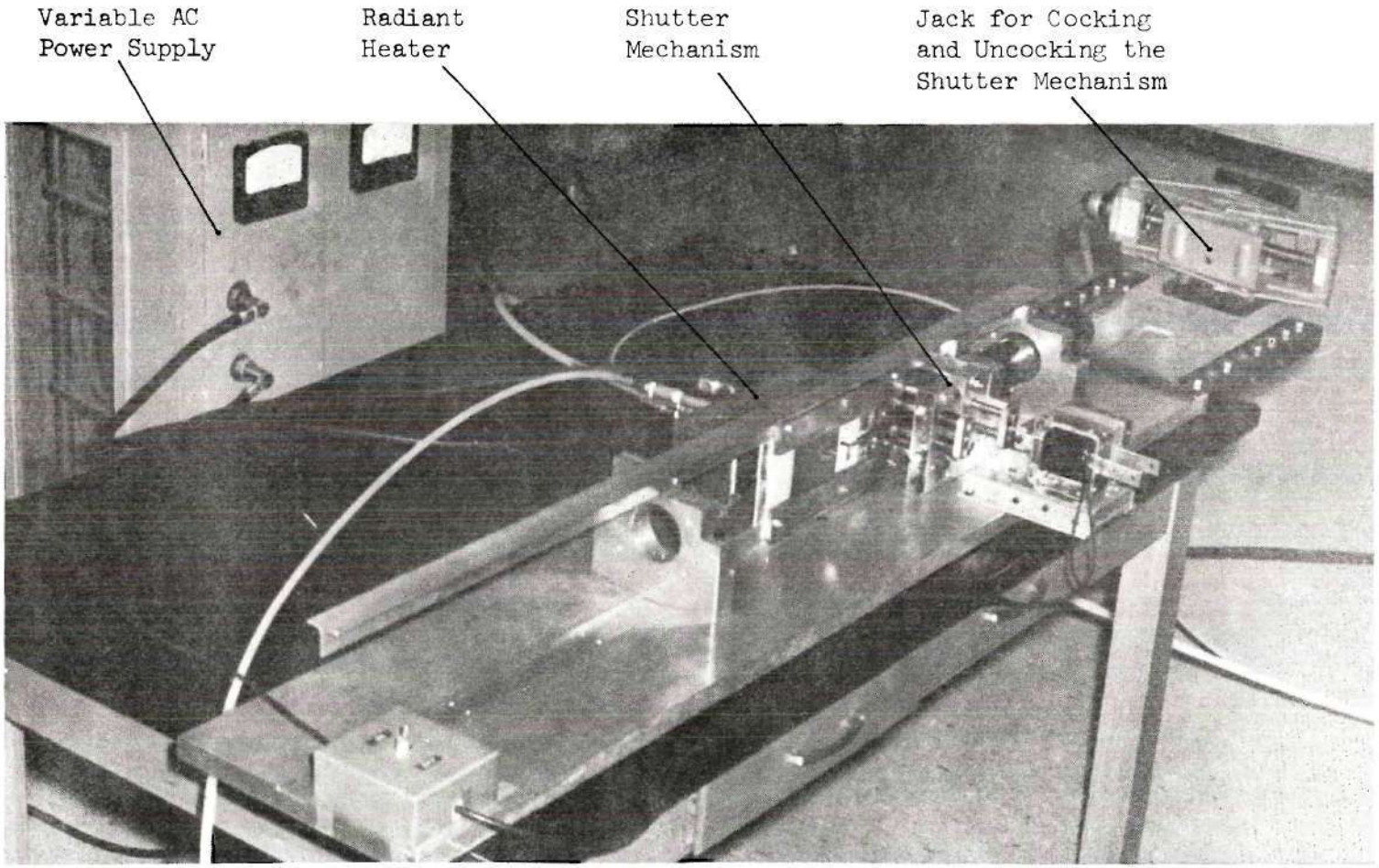


Figure 3. Ignition Time Apparatus Reproduced from Reference [2].

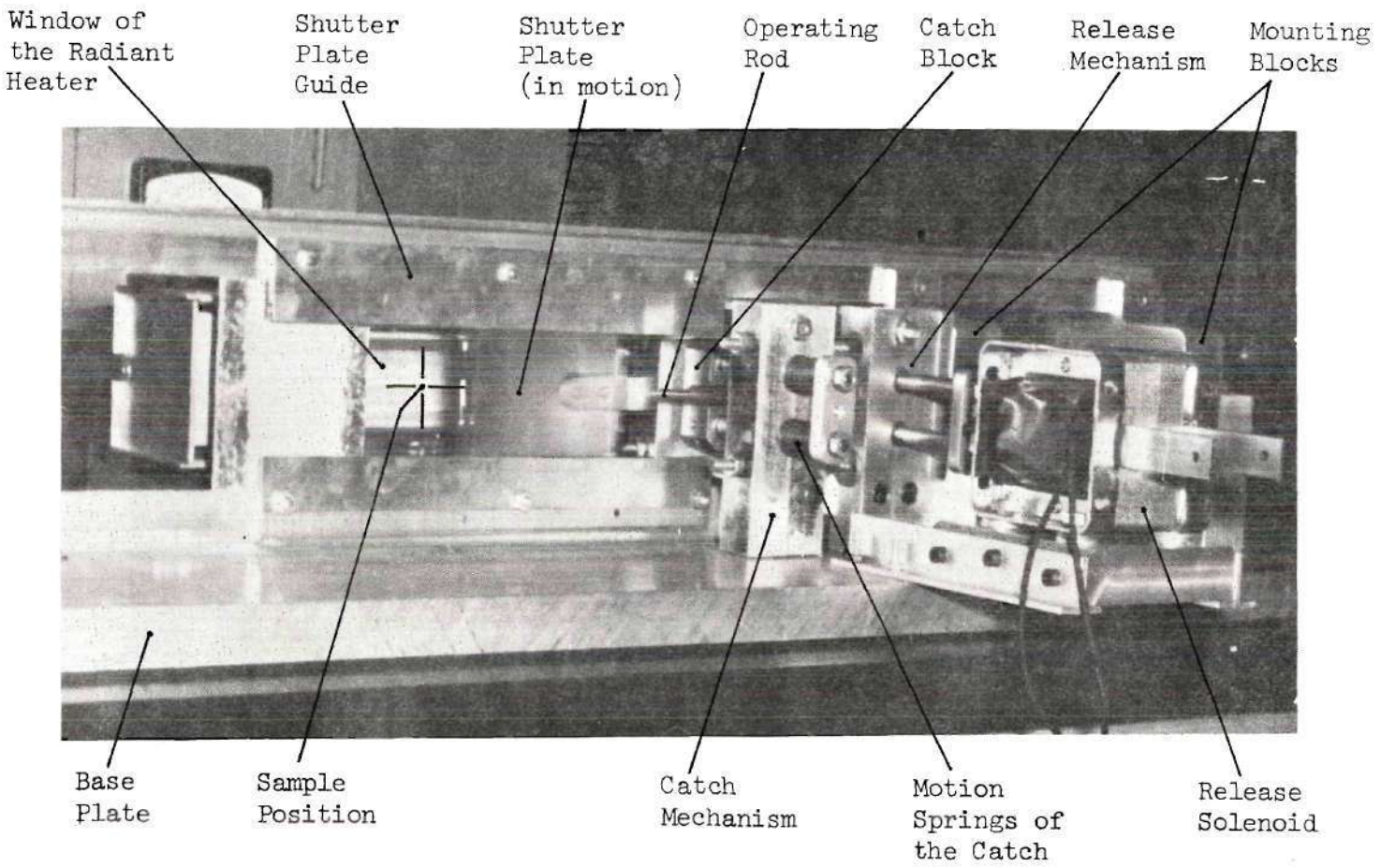


Figure 4. Ignition Time Apparatus - Shutter Mechanism.

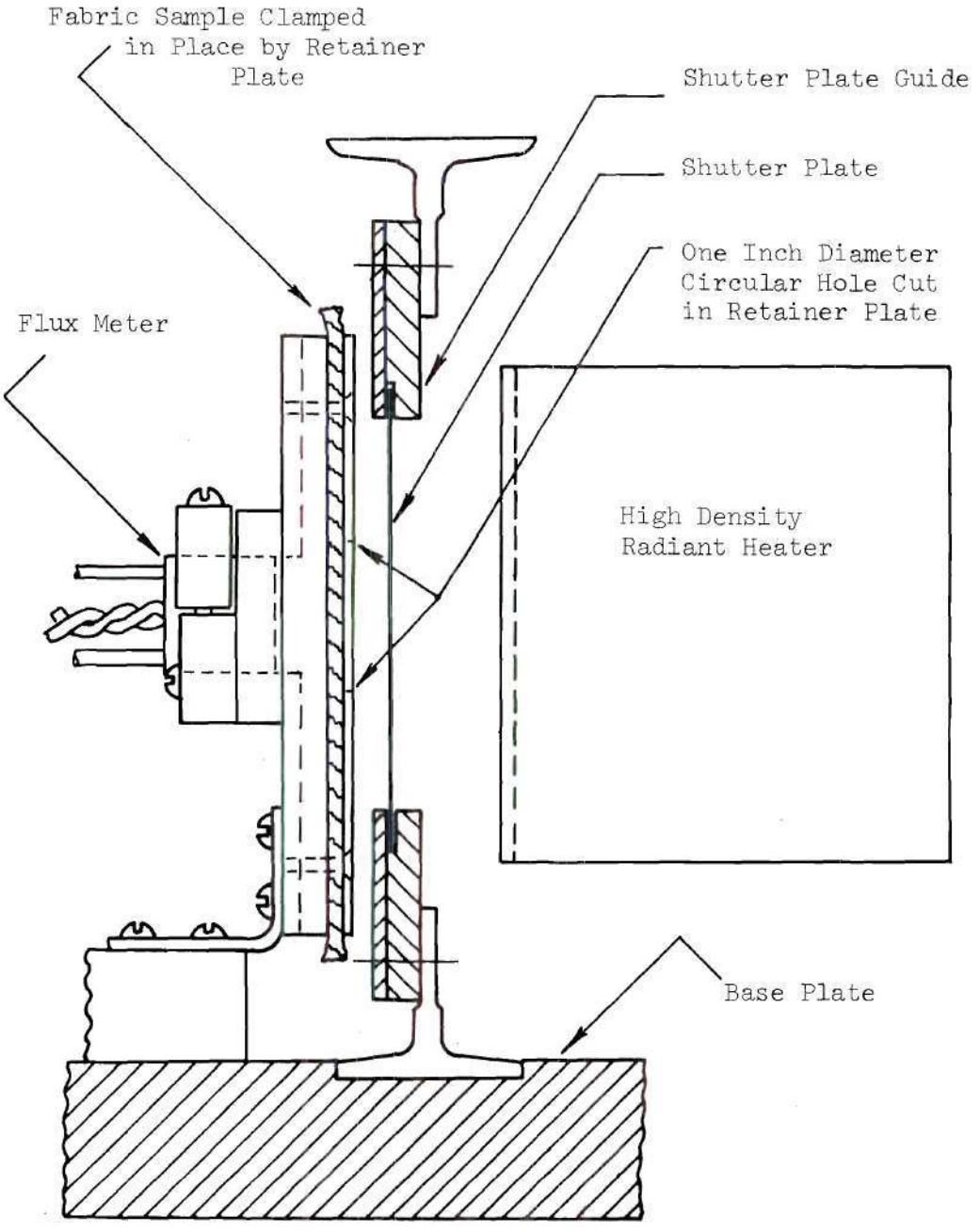


Figure 5. Cross Sectional View of Ignition Time Apparatus.

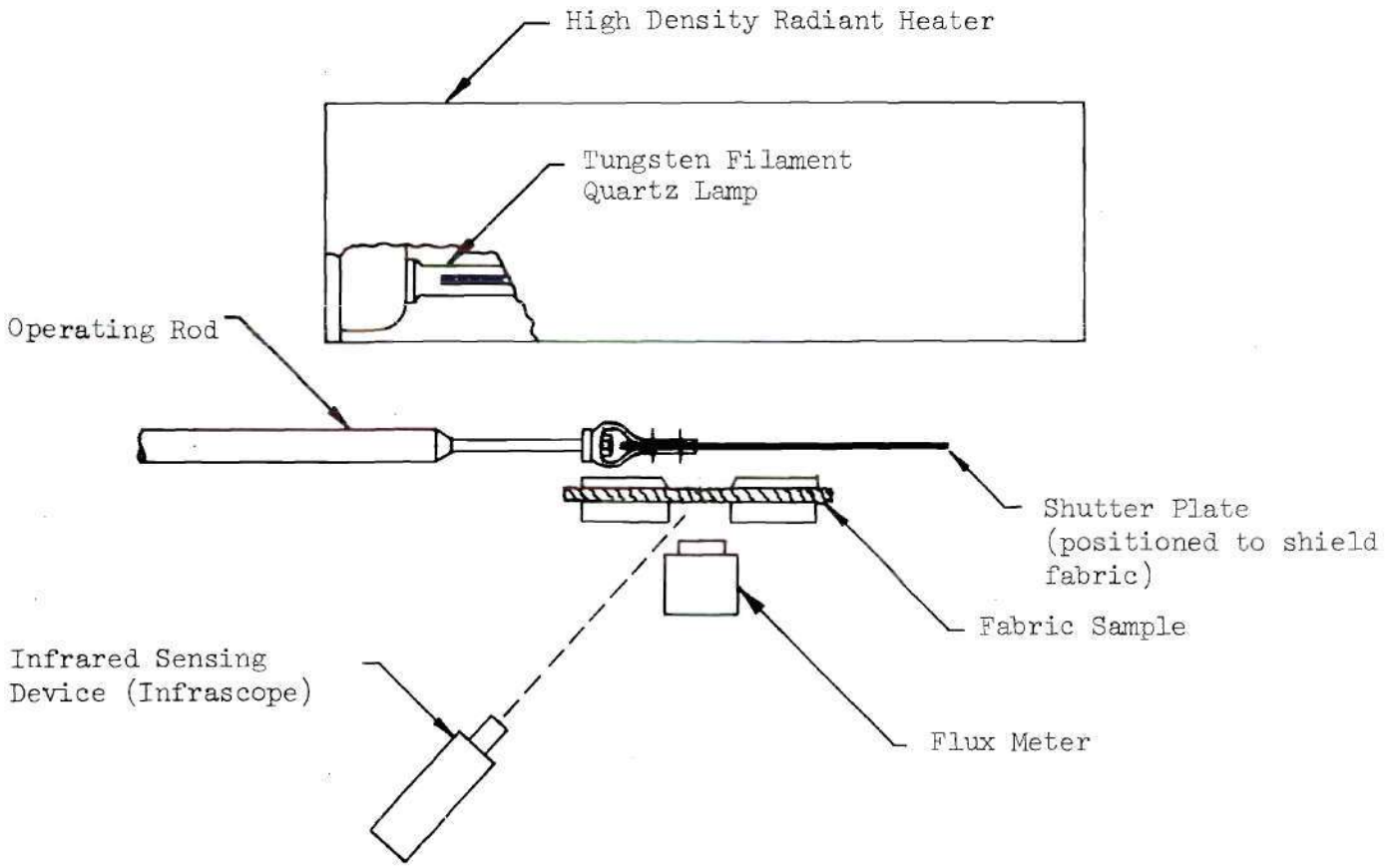


Figure 6. Ignition Time Apparatus - General Arrangement of Heater, Shutter Plate, Sample, and Sensors from Reference [1]

# CHAPTER III

## IGNITION TIME MEASUREMENTS

The Ignition Time Apparatus, described in the preceding chapter, was used to measure the ignition times for 10 different fabrics (bone dry), each irradiated at five different heat fluxes. Raw data obtained during the tests are presented in Appendix B. Final results are plotted in Figures 7 through 9.

### 3.1 Apparatus Check and Calibration

Active testing was preceded by radiant heater calibration. The flux meter (refer to Figure 5) was relocated from normal behind-sample center position to four different positions in the sample exposure area on the sample front face plane. While the meter was in each position, prescribed voltages were applied to the radiant heater, and consequent EMF signals from the meter were measured with a Leeds and Northrup Model 8686 millivolt potentiometer. The EMF at each voltage setting was then averaged and converted to incident flux via the manufacturer's calibration [5]. Maximum variation in heat flux over the circular sample area was approximately 4 per cent.

During the calibration, thermal equilibrium between heater and apparatus structure was achieved after about six minutes exposure. However, the EMF reading after 30 seconds exposure was at all heater power settings more than 98 per cent of the 240 second

reading. During subsequent testing, the heater was powered to desired intensity and allowed to heat the apparatus for at least 30 seconds before the shutter was released to initiate fabric exposure.

After the first 40 tests were completed, the heater was checked again to measure any variation of radiant heater output at the prescribed heater voltages. The flux meter was repositioned to the center of the front face plane and the radiant heater powered to the preselected voltages. Recheck demonstrated that incident flux rates were essentially unchanged from the initial calibration values [5].

## 3.2 General Test Procedure

The test procedure followed has been outlined in the previous chapter. A test included the following operations [5]:

(a) Sample dried by storage in calcium chloride desiccators for 48 hours or longer to produce bone-dry condition.

(b) Sample mounted by clamping a cut cloth section into the sample holder and trimming to fit.

(c) Sample positioned 1.18 in. from the radiant heater window. This position was obtained by locating the sample holder 0.15 in. from the brass shutter plate guide. Figure 5 illustrates the configuration.

(d) Ignition Time Apparatus cocked, with shutter plate in position to shield the fabric sample from radiant heat.

(e) Radiant heater powered to desired intensity. Incident

heat fluxes of 23,900, 34,000, 47,300, 63,300 and 72,700 Btu/hr-ft$^2$ were applied to the fabric front face.

(f) Shutter released to expose fabric sample. The switch which activated the solenoid to release the shutter also triggered oscilloscope traces. Immediately after exposing the sample, the shutter plate cammed on a microswitch to generate a pulse on the oscilloscope traces and identify that instant of exposure initiation. In addition, the operator started a stopwatch at shutter release in order that visually detected times to ignition could be measured.

(g) Upon fabric destruction, ignition or melting, the heat source was de-energized.

## 3.3 Description of Test Observations

Following sections list detailed observations from the experiments. The discussions have been listed by order of fabric types, rather than chronologically by order of test. Appendices A and B, with the following discussions, couple to describe fully the experimental results. It should be emphasized that thermodynamic processes contributing to fabric destruction are quite complex. Detection of various stages is not always clear cut. Thus, inclusion of these discussions of the test is entirely appropriate.

The "time" quantities quoted in these following discussions were taken from oscilloscope tracings of flux meter output unless exposure time exceeded 45 seconds, in which case stopwatch readings were used. The ignition process caused a large increase in heat flux recorded by the flux meter. Onset of melting (fabrics woven of man-made

materials) similarly was indicated by readily obvious variations in the heat flux incident to the calorimeter. Appendix B includes tracings from photographic records of the oscilloscope tracks. These tracings were used to measure time to ignition (or melting) and the magnitude of transmitted flux. Quantities determined are tabulated in Appendix A. In addition to the application of flux meter output to evaluate ignition time, visual estimations of time to front face ignition were recorded with the stopwatch and correlated with the photographic records. Variations in time elapse from that instant of fabric exposure until destruction ranged from 2 to 90 seconds.

3.3.1 Test of GIRCFF Fabric No. 2

Fabric No. 2 is a thin, light weight (7.51 mg/cm$^2$) yellow textured blouse material, woven of 100 per cent polyester.

(a) Test 9A - Incident flux of 23,900 Btu/hr-ft$^2$. Progressive melting without ignition. After 85 seconds exposure, a spider web pattern of material wholly different from original weave remained over the exposure area. Material had melted and accumulated near the bottom of the exposure area in boiling pools. The test was terminated at this point.

(b) Test 6 - Incident flux of 34,000 Btu/hr-ft$^2$. Progressive melting without ignition. Material degraded much as occurred in Test 9A except that deterioration had ceased after 35 seconds exposure when the test was terminated.

(c) Test 7 - Incident flux of 47,300 Btu/hr-ft$^2$. Progressive melting without ignition. Material melting was rapid and complete. After only 12 seconds irradiation, the exposure circle was an open

hole with no remaining material in the area.

(d) Test 8 - Incident flux of 62,300 Btu/hr-ft$^2$. Rapid melting without ignition. The exposed area of fabric melted completely within 8 seconds. None of the fine residual grid such as noted in Tests 9A or 6 remained after test termination at 9 seconds.

(e) Test 41 - Incident flux of 72,700 Btu/hr-ft$^2$. Immediate melting without ignition. Deterioration began immediately after exposure, and all irradiated material had melted after 5 seconds.

3.3.2 Test of GIRCFF Fabric No. 5

Fabric No. 5 is a white jersey "T-shirt" material, woven from 100 per cent cotton. The material weighs 13.71 mg/cm$^2$.

(a) Test 8A - Incident flux of 23,900 Btu/hr-ft$^2$. Fabric ignition after discoloration. Irradiated fabric browned progressively darker until ignition at 28.8 seconds. Flame began near the top of the exposure area, and destroyed all fabric within the exposed circle.

(b) Test 9 - Incident flux of 34,000 Btu/hr-ft$^2$. Fabric ignition after discoloration. The fabric destruction sequence was identical to that of Test 8A, except that occurrence was more rapid. Flame first appeared near the top of the exposure area at 14.0 seconds.

(c) Test 10 - Incident flux of 47,300 Btu/hr-ft$^2$. Fabric ignition after discoloration. Rapid fabric discoloration preceded ignition at 8.8 seconds exposure.

(d) Test 11 - Incident flux of 62,300 Btu/hr-ft$^2$. Immediate fabric discoloration, with ignition after 5.5 seconds.

(e) Test 42 - Incident flux of 72,700 Btu/hr-ft$^2$. Immediate fabric discoloration, with ignition after 4.9 seconds.

3.3.3 Test of GIRCFF Fabric No. 8

Fabric No. 8 is a white jersey "T-shirt" material, woven from a fiber mixture, 65 per cent polyester and 35 per cent cotton. The material decomposition and destruction during test irradiation was significantly different from the 100 per cent cottom "T-shirt" material, in that a melting of the polyester preceded and delayed ignition of the cotton. Fabric No. 8 is slightly heavier than the tested 100 per cent cottom "T-shirt" and weighs 16.91 mg/cm$^2$.

(a) Test 10A - Incident flux of 23,900 Btu/hr-ft$^2$. Melting followed by ignition. Polyester protions of the fabric began melting after 4.8 seconds exposure. A fine grid of cotton was left stretched over the exposure circle at the end of 16.1 seconds. The residual cotton grid ignited at 28.1 seconds.

(b) Test 25 - Incident flux of 34,000 Btu/hr-ft$^2$. Melting followed by ignition. Melting began at 3.0 seconds and was complete at 11.5 seconds, leaving a fine cotton grid. The cotton grid ignited at 15.0 seconds.

(c) Test 26 - Incident flux of 47,300 Btu/hr-ft$^2$. Melting followed by ignition. Test history was the same as Tests 10A and 25 except that time elapses to each occurrence were shorter. Ignition occurred after 8.8 seconds exposure.

(d) Test 27 - Incident flux of 62,300 Btu/hr-ft$^2$. Melting was followed by ignition at 5.4 seconds.

(e) Test 35 - Incident flux of 72,700 Btu/hr-ft$^2$. Melting

was followed by an almost explosive ignition at 4.8 seconds.

During the tests at progressively higher incident heat flux, the ignition time approached progressively closer to that of the 100 per cent "T-shirt" material. The ignition time delay caused by melting of the polyester became less significant as heating rates were increased. At maximum heating rate, either the cotton portion of the cloth ignited before molten polyester could flow from the exposed area, or else the polyester itself ignited while the molten material remained under exposure.

3.3.4 Test of GIRCFF Fabric No. 10

This fabric is a thin light weight purple batiste, woven from 100 per cent cotton. The material weight is 6.65 $mg/cm^2$. During testing at low heating rates, the material charred to a dark brown color before finally igniting. At heating rates in excess of 47,300 $Btu/hr\text{-}ft^2$, any charring that might have occurred was followed so quickly by ignition that visual observation of the material changes was not possible.

(a) Test 7A - Incident flux of 23,900 $Btu/hr\text{-}ft^2$. Eventual discoloration followed by ignition. Fabric appearance was unchanged for almost 15 seconds exposure. Once charring began, discoloration progressed steadily as the material became increasingly darker brown until flame at 41.5 seconds exposure.

(b) Test 2 - Incident flux of 34,000 $Btu/hr\text{-}ft^2$. Fabric began to char and become discolored after 6 seconds. Ignition occurred at 18.2 seconds.

(c) Test 4 - Incident flux of 47,000 Btu/hr-ft$^2$. Fabric charring developed rapidly after exposure was begun. Fabric ignition was detected after 7.2 seconds exposure.

(d) Test 5 - Incident flux of 62,300 Btu/hr-ft$^2$. Fabric seemed to char and ignite simultaneously. The discoloration and flame occurred at 3.8 seconds exposure.

(e) Test 43 - Incident flux of 72,700 Btu/fr-ft$^2$. Fabric ignited after 2.7 seconds exposure.

3.3.5 Test of GIRCFF Fabric No. 11

Test fabric No. 11 is woven from man-made materials, a white tricot, 80 per cent acetate and 20 per cent nylon weighing 11.31 mg/cm$^2$. At maximum test heating rates, there seemed to be a flame which consumed all material in the test area. At the lower heat fluxes, however, the fabric melted away with a moderate amount of smoke.

(a) Test 4A - Incident flux of 23,900 Btu/hr-ft$^2$. Gradual fabric melting without ignition. Fabric melting began after only two seconds heat exposure. The fabric deteriorated progressively during the subsequent 100 seconds of exposure. The sample test area was strung with intact solid material after the test was halted.

(b) Test 28 - Incident flux of 34,000 Btu/hr-ft$^2$. Gradual fabric melting with no ignition. Fabric melting began immediately after exposure. Fabric degradiation ceased after 43 seconds leaving a spider web grid over the exposure circle. The test was terminated after 60 seconds.

(c) Test 29 - Incident flux of 47,300 Btu/hr-ft$^2$. Gradual fabric melting with a terminal flame. Fabric melting began immediately after start of exposure and progressed continually until a small flame at 46.2 seconds destroyed all fabric remaining in the exposure area. The test was terminated after 60 seconds.

(d) Text 30 - Incident flux of 62,300 Btu/hr-ft$^2$. Rapid fabric melting followed by a small flame. Melting began after less than a second of exposure and continued until flame at 11.2 seconds destroyed all fabric left within the exposure area. The test was terminated at 18 seconds.

(e) Test 34 - Incident flux of 72,700 Btu/hr-ft$^2$. Rapid melting began after only 0.4 seconds exposure. A terminal flame occurred at 7.2 seconds and destroyed all exposed material within the next 4 seconds. The test was terminated after 15 seconds.

3.3.6 Test of GIRCFF Fabric No. 12

GIRCFF Fabric No. 12 is a white tricot, material weight 8.91 mg/cm$^2$, woven from 100 per cent mylon. In all tests of this cloth, ignition never occurred. All exposed material melted completely in each test.

(a) Test 3A - Incident flux of 23,900 Btu/hr-ft$^2$. After initiation of exposure, melting began at 6.0 seconds. Molten matter drained down from the exposure area for the next 6 seconds at which time no fabric material remained within the irradiated circle.

(b) Test 31 - Incident flux of 34,000 Btu/hr-ft$^2$. Fabric melting began after 3.9 seconds exposure, and was complete after 7.3 seconds.

(c) Test 32 - Incident flux of 47,300 Btu/hr-ft$^2$. All material within the exposure circle had melted after 5.2 seconds exposure.

(d) Test 33 - Incident flux of 62,300 Btu/hr-ft$^2$. All exposed material was melted away within 3.1 seconds.

3.3.7 Test of BIRCFF Fabric No. 13

This cloth is a white tricot woven from 100 per cent acetate weighing 9.40 mg/cm$^2$. Fabric No. 13 melted without ever igniting during any of the five tests.

(a) Test 2A - Incident flux of 23,900 Btu/hr-ft$^2$. Fabric deterioration was characterized by progressive melting which was incomplete even after 112 seconds exposure.

(b) Test 19 - Incident flux of 34,000 Btu/hr-ft$^2$. Fabric deterioration under heat exposure continued progressively at a diminishing rate for 40 seconds without complete destruction.

(c) Test 20 - Incident flux of 47,300 Btu/hr-ft$^2$. The exposed material was not completely destroyed even after 40 seconds exposure.

(d) Test 21 - Incident flux of 62,300 Btu/hr-ft$^2$. In this test, complete destruction of the exposed material did occur. After exposure of only 13.2 seconds, no material remained in the exposure circle but was boiling in a pool at the bottom of the sample holder.

(e) Test 39 - Incident flux of 72,700 Btu/hr-ft$^2$. Test results were similar to Test 21 results except that complete fabric destruction had occurred after 9.4 seconds.

### 3.3.8 Test of GIRCFF Fabric No. 14

This sample is white batiste material woven of 65 per cent polyester and 35 per cent cotton which weighs 8.55 mg/cm$^2$. In the four tests at incident heat fluxes in excess of 30,000 Btu/hr-ft$^2$, a melting phase was followed by a terminal flame. At the lowest incident flux rate, ignition did not occur.

(a) Test 6A - Incident flux of 23,900 Btu/hr-ft$^2$. The polyester portion of the weave melted within 25 seconds, but the fine residual cotton grid withstood another 45 seconds of exposure without igniting.

(b) Test 22 - Incident flux of 34,000 Btu/hr-ft$^2$. The melting portion of the fabric had flowed molten from the exposure area after 17.0 seconds. The remaining material, a fine grid of cotton, ignited 24 seconds later and was destroyed.

(c) Test 23 - Incident flux of 47,300 Btu/hr-ft$^2$. Again there was a melting phase followed by ignition. Melting was completed after 7.0 seconds, and ignition occurred after 11.4 seconds exposure.

(d) Test 24 - Incident flux of 62,300 Btu/hr-ft$^2$. All melting had been completed after 3.2 seconds exposure. The remaining material ignited and was destroyed at 5.8 seconds.

(e) Test 36 - Incident flux of 72,700 Btu/hr-ft$^2$. Melting was completed at 2.8 seconds. Ignition occurred at 4.8 seconds.

### 3.3.9 Test of GIRCFF Fabric No. 18

This cloth is a white cotton (100 per cent) flannel, the same

as is frequently used for night clothes. Fabric weight is 12.88 $mg/cm^2$. The fuzzy side of the material was oriented toward the radiant heater during the tests. Subsequent tests indicated that orientation is not a significant factor in determination of ignition time [4]. In all tests, the fabric initially charred and became discolored while smoking slightly. The eventual ignition occurred after the exposed material had become quite dark brown in color. Terminal flames destroyed the entire exposed area.

3.3.10 Test of GIRCFF Fabric No. 19

Fabric No. 19 is a white flannel material, 100 per cent cotton, treated with fire retarding compound. The material weight is 14.81 $mg/cm^2$. Tests were conducted with fabric fuzz oriented toward the heat source. This fabric demonstrated more rapid ignition than any of the other nine tested materials. Flames broke out soon after exposure was begun, but flames died without burning through the primary weave of fabric. The burned areas were considerably thinner than the unharmed material. At an incident flux of 72,700 $Btu/hr\text{-}ft^2$, Test 38, some degradation did occur under prolonged exposure; but additional flaming did not occur. Table A8 lists results from tests of this fabric.

3.3.11 Tests of Room Stored Samples

Subsequent to completion of the 50 tests described above, an additional six experiments were conducted on room stored cloth samples. Test irradiances from these terminal tests were 23,900 ($Btu/hr\text{-}ft^2$). The relative humidity of the room air was measured to

be 55 - 60 per cent. These experiments included 5 tests of single fabric layers and another single test of a two-layer sample.

(a) Test 11A - Fabric 19. The cloth browned, then ignited after 11.2 seconds exposure.

(b) Test 12A - Fabric 5. Destruction occurred in the same sequence as was described for the "bone-dry" samples. Ignition was delayed until 45 seconds exposure; however, that delay was the result of fabric tension. The sample was stretched more tightly than normal, and the fabric was more transparent than usual.

(c) Test 13A - Fabric 5. Ignition after 24.5 seconds. The shorter ignition time reflects the test effort to make the sample as relaxed as possible and yet remain plane.

(d) Test 14A - Fabric 5. Ignition after 29.7 seconds. The fabric tension was consistent with previous tests. The ignition time was less than a second later than was recorded for the "bone-dry" sample, Test 8A.

(e) Test 15A - Fabric 19. Front surface ignition in 9.8 seconds. A blackened grid of intact material remained after the flames died and throughout the remaining period of exposure.

(f) Test 16A - Fabric 5. A description of this test with two layers of material is included in section 6.3.2.

The follow-on tests demonstrated that moist samples ignite somewhat later than "bone-dry" samples removed from the desiccators just prior to testing. The variation between ignition times was caused, probably, by differences in fabric tension or by variations

in the weaves of the samples.

## 3.4 Test Results

The following graphs, Figures 7 through 9, were plotted from tables in Appendix A and present the test data in terms of intensity of incident radiant heat flux versus time to ignition, melting, or destruction. No corrections have been applied to account for reflected or transmitted energy.

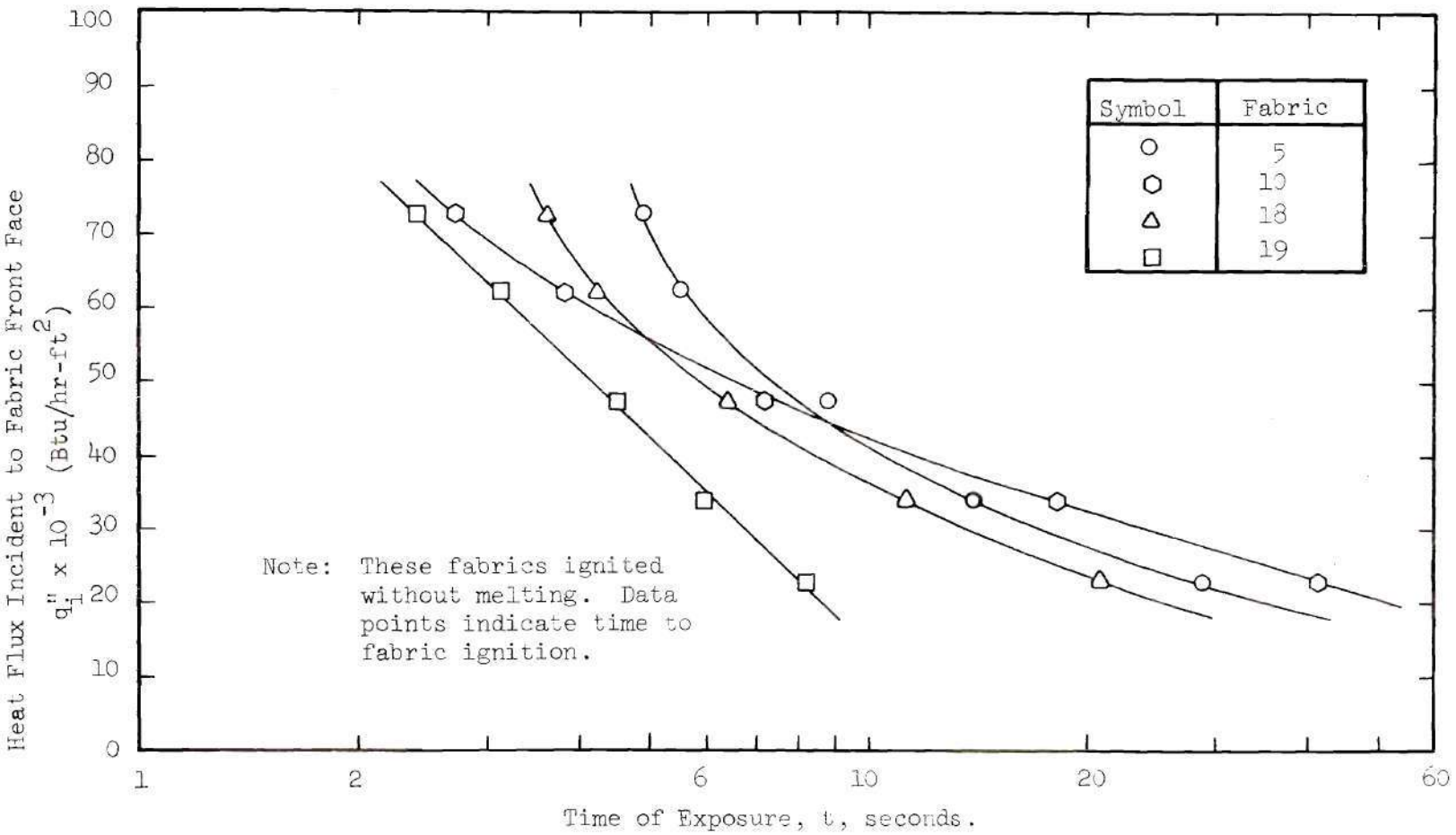


Figure 7. Time Elapse to Fabric Destruction Versus Incident Heat Flus Intensity Igniting Fabrics.

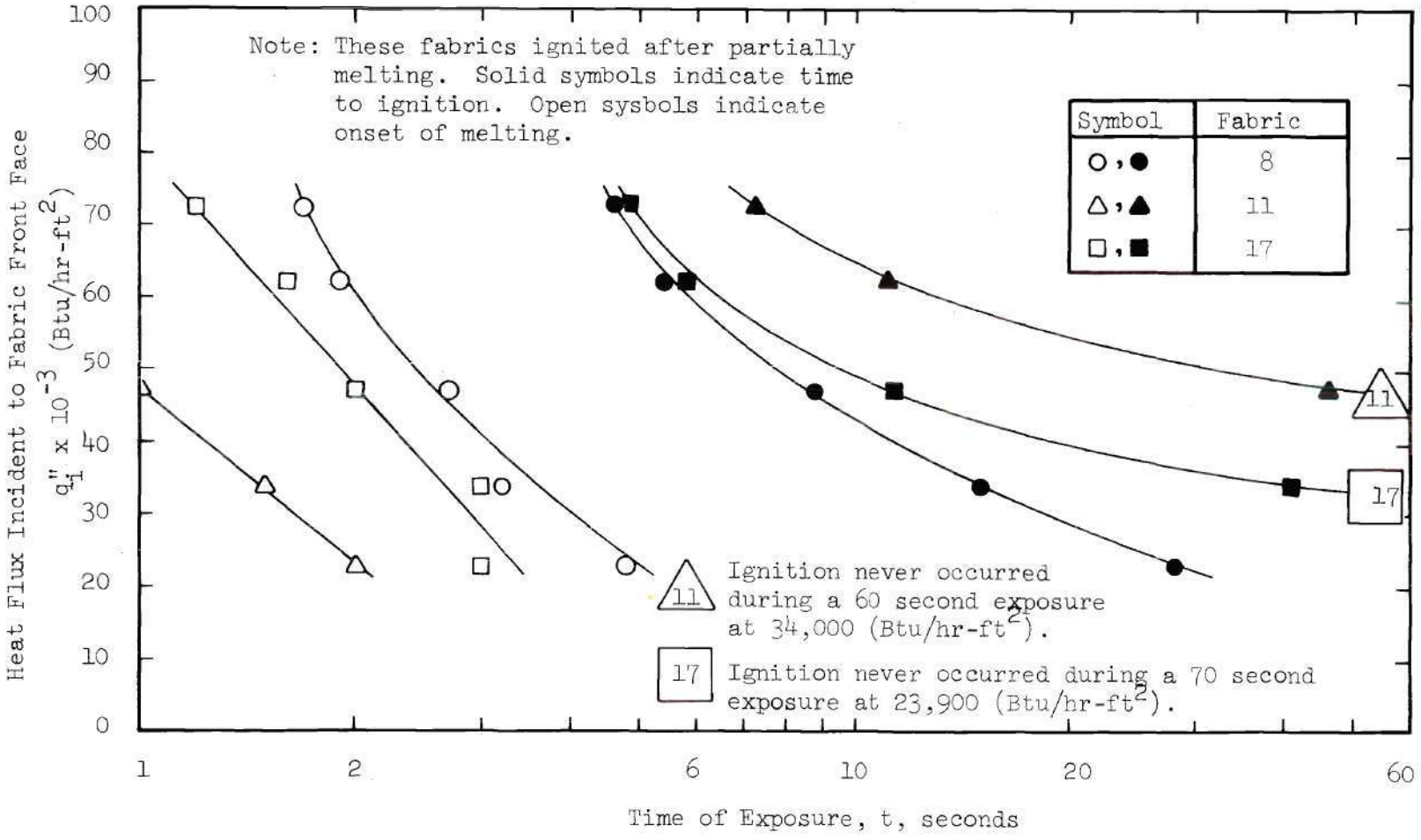


Figure 8. Time Elapse to Fabric Destruction Versus Incident Heat Flux Intensity, Igniting Fabrics with a Preliminary Melting Phase.

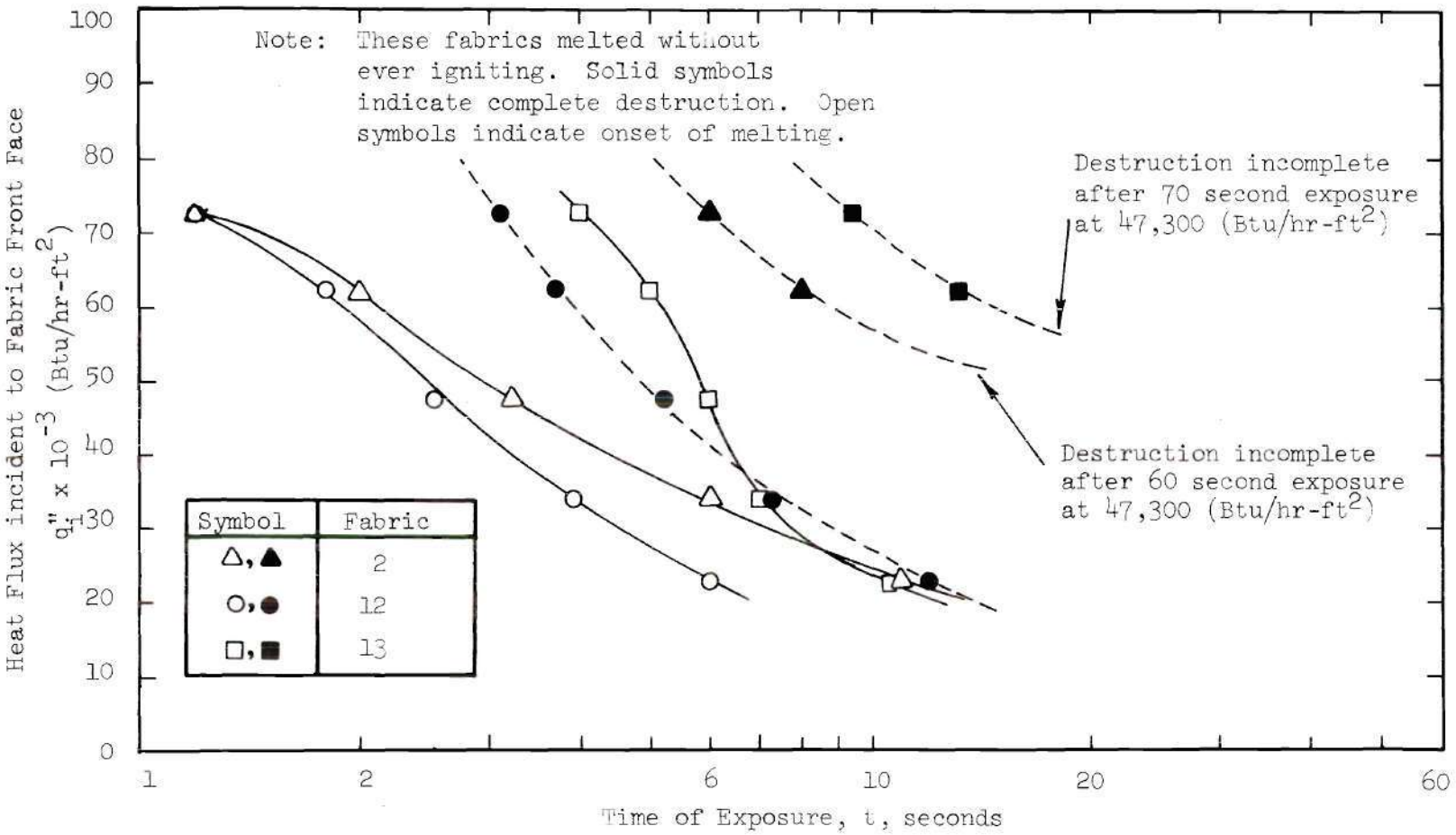


Figure 9. Time Elapse to Fabric Destruction Versus Incident Heat Flux Intensity, Melting Fabrics.

# CHAPTER IV

# FABRIC IGNITION ANALYSIS

## 4.1 Introduction

Results from the Ignition Time Tests are discussed in the previous chapter. Those data are from tests of single layers of fabric oriented with the fabric perpendicular* to incident heat flux. For that orientation, the data represent the quickest ignition (or melting) time possible for each of the tested cloths.

If the test situation could be analyzed such that fabric ignition can be predicted by the solution of a differential equation, the need for additional ignition time tests could be reduced to proof of the analytical method. Fabric physical and thermal properties considered significant for such analysis include:

(1) Thermal conductivity, $k$,

(2) Specific heat, $C_p$,

(3) Density, $\rho$,

(4) Fabric thickness, $\delta$,

(5) Fabric reflectivity, $\rho_o$,

(6) A fabric ignition criterion such as ignition temperature, $T_i$.

---

* The situation where an edge of a fabric is heated, i.e., heat input parallel to the plane of cloth, shall not be considered.

Alvares et al. [65], Patten [66], and Simms [69] have suggested that thin cellulostic materials will ignite spontaneously when any point on the fabric surface attains some characteristic ignition temperature, $T_i$. Wulff, Zuber et al. [1-4], likewise, have assumed the ignition temperature criterion valid for all igniting cloths. For melting fabrics, a characteristic melting temperature, $T_m$, is assumed attained on the fabric front surface when "onset of melting" occurs. These assumptions also will be used for the present analysis.

A literature survey by M. J. Kirkpatrick [1,4] reported the thermal properties of numerous fabrics and pointed out variations in the properties caused by use and treatment. While this survey has provided representative values for the thermal conductivities and specific heats of fabrics, accurate model verification is possible only with accurate property values measured for the test fabrics of interest. Material properties for the 10 tested fabrics, have been measured and reported by Wulff, Zuber et al. [3,4].

## 4.2 Fabric Ingition Model - Transient Conduction Through an Opaque Slab

As suggested previously, fabric ignition analysis can be simplified to a determination of that time elapsed, during which a plane fabric is heated at constant rate, before the front face has reached "ignition temperature". The simplest possible model of the temperature-time variation in a fabric would idealize the cloth as some finite thickness of a one-dimensional, semi-infinite, opaque, thermally isotropic conducting solid with constant properties. Radiant energy is absorbed at the slab front surface. Back-side boundary conditions,

side next to the skin, can be chosen to describe situations of skin contact with the cloth or of an air gap between the cloth and skin.

4.2.1 Model Definition

The model is described by Figure 10. A constant heat flux, $q_i''$, is incident to the front face of a homogeneous opaque solid. A portion, $\rho_o$, of the incident energy is reflected. A semi-infinite body, skin, is located behind the cloth, separated by a thin air gap.

Initially, the fabric, the air trapped between cloth and skin, and the skin surface are assumed to be at uniform temperature. This approximation neglects temperature differences of perhaps 15 - 20°F between skin surface and the fabric outside surface in a typical room temperature environment. However, this error represents no more than 4 per cent of the temperature increase expected for fabric melting or ignition. Conductive and radiative heat exchanges between the fabric front-face and adjacent air shall be neglected as insignificant when compared to incident flux intensities.

The following differential equation is a simplification of the Fourier heat conduction equation for the situation of one-dimensional conduction through an isotropic material with constant thermal conductivity, constant specific heat, and constant density.

$$\frac{\partial^2 T(x,t)}{\partial x^2} = \frac{1}{\alpha} \frac{\partial T(x,t)}{\partial t} \qquad (1)$$

$$\alpha = (k/\rho c_p) = \text{constant} \qquad (2)$$

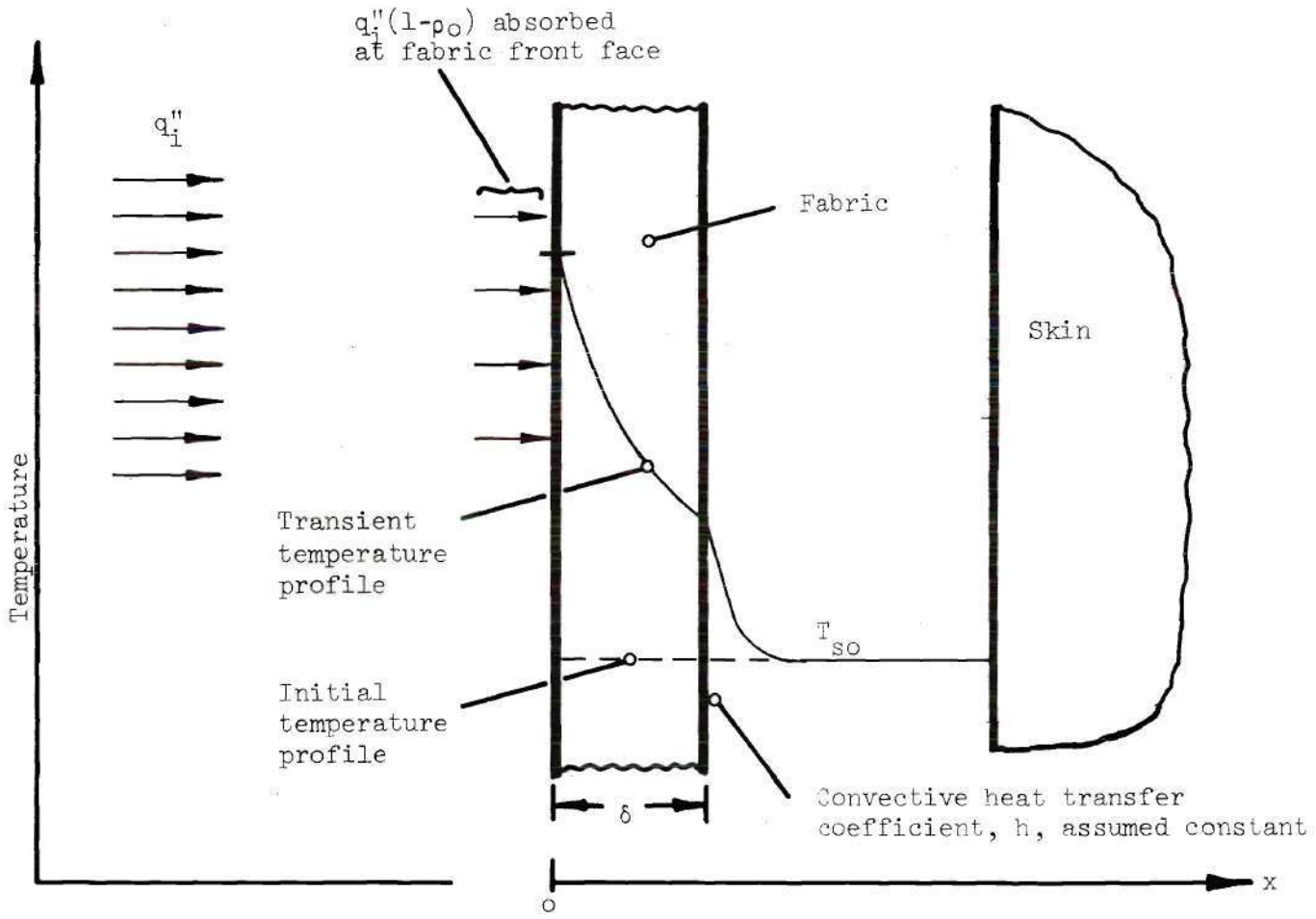


Figure 10. Transient Conduction Fabric Ignition Model.

The front-face boundary condition at x = 0:

$$(q_i'') \ (1 - \rho_o) = -k \left(\frac{\partial T}{\partial x}\right) \tag{3}$$

The back-face boundary condition at x = $\delta$:

$$-k \left(\frac{\partial T}{\partial x}\right) = h(T - T_{so}) \tag{4}$$

The initial condition:

$$T(x,o) = T_o = T_{so} \tag{5}$$

The solution for the case of heat loss from the slab back-face was completed and evaluated numerically by Newman and Green [67]. Their results are plotted in Figure 11 in terms of non-dimensional groups. Values for the fabric front-face, $(x/\delta) = 0$, and fabric back-face, $(x/\delta) = 1$, are plotted.

4.2.2 Conduction Model Evaluation

Model validity can be determined by comparing analytical predictions with experimental results. Plotting experimental data on the analytical curves will generate an obvious comparison. The model was predicated on the criterion of fabric ignition whenever the fabric front face attains "ignition temperature". This simplification suggests that analysis at $(x/\delta) = 0$, only, need be considered in making the comparison between theory and experiment.

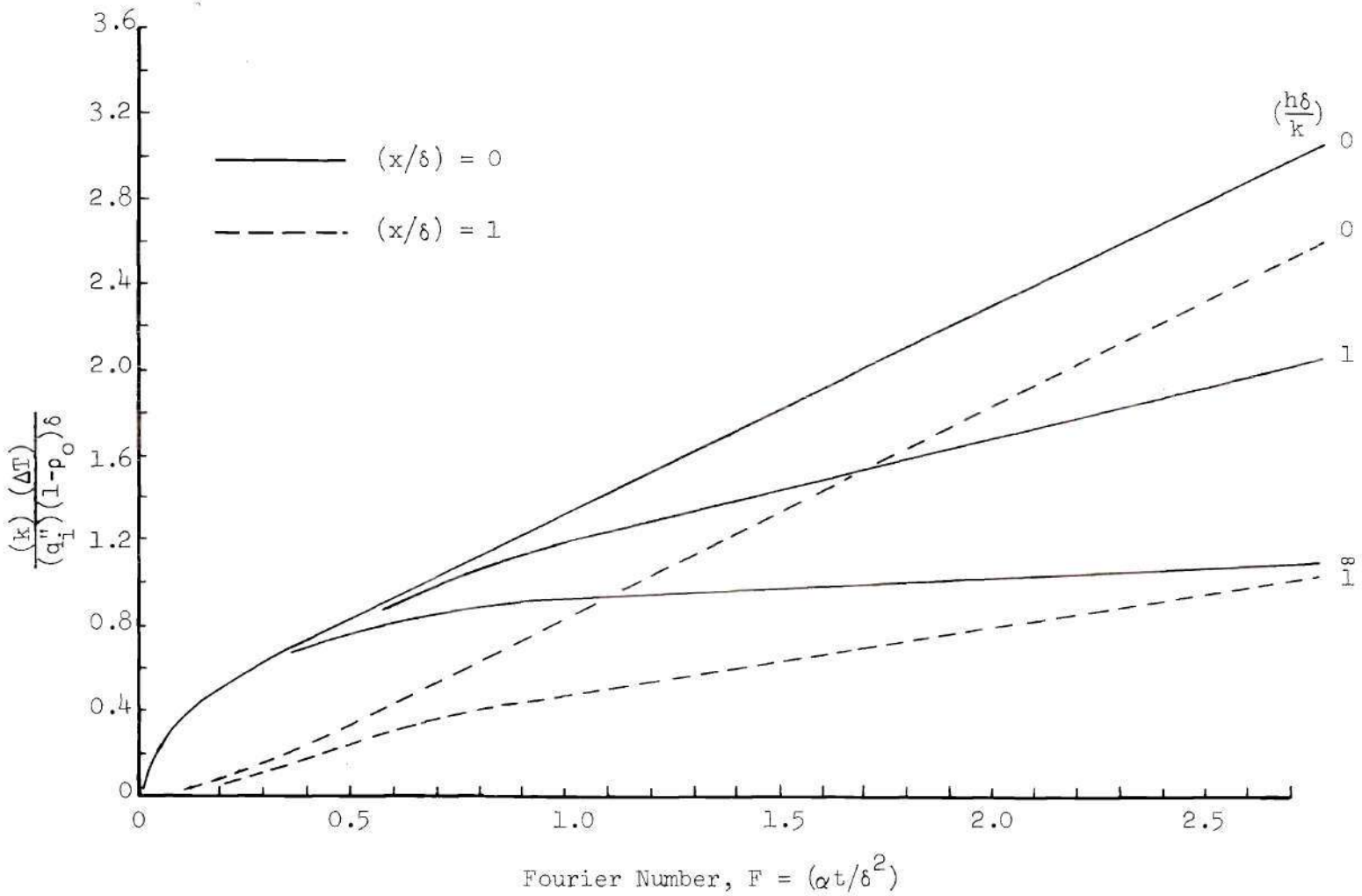


Figure 11. Analytical Results - Transient Conduction Through an Opaque Slab.

The ignition time test data* can be reduced readily to a dimensionless form by applying fabric thermophysical properties. The appropriate front-face temperature response curve can be determined by a realistic evaluation of the boundary condition parameter $(h\delta/k)$.

For the ignition time test conditions, the convective film coefficient, h, should lie between 1 and 10 (Btu/hr-ft$^2$ - $^oF$). Using values of k and $\delta$ for the tested fabrics [4],

$$0 < (h\delta/k) < 1$$

The front face temperature response curves for $(h\delta/k) = 0$ and $(h\delta/k) = 1$ are plotted together with data from the ignition time tests in Figure 12.

It is apparent that analytical predictions with the simple conduction model on a front-face "ignition temperature" criterion, do not agree well at all with experimental results. The model predicts fabric ignition typically an order of magnitude quicker than measured during the tests.

Several possible reasons for this difference between theory and experiment are discussed below:

(1) change in fabric thermal properties with temperature

* Ignition time data for Fabrics 5, 8, 19, and 19 have been reduced and plotted with the temperature response curves in Figure 12, using fabric thermophysical properties reported in Reference [4].

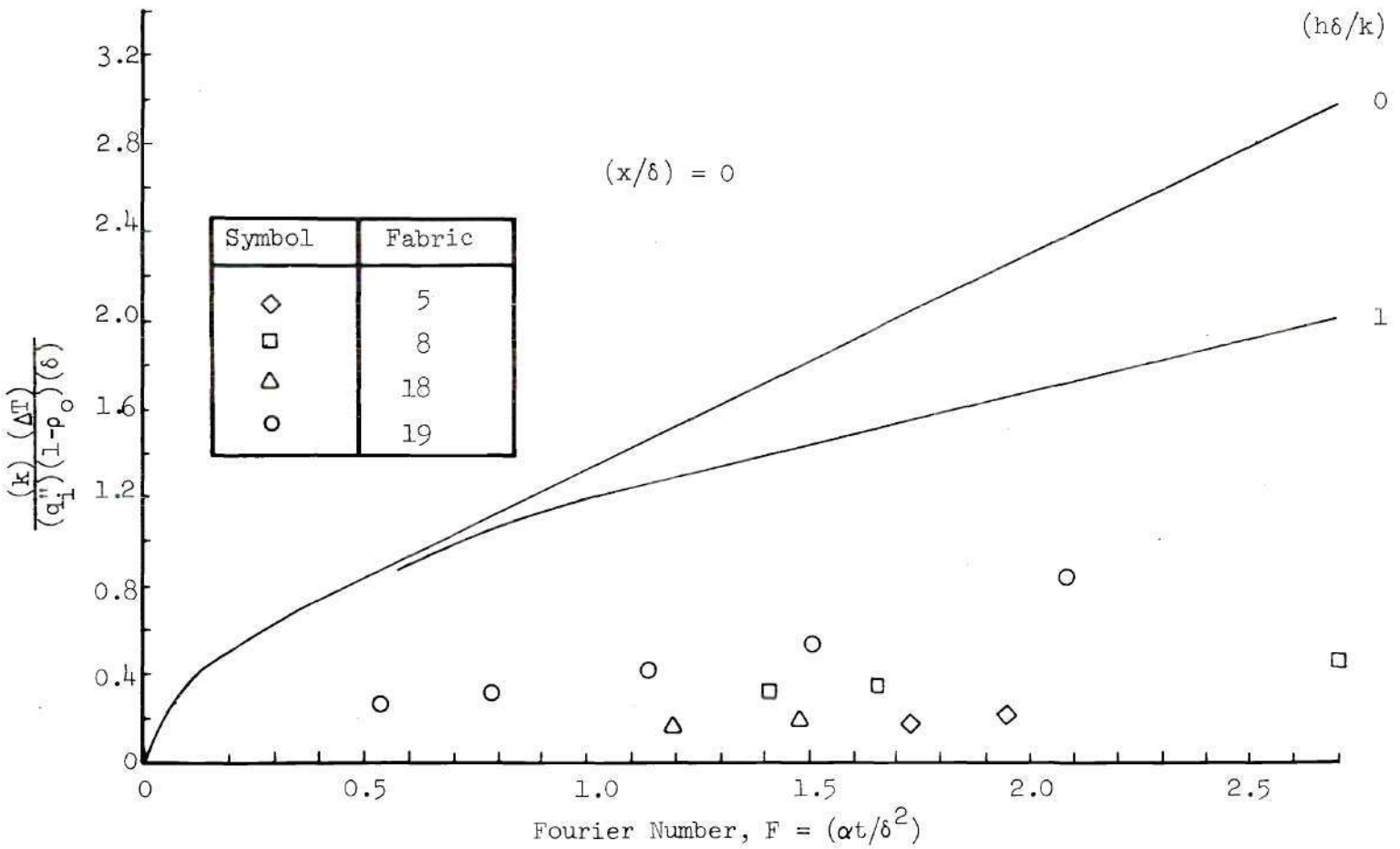


Figure 12. Simple Conduction Model - Comparison of Theory and Experiment.

increases,

(2) neglect of radiative dissipation,

(3) significant fabric transparency so that absorbed energy (which causes temperature increases) is considerably less than the net energy entering the fabric front face, and

(4) neglect of pre-ignition endothermic reactions.

Discrepancies arising from variation in the thermal properties k, $\rho$, and $C_p$ are thought to be small [67]. Radiative dissipation at the fabric front-face is not thought to be large, no greater than the convective losses.

The neglect of fabric transmittance is a very significant omission in the conduction model. The ignition time measurements recorded transmittances ranging from 0.14 to 0.27. Optical transmittances for the same fabrics were measured and reported by Wulff, Zuber et al. [4] in the range of 0.19 to 0.43. Fabric reflectances were reported by Wulff, Zuber et al. in the range 0.397 to 0.602. These values are consistent with the experimental results of Dunkle et al. [64] for fabrics irradiated with short wave length energy.

On a basis of comparison with experiment, the simple conduction model of fabric ignition must be discarded as insufficiently accurate. Measured magnitudes of transmitted flux prompt consideration of the more complex diathermanous model. In such model, fabric transmittance will be included by assuming that radiative heat flux within an irradiated fabric varies in accordance with the Beer-Lambert Law.

## 4.3 Fabric Ignition Model - Radiant Energy Transmission Through a Semi-Transparent Slab

A more natural but somewhat more complex model treats igniting fabrics as semitransparent, thin, diathermic solids. Bates and Monahan [50] were among the first to suggest that a diathermic model might describe the fabric temperature response to heat inputs. Transmitted energy, recorded during the experiments, varied between 15 and 27 per cent of the net incident energy.

### 4.3.1 Diathermanous Model Definition

The system considered in this analysis is shown schematically in Figure 13 and consists of three separate sections, 1) a thin fabric, idealized as a semitransparent slab, 2) the skin, and 3) an air gap which separates skin and cloth. Fabric ignition will be assumed to occur whenever some "ignition temperature", characteristic of the cloth in question, has been reached at the fabric front surface.

The model derivation below, reported by Wulff, Zuber et al. [2] and by Kalekar and Kung [6], is based on these following assumptions and approximations:

a) One-dimensional heat flow

b) Constant fabric thermal and optical properties throughout the duration of any thermal exposure incident.

c) Fabric idealized as a semi-transparent, energy absorbing and scattering material.

d) Radiant flux at any location, x, in the fabric defined by the Beer-Lambert Law,

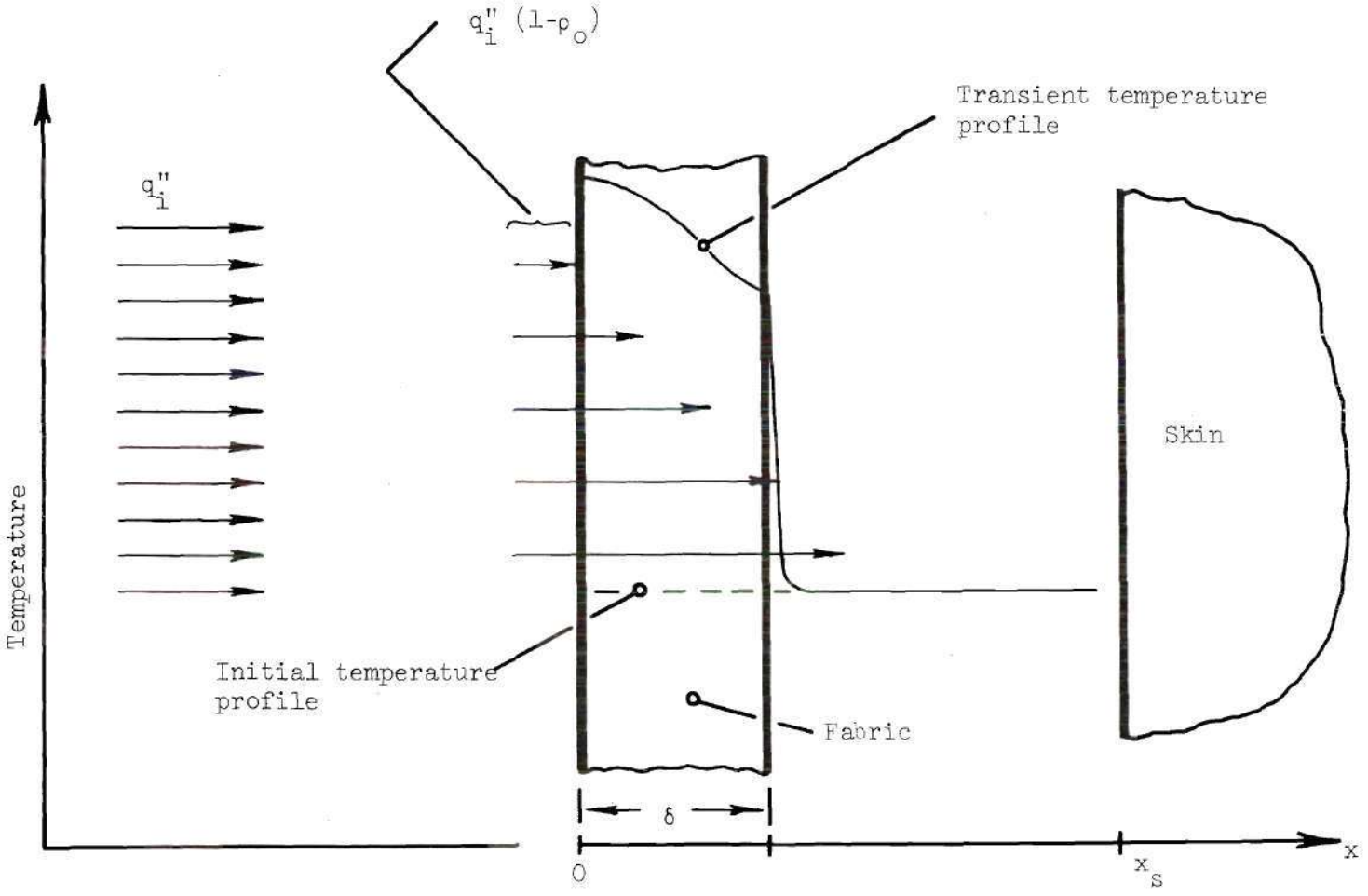


Figure 13. Coordinate System for Diathermanous Fabric Ignition Model.

$$I(x) = (q_i'') (1-\rho_o) \exp(-\kappa\chi) \qquad (1)$$

where

$q_i''$ = flux incident to fabric front face

$\rho_o$ = fabric reflectance

$\kappa$ = extinction coefficient

e) Effects of pre-ignition chemical kinetics negligible.

f) Convection effects on both faces of the fabric negligible.

g) Skin, air and fabric initially in thermal equilibrium.

h) Air assumed perfectly transparent with constant thermal properties.

i) Skin approximated as a homogeneous, semi-infinite, opaque solid with invarient thermal and optical properties.*

Applying these eight assumptions, the energy equations for each sub-system may be written.

For the fabric:

$$\rho C \left(\frac{\partial T}{\partial t}\right) = k \left(\frac{\partial^2 T}{\partial x^2}\right) + q_i'' \kappa(1-\rho_o) \exp(-\kappa\chi) \qquad (2)$$

For the air gap region:

$$\rho_a C_a \left(\frac{\partial T_a}{\partial t}\right) = k_a \left(\frac{\partial^2 T_a}{\partial x^2}\right) \qquad (3)$$

---

* This approximation shall be used in a subsequent modelling analysis of the temperature response of irradiated skin.

For the skin:

$$\rho_s C_s \left(\frac{\partial T_s}{\partial t}\right) = k_s \left(\frac{\partial^2 T_s}{\partial x^2}\right) \tag{4}$$

Boundary conditions between the system components would be coupled; but the coupling effects, convective heat transfer on the fabric boundaries, are negligible when compared with ignition time test radiant heat intensities, both incident to the fabric front-face and transmitted at the back-face. Comparing fabric front-face temperatures with heater element temperatures, radiant emissions by the fabric are negligible [6]. At the skin surface, conductive heat exchanges between air and skin would be negligibly small in comparison the transmitted radiant energy.

The resulting simplified boundary conditions are uncoupled between the different components of the system.

at $x = o, \delta$;

$$\frac{\partial T}{\partial x} = 0 \tag{5}$$

at $x = x_s$,

$$- k_s \left(\frac{\partial T_s}{\partial x}\right) = q_i'' \, (1 - \rho_o) \exp(-\kappa\delta) \tag{6}$$

and for $x \to \infty$,

$$T(\infty, t) = T_o \tag{7}$$

The initial condition,

$$T(x,o) = T_o \tag{8}$$

In order to develop a more usable solution, the modelling equations will be reduced to dimensionless form by incorporating the following non-dimensional groups, previously applied by Wulff, Zuber et al. [2].

$\theta = (T - T_o)/T_o$ normalized temperature

$F = (\alpha t/\delta^2)$ Fourier Number

$I_o^* = q_i'' (1 - \rho_o)\ \delta/k\ T_o$ non-dimensional heat flux ratio

$X^* = (x/\delta)$ relative position

$Bi = (h\delta/k)$ = Biot Number

Installing these relationships into the governing equations and boundary conditions for the fabric,

$$\frac{\partial\theta}{\partial F} = \frac{\partial^2\theta}{\partial X^{*2}} + I_o^* \kappa^* \exp(-\kappa^*) \tag{9}$$

$$\left\{\left(\frac{\partial\theta}{\partial X^*}\right)_{X^* = 0}\right\} = 0 \tag{10}$$

$$\left\{\left(\frac{\partial\theta}{\partial X^*}\right)_{X^* = 1}\right\} = 0 \tag{11}$$

$$\theta(\infty, F) = 0 \tag{12}$$

$$\theta(X^*, 0) = 0 \tag{13}$$

The energy incident to the skin,

$$\left\{\left(\frac{k_s}{k}\right)\left(\frac{\partial\theta_s}{\partial X^*}\right)_{X^* = X_s^*}\right\} = -\ I_o^* \exp(-\kappa^*) \tag{14}$$

These equations and relationships can be solved by Fourier transformation techniques.

A finite cosine Fourier transformation leads to a solution for the transient temperature variation across the fabric. For the particular case of no conduction into the fabric front-face, the solution, as reported by Wulff, Zuber et al. [2], is:

$$\theta\,(X^*,F) = I_o^* F[1 - \exp\,(-\kappa^*)] +$$

$$2 \sum_{n=1}^{\infty} \left\{\frac{1}{n\pi}\right\}^2 I_o^* [1 - (-1)^n \exp\,(-\kappa^*)] \left\{ \frac{1 - \exp\,(F[n\pi]^2)}{1 + \left[\frac{n\pi}{\kappa^*}\right]^2} \right\} \cos\,(n\pi X^*)$$

The first term in this equation represents the mean temperature rise within the fabric. The infinite series accounts for variation across the fabric thickness.

Equation (15) was evaluated by a short FORTRAN computer program for $0.40 < I_o^* < 8.00$ and for $0.20 < \kappa^* < 0.35$. These values cover the ignition time test conditions. The results for $\kappa^* = 0.23$, 0.29, and 0.35 were plotted in Figure 14 as representative of the test ranges.

4.3.2 Diathermanous Model Evaluation

The diathermic model predicts to almost constant temperature across the fabric thickness for the case of thin cloths. Figure 14 and Figure 15 present fabric front-face and back-face temperature response for $I_o^* = 0.60$ and $I_o^* = 5.00$, respectively. As shown in the plots, for optical thickness no greater than in the ten tested fabrics, $0.20 < \kappa^* < 0.35$, front and back surface temperatures are almost identical.

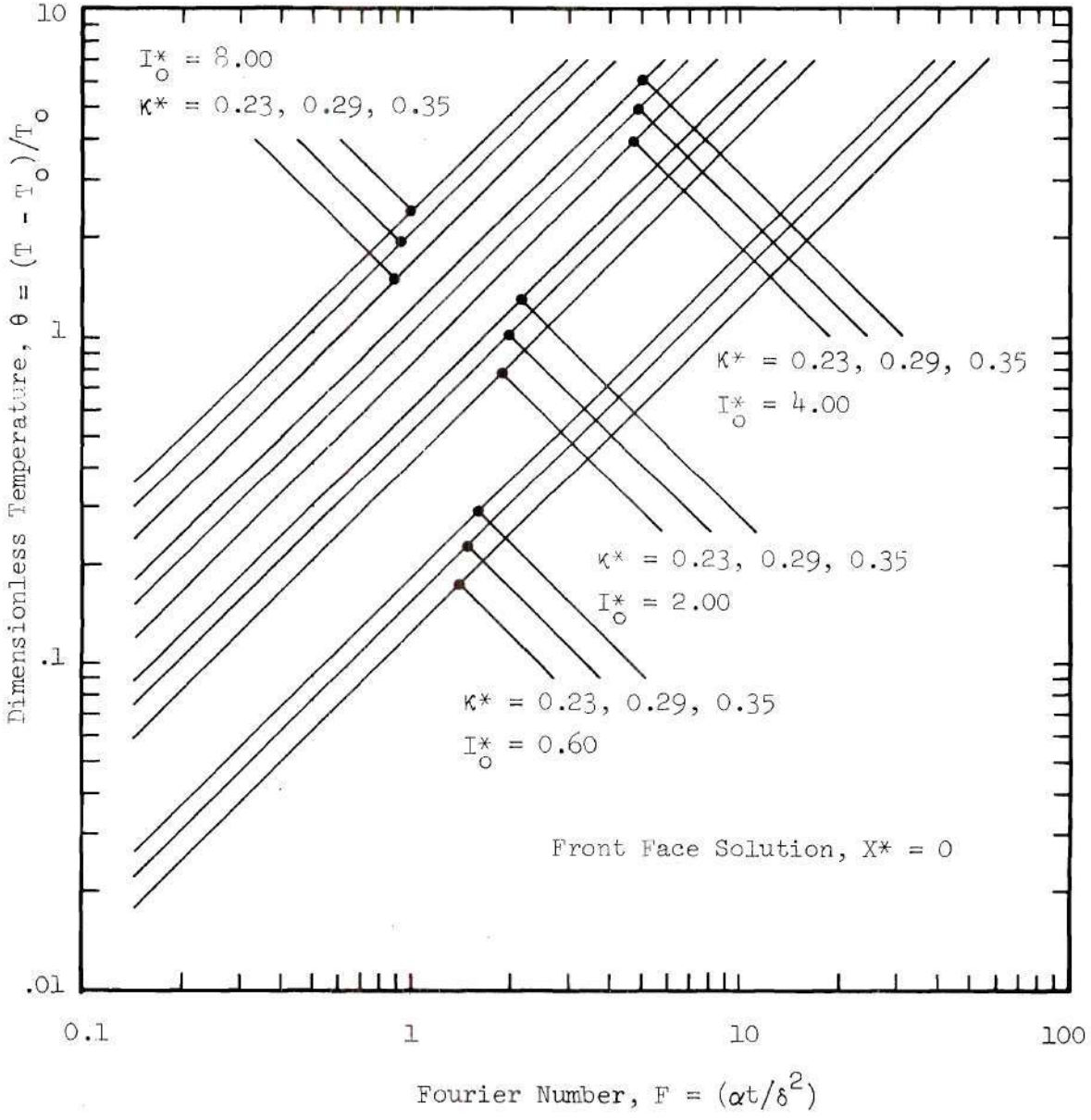


Figure 14. Temperature Response of Fabric Front Face According to the Diathermanous Fabric Ignition Model.

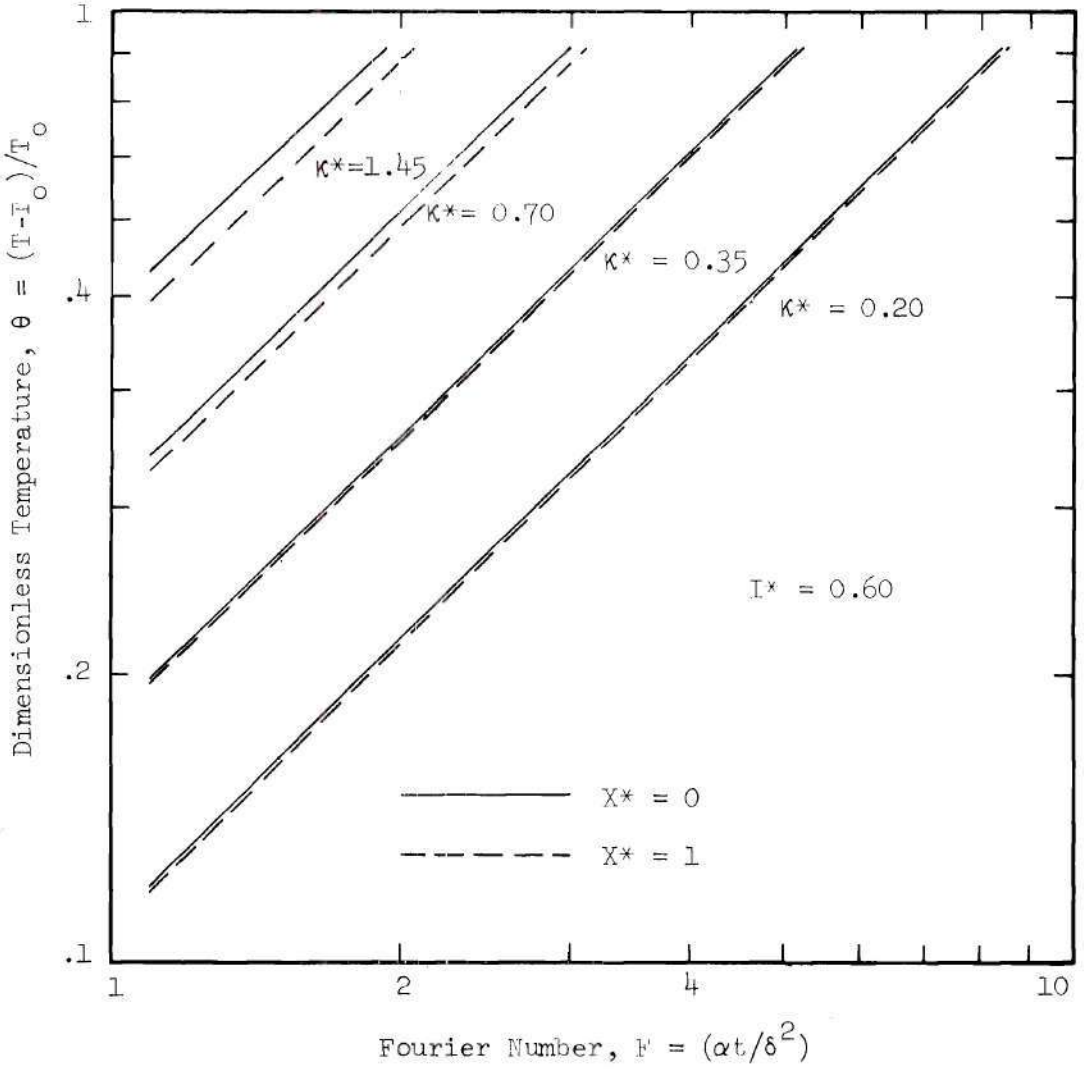


Figure 15. Diathermanous Model - Comparison of Front and Back Face Results for Minimum Test $I^*_o$.

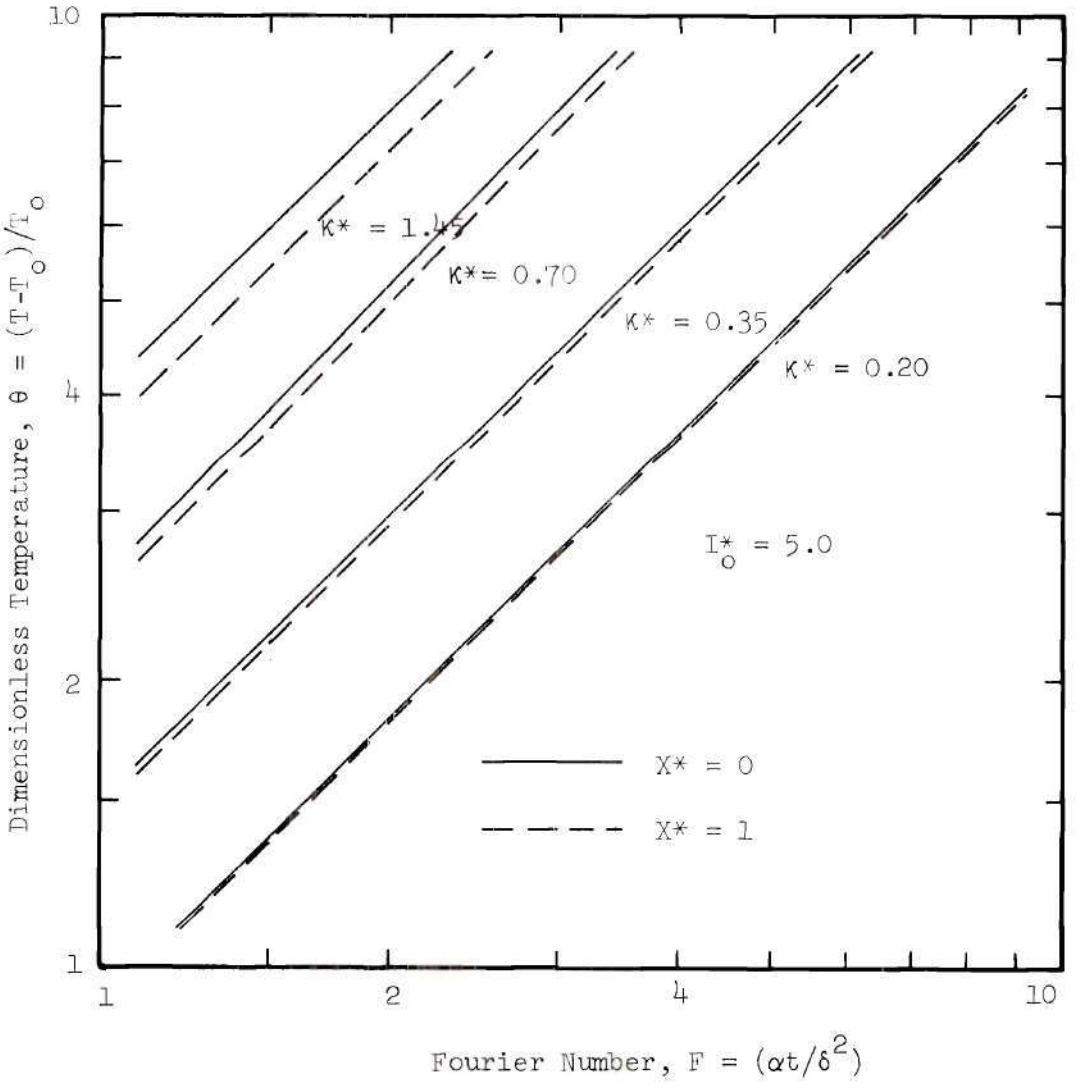


Figure 16. Diathermanous Model - Comparison of Front and Back Face Results for Maximum Test $I^*_o$.

The temperature uniformity indicates that with an ignition temperature criterion, fabric ignition would occur throughout the fabric thickness virtually simultaneously. Any region in a combusting fabric not ignited spontaneously would undergo pilot ignition. For the case of melting cloths, if fabric composition be absolutely invarient, then melting would begin at the fabric front face. However, the time difference between onset of front-face melting and onset of back-face melting would be negligible.

The analytical predictions of ignition time and time to onset of melting are plotted in Figure 17 and Figure 18 for Fabrics 2, 5, 8, 13, 18 and 19 along with the experimental results. These fabrics exhibit better correlation between analytical predictions and experimental results than do the remaining four. For each of these fabrics except the fire retardant flannel (Fabric 19), predicted ignition (or melting) times are less than the measured. Results for the unplotted fabrics are also conservative.

Model predictions approach experimental results as higher heating rates are imposed. One reason that the model becomes more accurate at greater heating rates is that the assumption of negligible convenction becomes more accurate [4]. Temperature uniformity across the fabrics indicates that an assumption of negligible convection must be applied at both faces. In the original assumption, the front-face convection was neglected because the ratio of convective heat loss, H, on fabric front-face to the incident heat flux, $q_1''$, was assumed to be negligible. However, due to temperature uniformity, the neglected convection is almost double the anticipated value. Natural convection heat losses, $H \sim 2(T-T_o)$,

at the anticipated maximum surface temperatures would range from 800 to 1200 (Btu/hr-ft$^2$). For the lower test heating rates, total losses by free convection could approach 10 per cent of the indicent heat. At the higher heating rates, however, the assumption of negligible convection is less inaccurate [55].

Values of optical properties inaccurate for the test conditions would reduce model accuracy. It was noted that fabric transmittances measured during this study were less than transmittances measured optically and reported by Wulff, Zuber et al. However, reducing fabric transmittance with constant reflectance would increase the energy absorbed by the fabric. Increased absorption would cause quicker ignition (or melting).

Another effect not considered, which might delay ignition, is porous weave. The fabrics not plotted in Figure 17 or Figure 18 for comparison between theory and experiment, are woven like screen wire. The resulting transparency apparently is incorporated into the optical thickness and fabric transmittance. However, these fabrics are so antisotropic that the modelling assumption that they be diathermanous isotropic slabs is inaccurate.

As evidenced by the evolution of combustible gases and smoke before ignition, ignition time depends strongly on pre-ignition chemical reactions. The Fabric Flammability program at Georgia Tech has continued development of more accurate fabric ignition models. The effects of pre-ignition pyrolysis and free convection have been included in recent modelling efforts [4].

## 4.4 Conclusion

Overall, the diathermanous slab model of the fabric ignition

process is more accurate than the conducting opaque slab model. In all tested fabrics except the fire retardent flannel (Fabric No. 19), the predictions were conservative, that is, predicted ignition sooner than actually occurred. Therefore, the analytical predictions could be applied to derive some sort of time to danger prediction which actually would be less than the real time to danger.

The model conservatism was expected. Simplifications necessary to solve the mathematics were chosen consistent with engineering practice such that the model solution would yield the most unfavorable answer possible. The real situation, beyond doubt, would be more favorable. As shown in the comparison of theory and experiment, at low heat fluxes, the model becomes unrealistically conservative.

The rather extended period of exposure required to produce fabric ignition, during which time underlying skin is being heated, brings up a curiosity about skin response to heating. Modelling the ignition of garment fabrics, divorced from the variables of clothing users, is a partial solution at best. The human factor must be considered before final judgements about the ignition of clothing can be made. It is conceivable that a clothing wearer would never tolerate an exposure sufficiently extended to permit his garments to ignite. These doubts encourage an investigation into the total system of man plus garment.

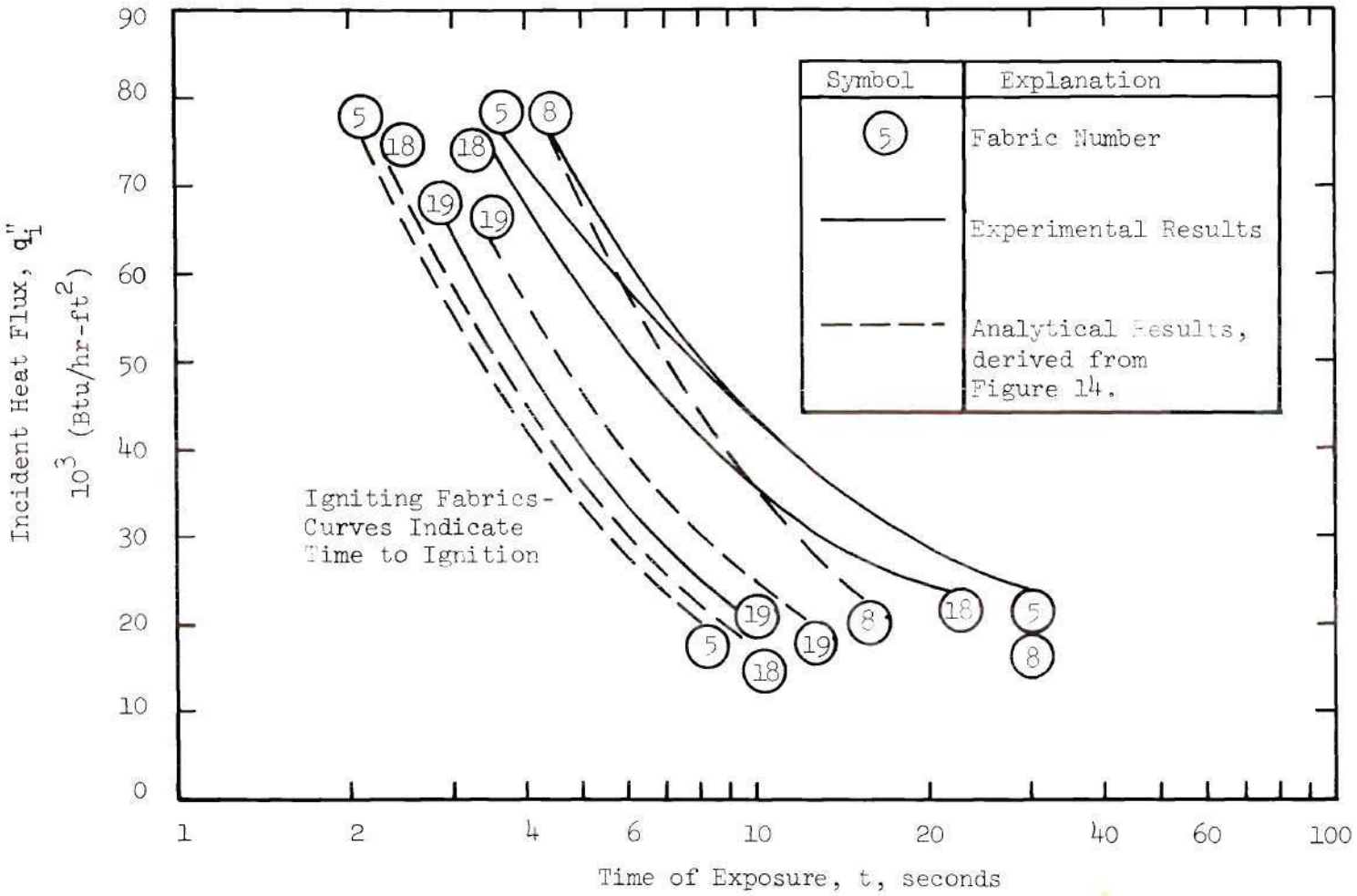


Figure 17. Diathermanous Model - Comparison of Theory and Experiment for Igniting Fabrics.

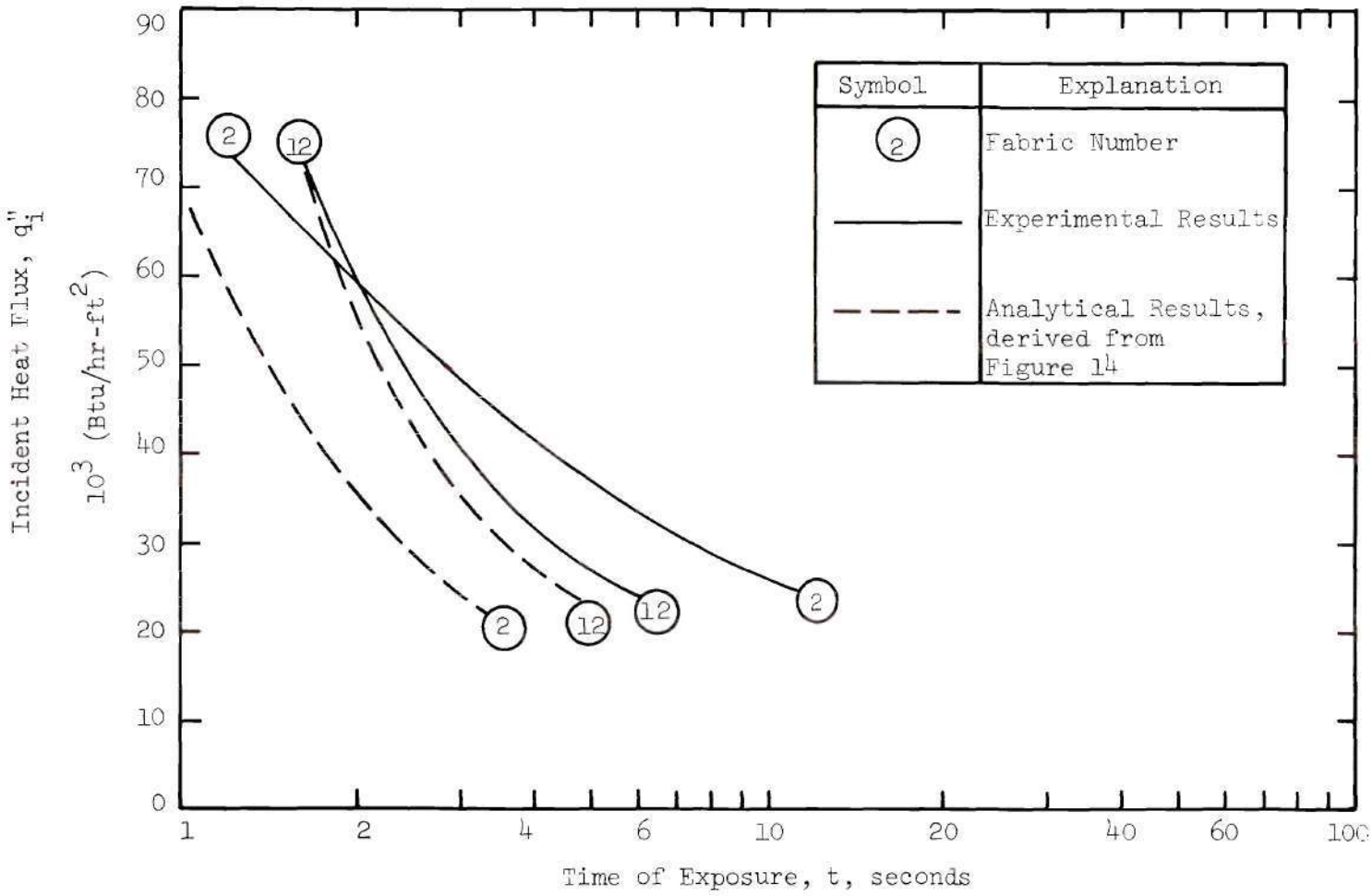


Figure 18. Diathermanous Model - Comparison of Theory and Experiment for Melting Fabrics.

# CHAPTER V

# BURN INJURY ANALYSIS

## 5.1 Introduction

Wulff, Zuber et al. [1 - 4], and Kalelkar and Kung [6 - 8] have analyzed the fabric ignition process to determine the probability of danger. The assumption is that burn injury is contingent upon fabric ignition. Conversely, Stoll, Chianta, Munroe, and others [43, 52, 53, 59 - 63] have analyzed that measure of protection from heat sources provided a man by the woven fabrics he wears. This contrast in concern raises the fundamental question of whether or not a man exposed to a high energy heat source will be injured because his garments ignite or because his clothes give insufficient protection to prevent skin damage prior to ignition.

To explore this question of physiological danger, the nature of burn injury as well as human response to heat stimuli must be investigated. This chapter includes a biological description of human skin and thermal damage to skin tissue, a thermal modelling analysis of skin as a semi-infinite conductor, and discussion of human reaction to noxious stimuli. This information is used then to develop the concept of degree of thermal protection provided by the typical fabrics tested in the present study.

## 5.2 Biological Description of Skin Structure and Cutaneous Burn Injury

Human skin can be described as the outer-most protective covering

of the body and comprises approximately 6 per cent of total body weight. Skin thickness varies from 1/2 to 5 mm with a usual value of 1 or 2 mm [43]. Without skin, the fluid environment of the body cell structure could not be maintained. For the human, whenever as much as 40 per cent of the skin has been destroyed, the life of the injured individual is in grave jeopardy [43].

Before presenting a development of mathematical formulations by which to describe thermal injury and heat sensation, the biology of human skin is presented to form a basis for the necessary modeling assumptions. Figure 19 presents the nomenclature of human skin.

### 5.2.1 Skin Layers

Of the two layers of human skin, the deeper fibrous layer is the dermis (or corium) while the superficial, cellular layer is termed epidermis. The dermis includes both elastic and non-elastic fibers. Elastic fibers produce skin pliability and provide skin resistance to deformation. Adjacent to the epidermis, the dermis is grossly irregular and generally corrugated. The epidermis conforms in outline to those dermal corrugations (papillae), and resulting ridges, in the hands, for example, increase grasping efficiency while forming the surface ridges known as finger points. Dermal cells become progressively less densely packed in the deeper regions, and no clear cut line of demarcation separates the dermis from the loose internal fatty tissue.

### 5.2.2 Nails and Hairs

These elements differ considerably from the dermis and epi-

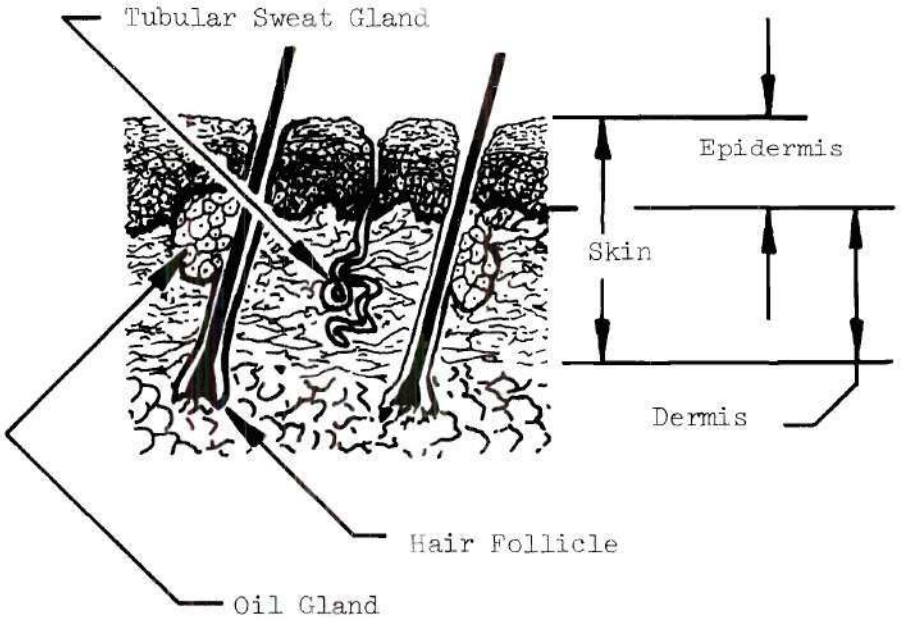


Figure 19. Schematic Drawing of Human Skin Structure.

dermis but are developments from skin tissue. While nails provide protection for the sensitive digital tips, hairs form part of the sensory perception mechanism.

Hairs begin as tubular down-growths of the skin layers. These down-growths reach past the dermis into underlying tissue to form hair follicles. From the follicles, hairs grow outward past the skin surface. At the bottom of each follicle, numerous sensory nerve fibers are terminated. Hair growth patterns vary considerably between the sexes and between individuals of the same sex. Different types of hair, course, fine or intermediate, cover all portions of the body except soles of the feet, palms of the hands, and moist mucus membraneous regions of the body such as lips. Hair color is determined by the amount of the pigment, melanin, in the follicles [12].

5.2.3 Oil and Sweat Glands

Above the hair follicles, closer to the skin surface and adjacent to each hair shaft, oil glands (sabaceous glands) lie in the dermis to provide oils for skin and hair. Tubular sweat glands also are situated in the skin structure. These glands are highly coiled delicate tubes lying deeper in the dermis than the oil glands. Long sweat ducts extend to the skin surface along irregular courses. Sweat glands are distributed all over the entire body skin, but are particularly large and numerous in groin and underarm areas. Sweating is an important aid to the lungs and kidneys in the elimination of excess quantities of water and salts [12]. The processes of sweating also are a vital function in the

regulation of internal body temperature.

5.2.4 Fluid Flow Networks Within Skin

Blood vessels in skin terminate in the dermis such that the epidermis is essentially avascular [42]. Arteries are located in the under skin fatty tissues; and, from those arteries, two networks of arterioles are formed. The first network lies in the deepest sections of the dermis, the other just below the papillae which form that irregular junction between dermis and epidermis. From that second arteriole network, capillaries connect to the papillae forming the outermost vascular tissue layers [12].

Arterioles are blood networks similar to the arteries* but which expand or contract to regulate the quantity of blood delivered to a capillary field [12]. This blood flow regulation is accomplished according to functional activity, tissue temperature, and sometimes emotional situations, for instance, blushing or the blanching of fear [12].

An average capillary is not much more than a millimeter in length with an internal diameter just large enough to permit passage of red blood cells in single file. Interchange between blood plasma and tissue fluids is accomplished such that blood emerging from a capillary network has delivered oxygen and nutriments to the cells and picked up carbon dioxide and waste products [12].

Another profuse network in the dermis is formed by lymphatic vessels. These dermal networks drain into larger and deeper lympth

* Arteries are passive in nature. Arterial expansion or contraction is a function of blood pressure and artery elasticity.

vessels (lymphatics) which are situated in sub-skin strata of fatty tissue and muscle [12]. Lympth is that colorless fluid drained from the tissue by lympth capillaries forming an alternative pathway for the return of tissue fluid to the blood stream.

5.2.5 Cutaneous Sensory System

The cutaneous nerves end in both skin layers and are particularly numerous around hair follicles. Sensory nerves convey impulses toward the central nervous system, while the organs receiving stimuli are the sensory receptors [10]. Stimuli received from outside the body are received by special and elaborate automical structures. The body can sense stimuli which are perceived as smell, sight, hearing, taste, touch, temperature, and pain [12]. For the stimulus pain, no special end-organs are required since the nakes ends of nerve fibers themselves can receive adequate stimulus directly [28]. The other stimuli require very special end-organs such as taste buds, eyes, etc. for reception.

5.2.6 Sub-skin Structure

Subcutaneous tissue, lying below the skin, is a loose tissue with widely varying fat cell content. The subcutaneous layer of fat, which is almost the rule among well nourished persons, is a storage depot which is consumed whenever food intake does not meet the needs of the individual. Generally, subcutaneous tissue is loose, but in some areas it is dense and tough to moor the skin to underlying bone and muscle [12].

5.2.7 Cutaneous Burn Injury

Skin destruction by heating is a complex occurrence wherein

body protective mechanisms are overwhelmed by the incident heat. The terms first, second, third and fourth degree burns indicate progressively more severe thermal injury.

Heating the skin at rates sufficient to raise sub-surface temperatures to levels considerably in excess of normal, leads to a series of local reactive changes. The severity of those changes is a function of the degree and duration of temperature elevation [29]. Changes that occur at some given depth below the surface of the exposed skin are determined by the severity of heating and by the nature of affected cell structure.

The mildest forms of heat induced epidermal injury do not involve recognizable alternation to cell structure. Such injuries are reversible, and the time required for reverting to normal cell state increases with the time required for injury production [29].

The earliest visable evidence of thermal injury to the epidermis is redistribution of the cell fluid chromatin within cell nuclei coupled with a swelling of the epidermal cell nuclei. Further injury results in disintegration of protoplasm within the basal cells and swelling of nuclei throughout the epidermal thickness [29]. These alternations impair attachment of epidermis to dermis such that friction or even collection of edema fluids* can cause detachment and blisters.

When a thermal exposure is sufficiently severe to cause a

---

* Edema fluid is clear liquid resembling blood plasma which floods heat damaged tissue. The liquid in a skin blister is this fluid.

progressive rise in subsurface temperature, transepidermal coagulation will occur. When the epidermal temperature is increased rapidly to about 55°C (131°F), coagulative changes may even mask both nuclear swelling and protoplasm disintegration. Further increases in temperature will produce progressive desiccation and, eventually, carbonization of the epidermal cells.

The first change in the dermis due to heating is a constriction of superficial blood vessels. Ordinarily, the constriction will be followed immediately by vasodilation.* Under extremely severe heating, though, the superficial vessels become permanently fixed in the initial constricted state. Vasodilation occurs only at deeper levels where temperature rise is less severe [29]. That vasodilation leads to increased vascular permeability, edema fluid collection, and the formation of blisters.

Human skin sensitivity to pain, pressure, temperature and heat exposure is very consistent among all persons regardless of race, age or sex. In addition, the thermal properties of human skin are very nearly the same among all persons. These consistencies and similarities enhance the feasibility and accuracy of mathematically modeling the processes of skin response to hyperthermic episodes [32].

## 5.3 Thermal Models of Human Skin

In the preceding section, a general biological description of human skin has been presented. Skin biological factors will be

* Vasodilation is the involuntary expansion of arteriole networks to flood a tissue area with protective fluid.

applied to justify approximations required in the ensueing developments of thermal skin models.

Human skin temperature response can be modeled by approximating the skin as a semi-infinite one-dimensional conducting body. Burn injury and pain perception are described in terms of protein destruction rate processes. Before defining any actual models, a discussion of the modelling parameters, thermal and optical properties of skin, is appropriate.

### 5.3.1 Thermal and Optical Properties of Human Skin

Almost all thermal and optical properties of human skin are difficult to measure accurately and vary considerably with changes in the physiological and physchological states of the tested individual. However, repeated testing demonstrates that variations between individual human beings are probably less than variations between different positions on the same human body [38, 41, 42, 43, 45]. Accurate measurement of thermal or optical properties in living skin is a difficult process. Generally, the property values are drawn by inference from experiment.

Thermal and sensory detectors within human skin are part of an efficient feedback control system which regulates the cutaneous blood flow system. The thermal properties of skin are adjusted by this involuntary skin sensor system and by voluntary cortex controls to protect the skin and the entire body from hazardous environments [43]. Local cooling generates vasoconstriction, arteriole contraction, and consequently decreases blood flow to the skin. Conversely, local heating causes vasodilation, flooding the heated skin in an attempt

to inhibit skin temperature rise to injurious levels. Prolonged local heating also brings about sweating on the heated area and adjacent non-heated areas. More intense heating may stimulate the sensations of pain and cause reflex withdrawal of a limb or even the entire body [9, 11, 43].

Thermal conductivity (k), density ($\rho$), and specific heat (C) are each affected severely by cutaneous blood flow. Generally, values stated in the literature for each of these thermal properties are derived from measurements of that product ($k\rho C$), termed the thermal inertia, and the thermal diffusivity ($\alpha = k/\rho C_p$).

The thermal inertia has been found to vary between $90 \times 10^{-5}$ and $400 \times 10^{-5}$ $\{(cal)^2/(cm)^4(sec)(^oC)^2\}$ depending upon prevailing physiological, physical, and physchological conditions [38, 42].* During any heating incident, the thermal diffusivity of skin remains very nearly constant. Similar increases occur in both thermal conductivity and heat capacity, with increased blood flooding [27,31,41, 44] such that the ratio of these quantities is virtually constant. During incidents of high intensity, short duration hyperthermic episodes, the mechanisms of vasodilation and local tissue flooding do not have time to develop [38,40,41], and thermal diffusivity, therefore, is even more nearly invarient.

Stoll [42] reports skin thermal diffusivity to be $7 \times 10^{-4}$ $(cm^2/sec)$. Values reported for the thermal conductivity, density and

* Lipkin and Hardy [38] report $(k\rho C) = 90 \times 10^{-5} - 100 \times 10^{-5}\{(cal)^2/(cm)^4(sec)(^oC)^2\}$ for exposures less than 20 seconds.

specific heat of skin are:

$$k = (8.0) \times 10^{-4} \left\{ \frac{cal}{cm\text{-}sec\text{-}^{o}C} \right\} \text{ excised epidermis} \quad [57]$$

$$k = 8.8 \times 10^{-4} \left[ \frac{cal}{cm\text{-}sec\text{-}^{o}C} \right] \text{ dermis} \quad [42]$$

$$C_p = 0.8 \left\{ \frac{cal}{gm} \right\} \text{ excised} \quad [43]$$

$$\rho = 1.20 \left\{ \frac{gm}{cm^3} \right\} \text{ excised} \quad [38]$$

Human skin is very nearly a black body radiator [21]. Skin pigmentation has little or no bearing upon the magnitude of skin emissivity [22,23,31,32,46]. These qualities have permitted development of various radiometric devices for the measurement of skin temperature, and for the mapping of the entire body surface by thermography [22,23,43,46,48,49]. Skin absorptivity has been found to be essentially invariant with pigmentation, and approximately equal to skin emissivity [41].

By restricting the analysis to cases of exposures sufficiently intense to induce tissue damage within 40 seconds, a one-dimensional conduction model is an accurate approximation to human skin. Skin burn injury models can be developed on the basis of chemical rate

processes. Both techniques have generated models which agree with experimental physiological data [41,44].

5.3.2 Skin Temperature Response to Intense Thermal Radiation

In view of the complexity of human skin, a general solution to the temperature-time relationship for skin exposed to intense radiant heating is impossible. However, a first approximation to the temperature history can be developed by imposing sufficient restrictions and approximations to permit solutions of the Fourier heat conduction equation:

$$\frac{\partial}{\partial x}\left(k_x \frac{\partial T}{\partial x}\right) + \frac{\partial}{\partial y}\left(k_y \frac{\partial T}{\partial y}\right) + \frac{\partial}{\partial z}\left(k_z \frac{\partial T}{\partial z}\right) = \rho C_p \left(\frac{\partial T}{\partial t}\right) \qquad (1)$$

Imposed initial and boundary conditions must be consistent with a skin heating incident.

The following assumptions and approximations reduce the above equation to tractable form:

(1) Human skin is assumed to be a solid conducting body composed of thermally isotropic homogeneous material. This assumption is quite accurate in avascular regions where tissue structure is a monotonous repetition of similar cells. Hairs, sweat glands and oil glands break up the homogeniety where they are located; but, generally, non-homogeneous regions occupy a rather small portion of the total volume of material under consideration.

(2) All thermophysical properties are assumed invariant with position and time. As discussed in the previous section, this approx-

imation is accurate for short-term exposures to high heat fluxes.

(3) The area exposed to heating is assumed sufficiently large that heat flow is one-dimensional. As discussed in the biological descriptions, skin is relatively thin. Therefore, the assumption that heat flow is normal to the surface is quite accurate.

(4) Skin is assumed to be an opaque solid not penetrated by the incident radiation. According to Oppel and Hardy [18], 90 per cent of far infrared radiation ($\lambda > 3\mu$) absorbed by human skin is absorbed within 0.05 mm of the surface. Furthermore, skin will be considered a black body. The emissivity, $\varepsilon$, of human skin at these wavelengths has been measured at $0.989 \pm 0.010$ [21,23]. For shorter wavelengths ($\lambda < 3\mu$), skin emissivity is only 0.25 with 50 per cent of the absorbed energy absorbed within 0.50 mm [18]. A "red hot" electric stove ($T = 1000^{\circ}K$) emits in the infrared ($\lambda > 2\mu$) with most of the energy in the higher ranges ($\lambda > 3\mu$) [23].

(5) Skin surface is assumed to be at some initial temperature,

$$T_{so} = T(0,0)$$

which exceeds the ambient temperature. Typical values of surface temperature range from $28^{\circ}C$ to $35^{\circ}C$ for a normally clothed both in room temperature ($23 - 26^{\circ}C$) environments [22,26,34,43]. During a thermal exposure incident, the ambient temperature is assumed constant. Heat losses by the body to the environment by mechanisms other than convection are assumed negligibly small. In addition, during a skin heating episode, the convective heat transfer coefficient between the

skin and atmosphere will be assumed constant.

(6) A linear temperature gradient is assumed to exist through the skin layers prior to onset of heat exposure.

$$T(x,t)\Big|_{t \leq 0} = T_{so} + \gamma x$$

where:

$$\gamma = \text{constant}$$

This gradient is maintained by internal heat generation due to body metabolism. This heat is dissipated to the environment.

(7) The heating incident is modeled as a step function input of radial energy beginning at zero time.

$$\frac{\partial T(x,t)}{\partial t} = \frac{k}{\rho C_p} \frac{\partial^2 T(x,t)}{\partial x^2} = \alpha \frac{\partial^2 T(x,t)}{\partial x^2} \tag{2}$$

Referring to Figure 20, the initial conditions are:

$$T_{so} = T\ (0,0) \tag{3}$$

$$H_o = h\ (T_{so} - T_o) = k \frac{\partial T}{\partial x} \tag{4}$$

$$T(x,0) = T_{so} + \gamma x \tag{5}$$

Referring to Figure 21, the exposure conditions are:

$$T_s = T(0,t) \tag{6}$$

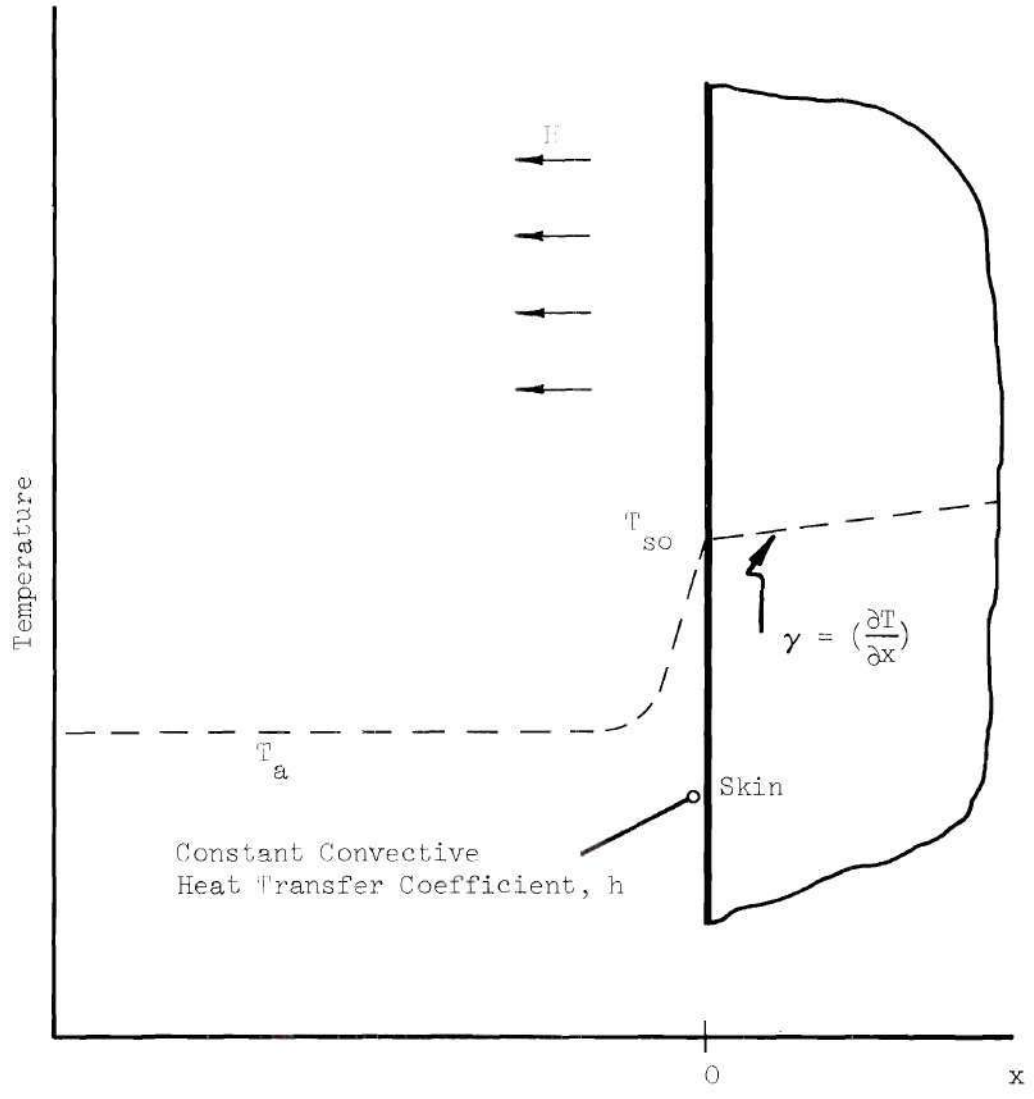


Note that the boundary condition at $x \rightarrow \infty$ is ignored.

Figure 20. Skin Temperature Response Analysis - Initial Conditions.

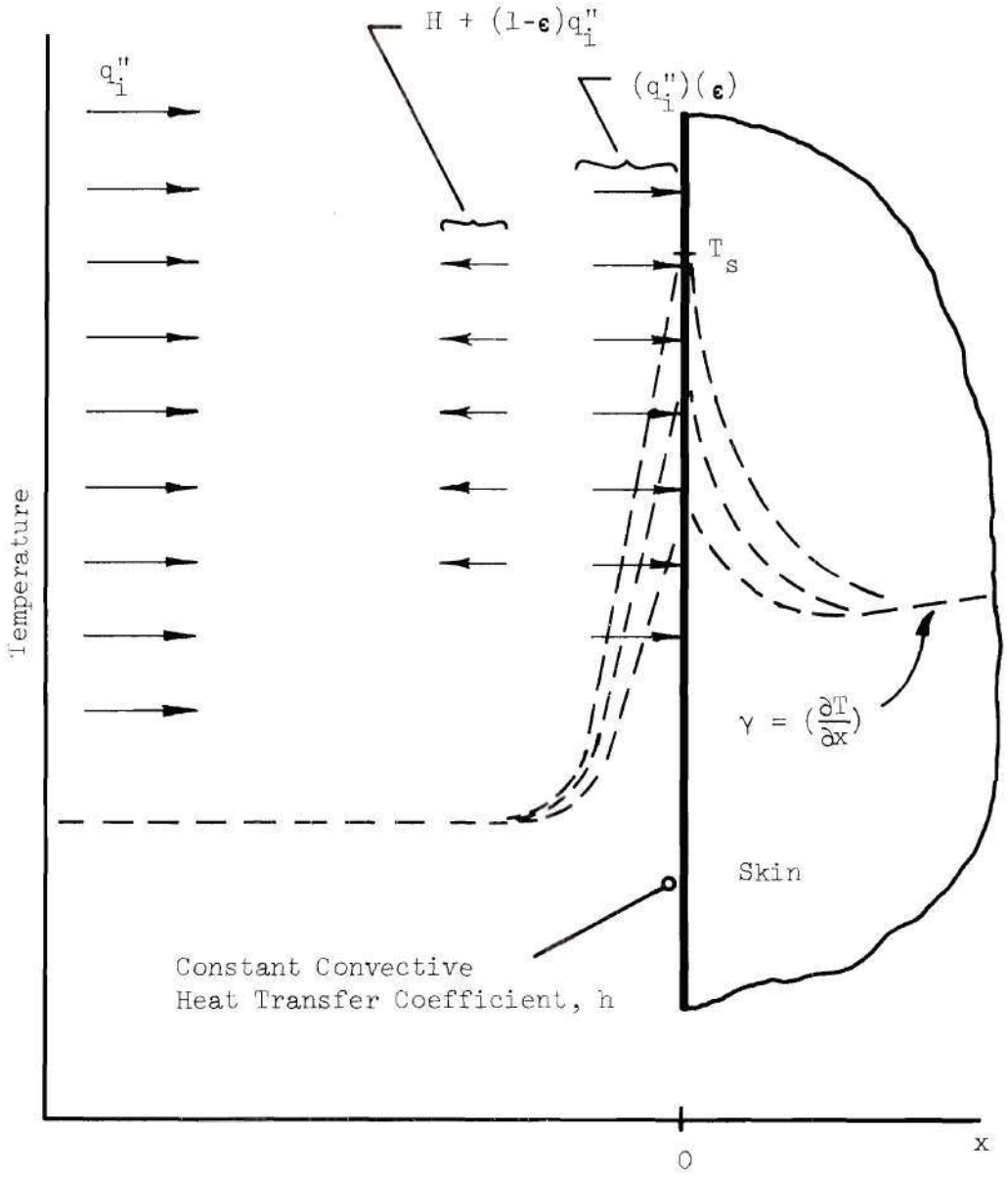


Note that the boundary condition at $x \rightarrow \infty$ is ignored.

Figure 21. Skin Temperature Response Analysis - Exposure Conditions.

$$H = h(T_s - T_a) > H_o \tag{7}$$

$$\varepsilon q_i'' - h(T_s - T_a) + k\left[\frac{\partial T}{\partial x}\right]_{x=0} = 0 \tag{8}$$

Applying methods of Laplace transformations [16], equation (2) can be written:

$$sT(x,s) - T(x,0) = \alpha \frac{d^2T(x,s)}{dx^2} \tag{9}$$

Introducing equation (5) into equation (9):

$$\frac{d^2T(x,s)}{dx^2} - \left(\frac{s}{\alpha}\right) T(x,s) = -\frac{1}{\alpha}\left(T_{so} + \gamma x\right) \tag{10}$$

The complimentary solution is given by:

$$[T(x,s)]_C = C_1 \exp\left\{\sqrt{\frac{x^2 s}{\alpha}}\right\} + C_2 \exp\left\{-\sqrt{\frac{x^2 s}{\alpha}}\right\} \tag{11}$$

The steady state solution is:

$$[T(x,s)]_{ss} = \frac{T_{so}}{s} + \frac{\gamma x}{s} \tag{12}$$

And the general solution is then:

$$T(x,s) = \frac{T_{so}}{s} + \frac{\gamma x}{s} + C_1 \exp\left\{\sqrt{\frac{x^2 s}{\alpha}}\right\} + C_2 \exp\left\{-\sqrt{\frac{x^2 s}{\alpha}}\right\} \tag{13}$$

Since

$$\lim_{s \to \infty} \{T(x,s)\} = 0$$

then

$$C_1 = 0$$

Evaluating $T(x,s)$ at $x = 0$:

$$C_2 = \frac{\epsilon q_i''}{h} \left\{ \frac{\sqrt{\frac{\alpha h^2}{k^2}}}{s\left( \sqrt{\frac{\alpha h^2}{k^2}} + \sqrt{s} \right)} \right\}$$

Equation (13) can be transformed directly back to the time plane by expressions given in Appendix 3 of Reference [16]. The resulting rather cumbersome equation seldom is used in thermal radiation experiments. Instead, the case of negligible convection is used ($h/k \cong 0$). Equation (13) thus can be simplified to:

$$T(x,s) = \frac{T_{so}}{s} + \frac{\gamma x}{s} + \frac{\epsilon q_i''}{k} \left[ \frac{\exp\left\{-x\sqrt{s/\alpha}\right\}}{s^{3/2}} \right] \qquad (14)$$

The inverse transformation is now readily stated:

$$T(x,t) = T_{so} + \gamma x + \left(\frac{2\varepsilon q_i''}{k}\right)\sqrt{\frac{\alpha t}{\pi}}\ \exp\left(-\frac{x^2}{4\alpha t}\right) \qquad (15)$$

$$\left(\frac{\varepsilon q_i''}{k}\right)\ \text{erfc}\ \left(\frac{x}{2\sqrt{\alpha t}}\right)$$

At the skin surface (x = 0) this reduces to:

$$T(0,t) = T_s = T_{so} + \frac{2\varepsilon q_i''\sqrt{t}}{\sqrt{\pi}\sqrt{k\rho C_p}} \qquad (16)$$

This solution has been reported in several references. Numerous researchers have applied the result to evaluate the quantity ($k\rho C_p$) of living skin. Others have published data demonstrating the function describes skin surface temperature response with accuracy on the order of the accuracy of skin surface temperature measurement [38,41,42].

5.3.3 The Significance of Thermally Induced Rate Processes in the Causation of Epidermal Injury

Numerous studies have demonstrated that epidermal injury results whenever the skin sustains sufficiently elevated temperatures over sufficiently extended time periods [27,28,29,43,52,53]. Henriques concluded that chemical rate processes, related to the denaturization of protein, produced the epidermal changes [30].

Development and evaluation of this chemical rate process analysis

require accurate knowledge of three parameters:

(a) duration of exposure

(b) tissue temperatures during the hyperthermic episode

(c) the degree of injury sustained

Skin temperatures can be estimated by computations with equations developed in the previous section using exposure intensity. The other parameters must be evaluated at the time of injury. According to Henriques [30] the following differential equation is applicable:

$$\frac{d\Omega}{dt} = (p)\ \exp\left\{\frac{-\Delta E}{R(T_t + 273)}\right\}$$

where:

$\Omega$ = an arbitrary epidermal injury function evaluated at the skin depth at which tissue temperature is $T_t$.

p = constant of proportionality determined from experimental results ($sec^{-1}$).

R = gas constant = 1.986 (cal/mole - $^{o}C$).

$T_t$ = tissue temperature at some time, t ($^{o}C$).

$\Delta E$ = activation energy for the chemical reactions occurring during thermally induced tissue destruction (cal/mole).

The injury function is given by:

$$\Omega = \int_0^t (p)\ \exp\left\{\frac{R(T_t + 273)}{\Delta E}\right\}\ dt$$

The absolute temperature ($T_t$ + 273) during some burn injury incident will not vary significantly. For exposures of only several seconds, $T_t$ would increase from 35° to perhaps 60°C, representing an absolute temperature change of only 8 per cent. Because the change is small, the temperature $T_t$ can be approximated by an invarient value, T, the steady state temperature. Using this approximation,

$$\Omega = (pt) \exp\left\{\frac{R(T_t + 273)}{\Delta E}\right\}$$

As demonstrated by Henriques and Moritz [27], the steady state temperature of all epidermal layers is approximately equal to the skin surface temperature. Henriques defined the tissue damage function, $\Omega$, to be 1 at the occurrence of complete transepidermal necrosis. For $\Omega$ =1, with convective heating,* Henriques computed the following values:

$$\Delta E = 150{,}000 \text{ (cal/mole)}$$
$$p = 3.1 \times 10^{98} \text{ (sec}^{-1}\text{)}$$

For these values of p and $\Delta E$, $\Omega$ = 0.53 was determined to be the maximum exposure possible without epidermal damage.

Stoll and Greene [42] in a subsequent experimental study,

* Convective heating was accomplished by exposing the skin to a continuous stream of hot water.

using radiant heat inputs, found that Henriques' damage rate function for convective heating was inaccurate for radiant heating episodes. It was theorized that with radiant inputs, the temperature variation through the basal layers of skin was different from the case when energy was convected into the skin. With convective heating, a less severe temperature gradiant was predicted. In addition, Stoll and Greene noted that during high intensity heating less total heat* was required to produce equivalent damage than during lower intensity heating. This phenomenon probably arises from a decreasing effectiveness of body protective mechanisms as heating intensity increases. Consequently, the investigation concluded that the damage rate function, $d\Omega/dt$, is discontinuous. Figure 22 describes variation of $d\Omega/dt$ with tissue temperature for both radiant and convective heat inputs.

An alternate method of evaluating $\Omega$ involves application of the plots in a finite difference technique:

$$\Omega = \sum_{j} \left(\frac{d\Omega}{dt}\right)_j (\Delta t)_j$$

Values of $(d\Omega/dt)_j$ can be read from the damage rate plots for each average temperature, $T_j$, which occurs in the skin during the time

---

* Total heat absorbed by the skin = $\int_0^t \epsilon q_i'' \, dt$

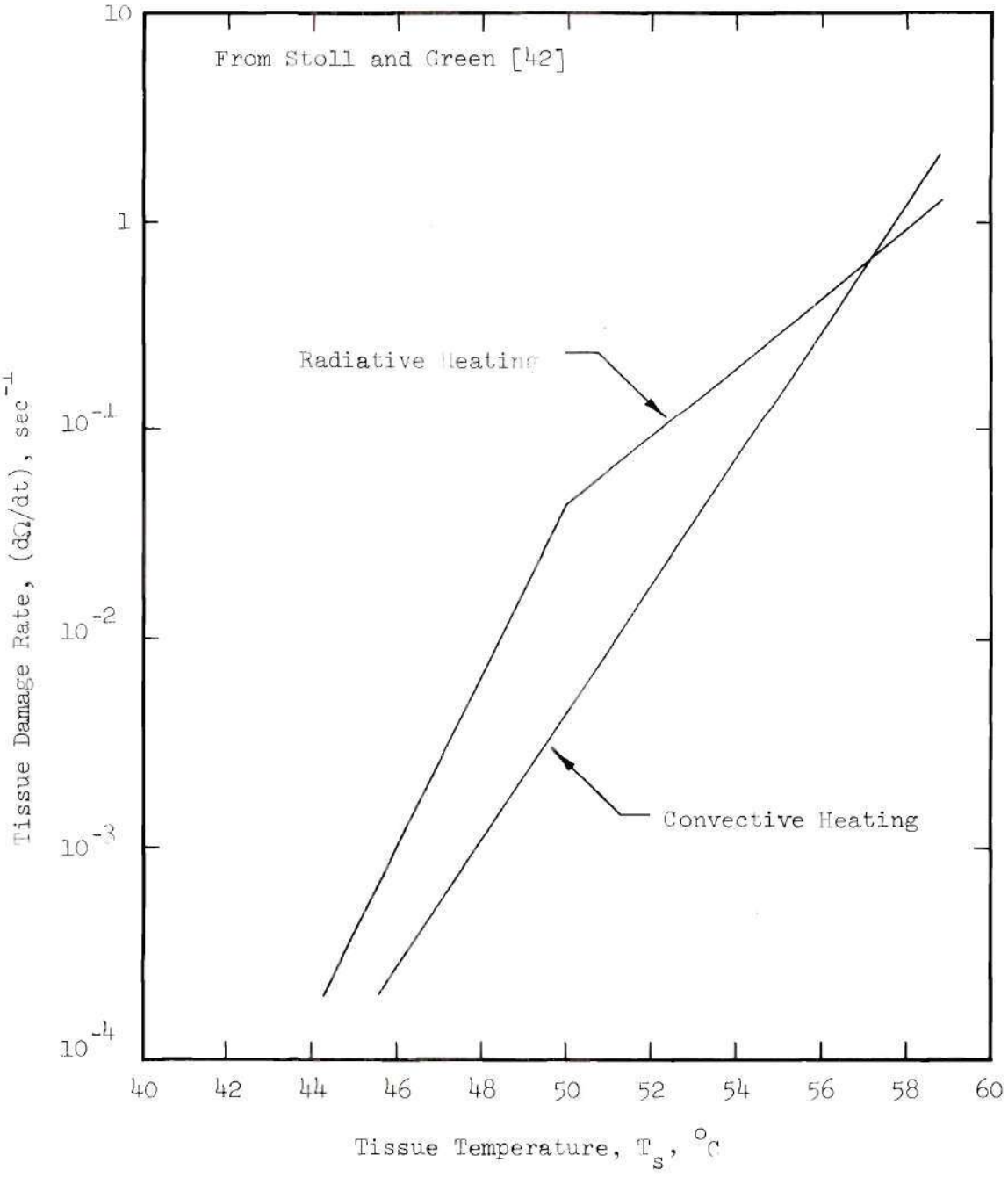


Figure 22. Skin Tissue Damage Rate Versus Tissue Temperature.

period, $(\Delta t)_j$. The skin tissue temperature can be computed from equations developed in the previous section.

Another aspect of tissue damage evaluation, not considered by Henriques, is the fact that significant percentages of total injury often occur after removal of the heat input while the tissue is cooling. For cases of higher tissue temperatures, as much as 35 per cent of total damage occurs during cooling [42]. A temperature - time history for tissue cooling can be developed along the lines of the tissue heating analysis, and the finite difference method continued over the entire period of elevated tissue temperature.

It is possible to damage the basal layers without the injured person feeling pain. This can occur whenever the basal layers of the epidermis are maintained at injurious levels while sensory nerve endings are maintained at sub-threshold levels. Sunburn is a common example of this phenomenon. In cases of heating rates sufficient to produce irreversible epidermal damage in time periods of less than 2 or 3 minutes, however, pain will precede damage [42,43,52].

5.3.4 Cutaneous Pain Sensation

Numerous studies report that pain occurs during "slow" heating incidents when the skin surface temperature has been elevated to approximately 45°C [34,35,43]. Slow heating incidents describe the situation where the temperature at the dermis-epidermis boundary remains very nearly the same as the skin surface temperature. For cases of more intense heating with shorter exposure time, skin surface temperatures as high as 49°C have been tolerated before pain

was reported [42,54]. These differences suggest that temperatures at some sub-surface position evoke pain sensation.

In a study by Stoll and Greene [42], pain receptors* were located at sub-epidermal depths, on the order of 0.18 to 0.24 mm below the skin surface on the forearm. Tissue temperature of 43.2 ± 0.4°C at those depths were reported to cause "pricking pain". Buettner [32] reported that tissue temperatures of 44.8 ± 0.5°C at 0.10 mm below the skin surface produce "unbearable pain". Other studies [34,35] conclude that during slow heating, surface and subsurface tissue down to depths of 0.2 to 0.5 mm achieve almost identical temperatures of roughly 45°C when "pain" occurs. An unsedated human, generally excluding paraplegics,** would become aware of his physiological danger, made aware by sudden local "warmness", before pain would occur. Time to pain, therefore, is a conservative estimate of the time elapse between exposure and awareness.

A number of references [42,45,52] have published time to pain data for human subjects exposed to radiation. Figure 23 summarizes these data. The data were taken from experiments with humans sub-

---

* Pain receptors, as described by Stoll and Greene [42], are sensory organs located beneath the skin surface which when sufficiently stimulated evoke the sensation of pain to the nervous system. These organs are nerve fibers, and evoke pain sensations whenever elevated to sufficient temperature or whenever subjected to sufficient pressure.

** Hardy [45] performed studies on a paraplegic female who, though paralyzed from spinal damage in her lower limbs, reacted for her safety whenever those paralyzed extremities were exposed to radiant energy.

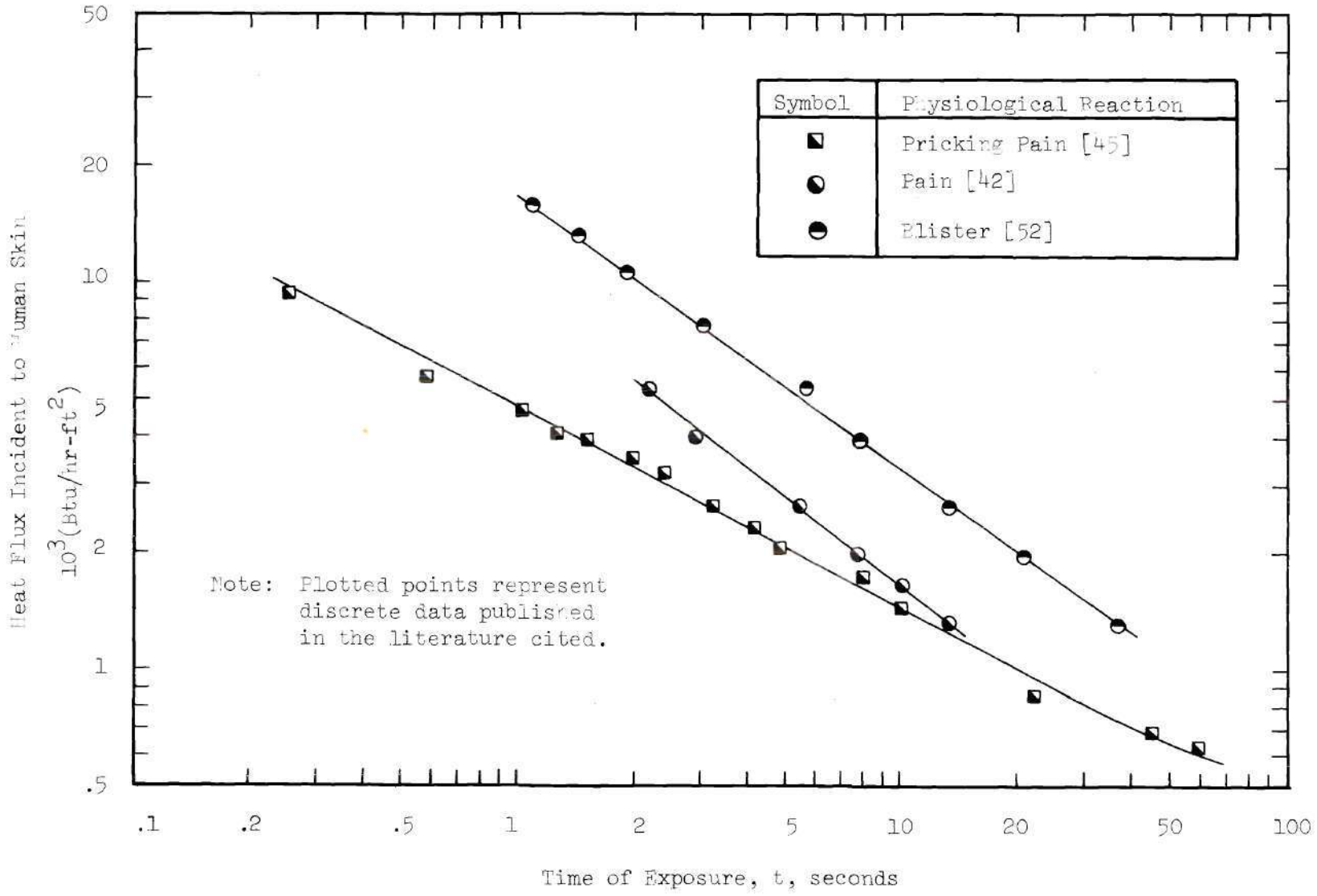


Figure 23. Time to Pain or Burn Injury Versus Skin Heating Rate.

jected to radiant heat incident to a small area of their bare skin. The tested individuals signaled when they felt pain. The time elapse between onset of exposure and report of pain was published as the time to pain for the test incident heat flux intensity.

A theoretical estimate of "time to pain" for thermally irradiated skin can be computed from the skin temperature response functions derived previously in Section 5.3.2:

$$\frac{k}{\epsilon q_i''} \; T(x,t) - T_{so} - \gamma x = 2\sqrt{\frac{\alpha t}{\pi}} \exp\left\{\frac{4\alpha t}{x^2}\right\} - x \operatorname{erfc}\left\{\frac{x}{2\sqrt{\alpha t}}\right\}$$

To evaluate time to pain, assume:

$T(x,t) = 45^{\circ}C$ when pain occurs

$T_{so} = 30^{\circ}C$

$x = 0.2$ mm

$\gamma = 1.1$ ($^{\circ}C$/mm) [41]

$\alpha = 7 \times 10^{-4}$ ($cm^2$/sec) [43]

$k = 8.8 \times 10^{-4}$ (cal/cm - sec - $^{\circ}C$) [57]

$\epsilon = 0.989$ [21]

Table A10 is a comparison between "time to pain" as measured by Stoll and Greene [42] and predictions by the function above. Predicted times in all cases are shorter than the measured, but several factors combine to account for the difference.

Small time elapses almost certainly exist between that instant when sufficient stimulus has occurred to cause pain and any report of

pain from the subject.* Increasing the thermal conductivity, k, of heated tissue will delay painful temperature levels. For example, increasing k from $8.8 \times 10^{-4}$ to $12 \times 10^{-4}$ [cal/(cm-sec-$^{o}$C)], for the case of skin irradiation at 0.20 [cal/cm$^{2}$ - sec], will increase the time to pain prediction from 3.2 to 5.0 seconds. The measured time [42] was 5.5 seconds. Although skin conductivity probably would not increase appreciably during such short duration exposures, the magnitude of k for living tissue, intact within the man, cannot be determined more accurately than the variation above.

## 5.4 Human Reaction Rates

Previous sections have explored questions of "time to pain" and "time to burn injury" by modeling the process of tissue damage. Another crucial parameter to be analyzed is the time required for a person to remove himself from danger once perceived. This time parameter will be termed the "reaction time".

Human reaction time involves two components; the time elapse between danger perception**and onset of movement, constitutes a small portion of the total. Time required for displacement of an endangered member or of the entire body forms the major part.

---

* To report pain, the subject must perform a controlled action, either speaking or somehow otherwise signaling.

** Danger perception is conservatively defined as that instant of pain sensation. Normally, a period of unusual local "warmness" would preceed the sensation of pain.

5.4.1 Time Elapse Before Onset of Movement

Reaction to noxious stimuli can involve either a voluntary action or an involuntary reflex [10]. Voluntary actions require employing the brain to control the motion. Reflex movements are involuntary muscle contractions initiated at nerve centers in the spinal chord before the brain can be notified [11].

Fearing [9] describes reflex actions as being:

(1) involuntary

(2) unlearned

(3) predictable and uniform

(4) not conditioned by consciousness

(5) for a protective purpose

(6) involving the synaptic* nervous system

(7) usually not involving the cerebral cortex

(8) much more rapid than voluntary actions.

The reflex actions are further described as being invariable and "machine-like", and follow a specific set of occurrences. According to Fearing [10], some stimulus will fall on some one or other nervous receptor and cause a nervous impulse. This nervous impulse is transmitted along nerve fibers to the central nervous system; here, on account of existing nervous connections, it gives rise to a fresh impulse. That secondary impulse passes along outgoing nerve fibers to

* This system involves a receptor for the stimulant, a conductor toward an inner nerve center, an effector (some body organ that becomes active upon stimulation), and an efferent conductor which conveys the "action" impulse back to those body organs which must react.

the active organ, where it excites a special activity in the cellular structures.

The time required for these activities to occur is quite short; reflex actions are initiated generally within 0.032 seconds and in many cases as quickly as 0.010 seconds for so-called "normal" subjects [10]. Reflex rate studies for unhealthy or aged persons are limited, but research with starved subjects has demonstrated considerable slow-down from results obtained during healthy periods with the same subjects [58].

Voluntary actions are guided by mental thought processes and usually require precise muscle control to effect complex motions. For even simple motions, Fearing [10] reports that voluntary actions in normal subjects require 0.225 seconds, or about 10 to 20 times as long as a reflex reaction. With elderly and unhealthy persons, the possibility of impaired muscle control must be recognized.

Restricting the consideration to normal subjects, reaction for protection should begin within 0.25 seconds of danger perception. As pointed out previously, this is a conservative estimate for "normal" persons, but uncertain when considering physically and mentally substandard persons.

### 5.4.2 Time of Motion

After becoming cognizant of his danger, a person must displace his endangered member or even his entire body to achieve safety. Brozek et al. [58] report that a "normal" person can move his arms through a $45^\circ$ rotation within 0.117 seconds. The same persons can rotate their legs about the hip $45^\circ$ within 0.122 seconds. Translation of the entire

body requires more time; but, within 0.50 seconds, the total body can be moved several inches.

Tests with persons having withered members* demonstrate that as much as three times normal time is required for identical limb movement [58]. Grossly incapacitated persons probably would be helpless to respond for safety. Such extreme situation, however, is impossible to evaluate properly or completely, and a conservative estimate of the usual situation shall be applied.

5.4.3 Total Time of Reaction

Summing the two components of response time provides an estimate of the lag between danger perception and safety. A conservative estimate of the time required would be 0.75 seconds for the "normal" human.

To analyze the situation of bare skin exposed to specified heat fluxes, the following examples have been selected:

(a) Heat Flux incident to skin = 14,000 (Btu/hr-ft$^2$)

From Figure 23,

time to pain $\cong$ 0.2 seconds

And time to safety $\cong$ 0.2 + 0.75

$\cong$ 0.95 seconds

but time to blister $\cong$ 1.5 seconds

(b) Flux incident to skin = 6000 (Btu/hr-ft$^2$)

time to pain $\cong$ 0.6 seconds

And time to safety $\cong$ 0.6 + 0.75 = 1.35 seconds

---

* The cited tests involved patients who had just been removed from limb casts or who had permanent disability.

but time to blister $\cong$ 4.5 seconds

In both examples, the individual probably could save himself from burn injury. Figure 24 presents a comparison of "time to safety" with physiological data on "time to pain" and "time to blister."

As even higher skin heating rates are encountered, the time available for removing an endangered member becomes less. A person who encounters heating rates near maximum household values, probably could not prevent injury. As shown by Figure 24, an encounter with heat sources capable of causing blistering in less than 0.75 seconds would probably result in a skin burn.

## 5.5 Conclusion

This chapter describes "normal" human physiological response to heat inputs. The fact that skin burns occur from time to time in every household illustrates that skin can be damaged from common heat sources before the victim has moved to protect himself.

The use of fabrics for thermal protection is a primary reason that even more burn injuries do not occur. Hot pads in every kitchen are used to protect the hands of the cook. A shirt sleeve will prevent skin burns should a covered arm brush some hot object. This concept of thermal protection provided by fabrics will be explored in the following chapter.

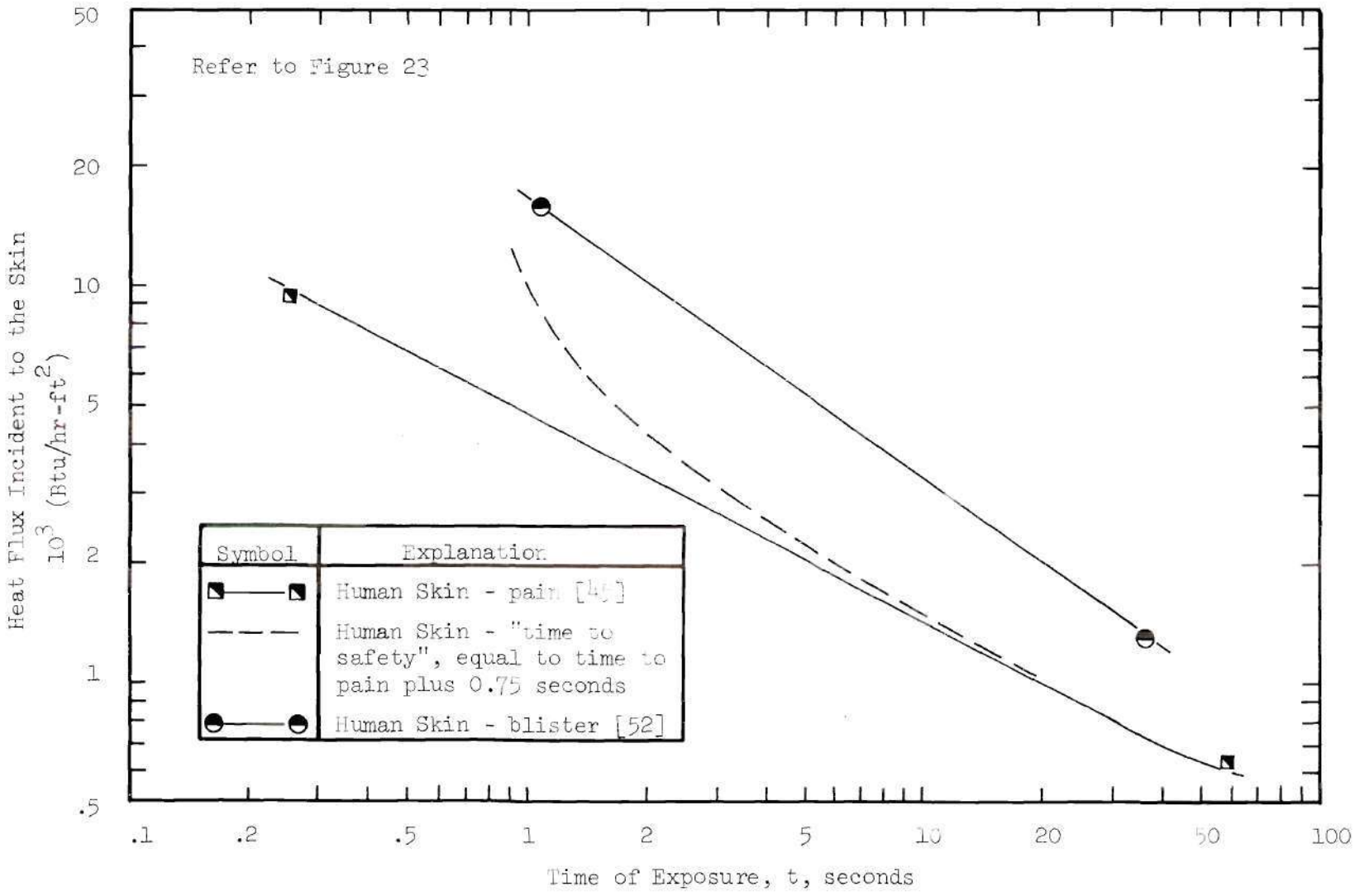


Figure 24. Comparison of Human Reaction with Skin Tissue Thermal Response.

# CHAPTER VI

# THERMAL PROTECTION OF CLOTHING

## 6.1 Literature Survey on Thermal Protection Studies

Apart from modesty or appearance considerations, man wears clothing for protection against the harshness of his environment. Normally, one would think of protection against cold, but protection against heat and solar radiation (sunburn) are also important.

In addition to providing protection from natural phenomena, clothing often prevents thermal damage to skin by insulating it from direct contact with hot objects or by shielding the skin from significant fractions of incident radiant heat. This benefit of clothing use is termed "thermal protection of clothing."

The mechanisms for protection are reflection of energy off the front surfaces of a fabric and heat absorbtion with an associated temperature rise in the cloth. Diverse factors, including material, weave, color, finish, thickness and cleanliness, determine the effectiveness of any particular garment in protecting the wearer.

Most studies on the thermal protection of fabrics have been sponsored by the military in development of safer flight suits. Pilots occasionally must run to safety through fuel fire conflagration to escape burning aircraft, relying on fabric flight suits for burn protection. Many studies have been published describing investigations of the thermal protection provided by various fabrics and fabric combinations [52, 53, 59 - 63]. The studies have speeded development of many

garments for special application. For example, suits for race car drivers are made from fabrics which afford significant thermal protection and which also are fire retardant. Clothing worn in steel mills normally is made to shield the worker from most of the incident heat.

The majority of studies on thermal protection under military sponsorship involve experimental measurements to determine whether or not a man wearing some clothing combination is sufficiently protected to escape an aircraft crash fire situation [52, 53, 60 - 62]. Numerous tests have been run where a mannequin with a neoprene skin simulant and clothed by various flight suit garments, was pulled through a raging fuel fire at man's running rate. Temperature sensors at various points on the dummy determined whether or not the skin simulant reached burn injury temperature during the exposure. Companion studies have compared the ratio of energy measured at the surface of a layer of fabrics to the energy measured behind the layer for various multiple layers of clothing.

An especially interesting study by Stoll [59] involved evaluation of a thermal protection index (T.P.I.) for certain types of cloth. In that study, anesthetized and depilated albino rats were placed behind fabric samples and subjected to rectangular pulses of radiant energy. A thermal protection index was quantized as the ratio of time to skin burn while the rat was shielded by a layer of fabric to the time to burn when it was not protected. The indices were evaluated only for an incident heat flux of 0.30 $cal/cm^2$-sec (3980 Btu/hr - $ft^2$). Probably, this thermal protection index would vary with different heating rates,

but her study did not include that factor.

The E. I. du Pont de Nemours and Company has invested considerable research into developing clothing which will afford thermal protection [63]. The du Pont research organization has defined a protective index, P. I., to be a ratio of energy blocked out by a cloth to the net incident energy. From the definition of fabric transmittance, $\tau_o$,

$$P.\ I. = (1 - \tau_o)$$

That company research found protective indices using two-layer combination of nylon and flame retardant cotton ranging from 0.68 to 0.91 for radiant incident heat [63].

Dussan and Weiner [68] have studied thermal protection from conductive heat inputs afforded by garment fabrics. The fabric was treated as a low thermal conductivity insulator in an analytical study.

Consideration of clothing as a physical hazard due to probability of ignition conflicts with use for thermal protection. The difference arises whenever clothes absorb sufficient energy that fabric ignition is impending. Determination of the probability of fabric ignition (and consequent burn injury caused by the flames) for some given exposure condition, must include evaluation of shielding effects and physiological response. Integrated evaluation of these parameters along with fabric ignition data should point toward a realistic determination of the probability of burn injury.

## 6.2 Thermal Protection Model and Application to Present Data

To describe the protection to covered skin afforded by a layer of cloth, fabric will be modeled as an inert, semi-opaque solid which absorbs and reflects a portion of the net incident energy. Figure 25 depicts details of the model. During a heating incident, the cloth will sustain a temperature rise, but not itself become a hazard by igniting and burning.

The heat felt by a clothed body is only a portion of the total energy incident to the covering fabric.

$$(q_i'')_{skin} = (\tau_o)\ (q_i'')_{net}$$

$$\tau_o = \text{fabric transmittance} < 1$$

Fabric transmittances were determined from flux meter outputs; refer to Appendix B. The transmittances will be assumed constant throughout an exposure period. Although this assumption does not agree precisely with experiment, the error is small and probably no greater than inconsistencies in the physiology of man.

The ten fabrics used in this study are all light colored and highly reflective, promoting rather low transmittances. Lower reflectances and possibly greater transmittances would be expected for dark colored cloths. In addition, if the fabrics be woven more tightly, with minimum air gap between individual fibers, fabric transmittance is reduced.

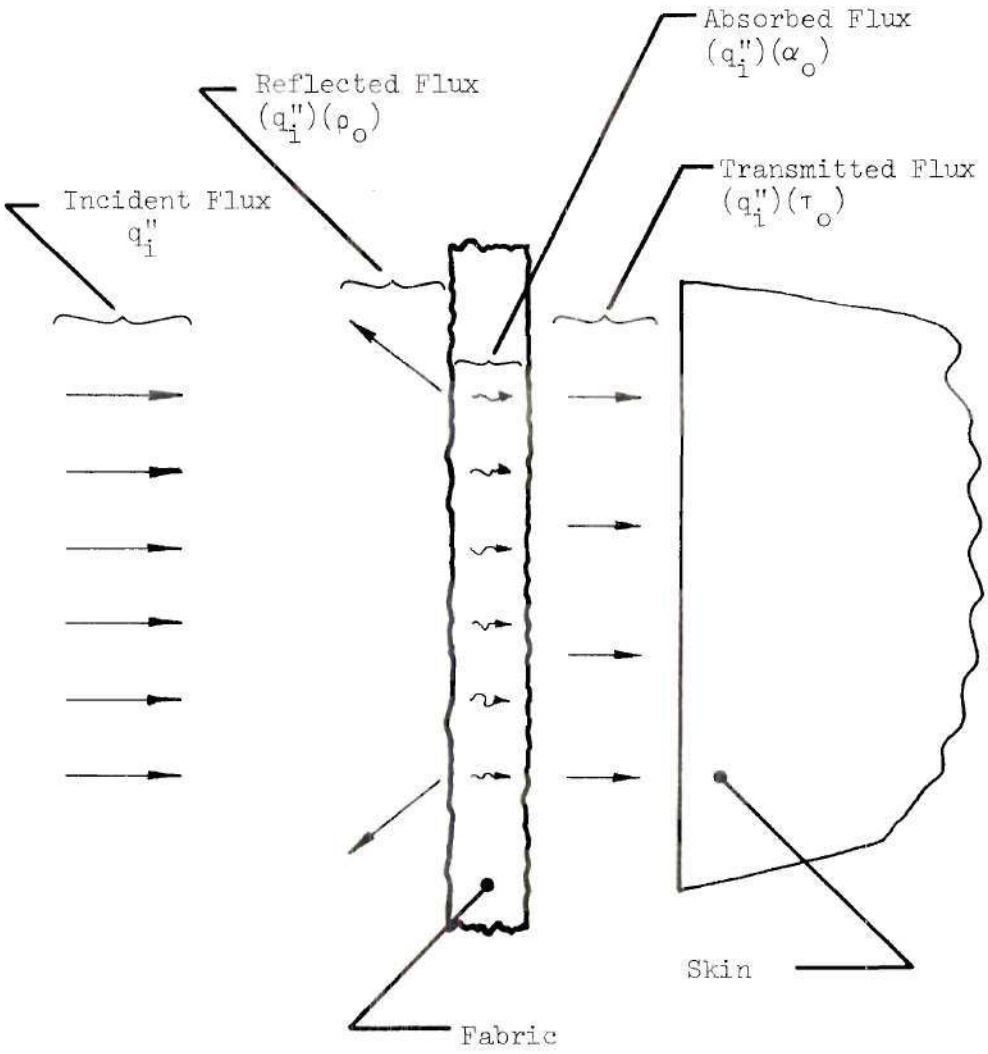


Figure 25. Thermal Protection Model.

Another important factor in evaluating fabric transmittances is wavelength of the incident energy. Dunkle, Ehrenburg and Gier [64] have published data on fabric reflectances for various wavelengths of incident light. The reflectances of closely woven cloth, for example, varied between 0.05 and 0.52. The value of 0.10 is fairly accurate with far infrared wavelengths ($\lambda > 7\mu$).

Fabric transmittances reported by Wulff, Zuber et al. [4] were determined by optical measurements with incident light in the short wavelength range, $0.6\mu$ to $2.5\mu$. The ignition time test measurements of fabric transmittances do not include evaluation of the incident energy wavelengths.

Information on transmittances of fabrics as functions of wavelength does not seem available. For this reason, transmittances measured during the ignition time tests are applied in solutions with the thermal protection model.

## 6.3 Thermal Protection From Ignition Time Tested Fabrics

The ten tested fabrics include cottons, mixtures of cotton and synthetics, and wholly synthetic fibers. The ten fabric group, as shown by the ignition time tests themselves, can present risks of melt drop hazard* as well as danger of fabric ignition.

Generally, thermal protection is a pre-ignition or pre-melting (only) benefit of clothing use, and with ignition, a garment becomes a

---

* Stoll [59] discusses melt drop hazard as a difficult problem with synthetic flight suits. The fabric material will become molten with heat exposure and drops of liquid will drop onto underlying skin and cause contaminated burns.

grave hazard to the wearer. Previous fabric ignition analyses were computation of the most rapid possible ignition. By developing such predictions of fabric ignition time, the minimum time to danger has been evaluated. In-use fabrics would become a hazard later than suggested by these predictions.

### 6.3.1 Definition of Time to Danger

The time elapse from onset of exposure until that instant when the fabric becomes a hazard to the user is termed time to danger. For a fabric which ignites and burns, time to danger is the ignition time. A definition of time to danger for a melting fabric, one which never ignites, is not so precise.

Generally, during the ignition time tests, melting fabrics would first melt rapidly, then melt slowly until complete destruction (if that ever occurred). A definition of time to danger for the melting fabric was selected to reflect Stoll's description of melt drop hazard [59]. Time to danger, melting fabrics, is the time elapse from onset of fabric exposure until that time halfway between onset of rapid melting and the beginning of slow melting. The wearer hazard is envisioned as molten material dropping onto the skin. The raw data presented in Appendix B will help clarify this definition.

Fabric ignition time data from Alvares [15], Bates and Monahan [50], and Welker et al. [51] are plotted in Figure 26 with data from this study in the format time to danger versus incident heat flux intensity. Figure 27 presents ignition time data from this study in a format of time to danger versus the intensity of transmitted flux. For

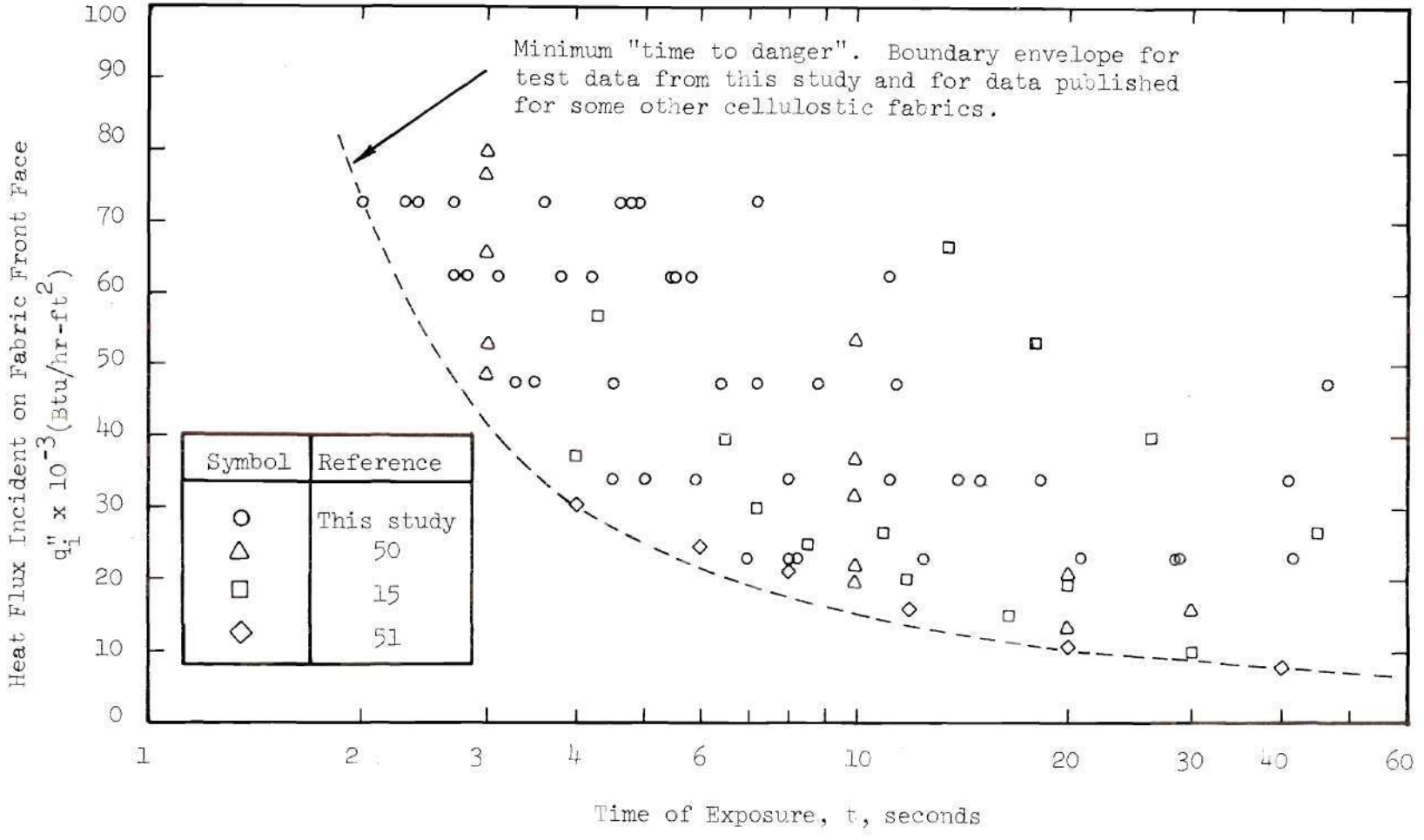


Figure 26. Time to Danger Versus Incident Heat Flux Intensity for Various Fabrics (Experimental Results).

the tested fabrics, at the maximum test heating rates, time to danger ranged between 2 and 5 seconds. For household heat flux intensities, the time to danger was varied between 7 and 40 seconds or longer.

6.3.2 Dangers of Excessive Thermal Protection

When considering flammable clothing, the question of how much thermal protection is desirable becomes a real concern. Obviously, sufficient fabric can be worn to block virtually all energy from the skin. This situation, though, is not desirable.

A person excessively clothed such that none of the energy incident to this clothing would reach his skin, might remain unaware of an exposure to dangerously intense heat until his clothes were aflame. This situation could render his clothing a grave hazard instead of a device for protection.

During the ignition time tests, a single test with two layers of 100 per cent T-shirt was performed. Two layers of cloth were mounted together and exposed at 23,900 Btu/hr-ft$^2$. That layer nearest the lamps ignited in 16.0 seconds, or in about two-thirds the single layer ignition time. The second layer ignited roughly 12 seconds later under continuing exposure. The two layer combination blocked some 20 per cent more energy than did a single layer of material. The second layer ignition occurred several seconds later than did ignition of a single layer.

When the concern is likelihood of burn injury from flaming garments, it is essential that time to safety , developed previously in Chapter IV, be less than fabric ignition time. In analyzing this problem, small values of transmittance would extend the time to safety

by delaying the sensation of pain.

## 6.4 Likelihood of Burn Injury Caused by Thermal Reaction of an Ignition Time Tested Fabric

Time to danger can be applied in conjunction with physiological data to predict burn injury probabilities. The investigation resolves to a determination of whether or not some normal person exposed to radiant heat, over body areas covered by a single layer of fabric, will be injured by thermal reaction of the garment itself before he can move for safety. If time to safety, defined previously, exceeds time to danger, the individual will be in jeopardy of burn injury form his clothing.

Figure 27 presents the information time to danger plotted versus the measured intensity of transmitted heat flux for each of the ten tested fabrics. By assuming that the measured transmitted flux is the flux incident to the skin, a composite description of time to danger and time to safety can be plotted for various exposure incidents. This information is presented in Figure 28.

It is interesting to note that for transmitted fluxes less than 10,000 (Btu/hr-ft$^2$), the time to safety is considerably less than time to danger . Since a net incident flux of more than 34,000 (Btu/hr-ft$^2$) was required to produce measured transmitted fluxes of 10,000 (Btu/hr-ft$^2$) with the ten primary GIRCFF fabrics, it can be inferred that in household exposure incidents* "normal" persons should escape

* Household heat sources should almost never exceed 30,000 (Btu/hr-ft$^2$). Refer to Table All.

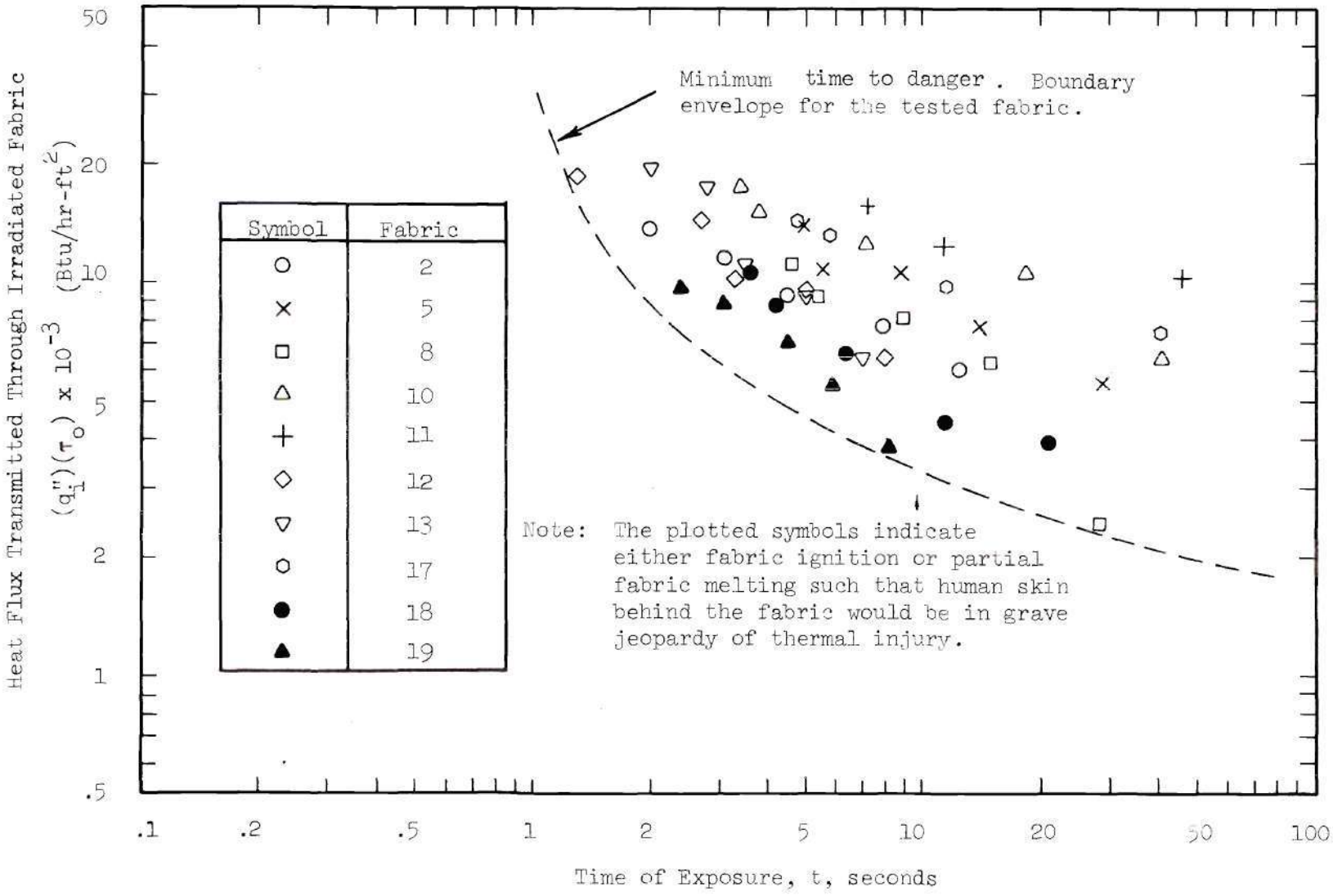


Figure 27. Time to Danger Versus Transmitted Heat Flux Intensity.

injury from fabric thermal reactions.

If clothing were not particularly transparent, probably it would ignite sooner. As discussed previously in the thermal protection model analysis, perfect protection probably is not really desirable. Optimum transmittance would allow the user maximum time to move to safety after becoming aware of heat exposure. Postponing his recognition of danger will impose greater risk of fabric fire, and consequently greater risk of burn injury.

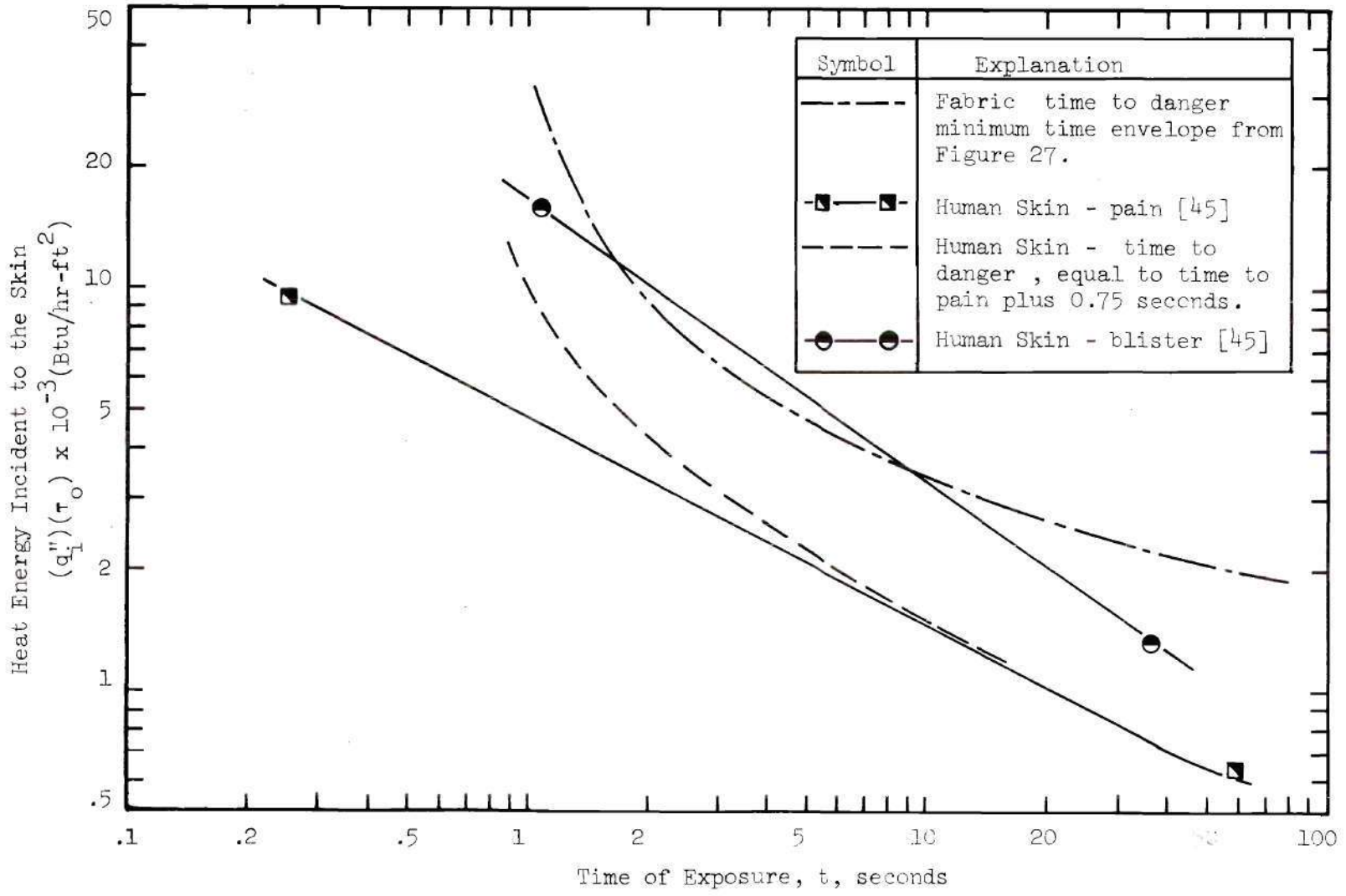


Figure 28. Comparison of Fabric Ignition Data with Physiological Response.

# CHAPTER VII

## CONCLUSIONS

The following conclusions can be drawn from this study of fabric ignition and burn injury probability:

(1) The Ignition Time Apparatus was satisfactory for measuring the ignition time of those fabrics tested. Shutter opening times were one per cent or less of the minimum ignition (or melting) time measured.

(2) Fifty six tests were run with the equipment on ten different fabrics for the range of incident heat fluxes:

$$23{,}900 \text{ (Btu/hr-ft}^2\text{)} < q_i'' < 72{,}700 \text{ (Btu/hr-ft}^2\text{)}$$

The ignition (or melting) times measured for the 56 tests varied between 3 and 90 seconds.

(3) Fabric transmittances were measured during each test and recorded. Values of transmittance were large, as expected for thin fabrics, and averaged 0.15 to 0.27 for the tests. Fabric transmittances tended to increase during exposure periods. This fact plus the visual observation of pre-ignation discoloration suggest that variation of fabric properties during exposure might affect ignition time.

(4) The diathermanous model of fabric ignition was much more accurate than the simple conduction model when compared with experimental data. The diathermanous model predicted ignition times which were less

than experimental results by about a factor of two. Generally, the analytical results are more accurate at higher heating rates.

(5) A review of the literature revealed that processes of thermal injury to the skin, as well as pain sensation, are heating rate dependent. The time elapse before occurence of either phenomenon is essentially inversely proportional to incident heat intensity. Additional literature research revealed that human reaction rates vary with age and physical or mental condition, but that some "normal" person probably can remove his limbs or his torso from any sort of dangerous situation within 0.75 seconds of his awareness of the peril.

(6) A "normal" person, clothed by a single layer of some optically thin fabric probably could escape burn injury should he be exposed to a radiant heat source of common household intensity. That is, the time to pain plus the probable time of action is less than the ignition times measured in this study or reported elsewhere in the literature during the period 1955-69. This conclusion neglects the possibility of delayed ignition, and assumes that removal is equivalent to attainment of safety.

(7) A review of the literature indicated that for the case of bare skin exposed to radiative sources, at heating rates associated with fabric decomposition, pain will precede injury. At extremely high heating rates, burn injury and pain are simultaneous or else pain is never felt because destruction of the sensory mechanisms occurs concurrently with tissue damage. At very low heating rates, on the order of solar radiation at the earth's surface, thermal damage can occur without pain.

(8) Using the values of fabric transmittance recorded during the ignition time tests, the ten tested fabrics provided protection to underlying skin from 60 per cent or more of the net incident radiant energy during the period of pre-ignition (or pre-melting) heating.

(9) Two layers of a fabric will provide more protection to underlying skin than will a single thickness. During a test with two layers of 100 per cent cotton "T-shirt" (Fabric No. 5), pre-ignition transmittance was 0.18. During a test at the same irradiance for a single layer of "T-shirt" material, the transmittance was 0.23.

# APPENDIX A

## SUMMARY OF PERTINENT DATA

# APPENDIX A

## SUMMARY OF PERTINENT DATA

Information in the following tables summarizes quantitative data applicable to this study. Each table is referenced in the body of the report; data information sources are indicated in the tables themselves.

Experimental ignition time data reported in Table A1 through Table A8 were obtained in this study with the Ignition Time Device. These data were first reported by Kirkpatrick and Bergles [5] at conclusion of the test sequence reported in Chapter III.

Physiological data given in Table A9 were accumulated through a rather extensive literature search. Table A10 summarizes analytical results of the skin temperature response model. Discussions of the information in both these tables are given in Chapter V.

Information in Table A11 was obtained from various references and lists radiant heat intensities associated with common sources. The radiant heater of the Ignition Time Apparatus can produce heat fluxes up to almost two times the maximum listed in the table.

Table A1. Ignition Time Test Results (Melting Fabric No. 2)

| GIRCFF Fabric No. | Test No. (1) | Incident Heat Flux (2) $\frac{Btu}{hr - ft^2}$ | Transmitted Heat Flux (3) $\frac{Btu}{hr - ft^2}$ | Time to (1) Onset of Melting (2) Completion of Melting |
|---|---|---|---|---|
| 2 | 9A | 23,900 | 6,100 (4) | (1) 11.0<br>(2) indefinite (6) |
| 2 | 6 | 34,000 | 7,720 (4) | (1) 6.0<br>(2) indefinite (6) |
| 2 | 7 | 47,300 | 9,340 (4) | (1) 3.2<br>(2) indefinite (6) |
| 2 | 8 | 62,300 | 11,690 (4)<br>34,250 (5) | (1) 2.0<br>(2) 8.0 (7) |
| 2 | 41 | 72,700 | 13,700 (4)<br>42,100 (5) | (1) 1.2<br>(2) 6.0 (7) |

(1) Refer to the raw data presented in the plots included in Appendix B.

(2) Heat flux incident to fabric front face.

(3) The transmitted flux was measured by a calorimeter located 0.400 inch behind fabric back surface.

(4) Transmitted flux measured prior to onset of melting.

(5) Flux at calorimeter position after fabric destruction by complete melting.

(6) Fabric degradation under heat exposure was a gradually increasing porosity. Individual fibers comprising the weave gradually diminished in diameter as molten material flowed away from the irradiated area or vaporized.

(7) At this time elapse after fabric exposure, no material remained in the irradiated area.

Table A2. Ignition Time Test Results (Igniting Fabrics)

| CIRCOT Fabric No. | Test No. (1) | Incident Heat Flux Btu / hr - ft$^2$ | Transmitted Heat Flux (2) Btu / hr - ft$^2$ | Time to Ignition (sec) |
|---|---|---|---|---|
| 5 | 8A | 23,900 | 5,470 | 28.8 |
| 5 | 9 | 34,000 | 7,775 | 14.0 |
| 5 | 10 | 47,300 | 10,610 | 8.8 |
| 5 | 11 | 62,300 | 10,920 | 5.5 |
| 5 | 42 | 72,700 | 14,000 | 4.9 |
| 10 | 7A | 23,900 | 6,490 | 41.5 |
| 10 | 2 | 34,000 | 10,610 | 18.2 |
| 10 | 4 | 47,300 | 12,950 | 7.2 |
| 10 | 5 | 62,300 | 15,025 | 3.8 |
| 10 | 43 | 72,700 | 17,600 | 2.7 |
| 18 | 6A | 23,900 | 3,925 | 20.9 |
| 18 | 12 | 34,000 | 4,450 | 11.2 |
| 18 | 13 | 47,300 | 6,670 | 6.4 |
| 18 | 14 | 62,300 | 8,910 | 4.2 |
| 18 | 37 | 72,700 | 10,610 | 3.8 |

General Shape of Calorimeter (2) Output for This Set of Fabrics

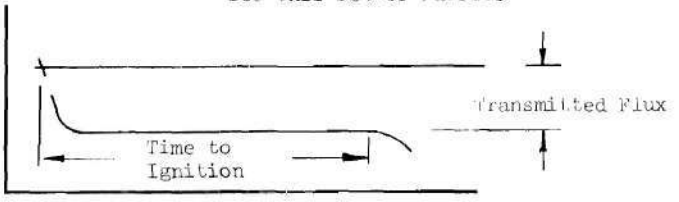


(1) Refer to the raw data presented by the plots included in Appendix B.

(2) The transmitted flux was measured by a calorimeter located 0.400 inch behind the fabric back face. The flux magnitude reported in this table were read at times before fabric ignition.

Table A3. Ignition Time Test Results
(Fabric Ignition After Partial Melting,
Fabric No. 8)

| GIRCFF Fabric | Test No. (1) | Incident Heat Flux $\frac{Btu}{hr - ft^2}$ | Transmitted Heat Flux (2) $\frac{Btu}{hr - ft^2}$ | Time to: (1) Onset of Melting (2) Completion of Melting (3) Ignition (seconds) |
|---|---|---|---|---|
| 8 | 10A | 23,900 | 2,425 (3)<br>5,870 (4)<br>- | (1) 4.8<br>(2) 16.1<br>(3) 28.1 |
| 8 | 25 | 34,000 | 6,270 (3)<br>10,510 (4)<br>- | (1) 3.2<br>(2) 11.5<br>(3) 15.0 |
| 8 | 26 | 47,300 | 8,100 (3)<br>12,940 (4)<br>- | (1) 2.7<br>(2) 6.8<br>(3) 8.8 |
| 8 | 27 | 62,300 | 9,300 (3)<br>15,850 (4)<br>- | (1) 1.9<br>(2) 3.8<br>(3) 5.4 |
| 8 | 35 | 72,700 | 11,319 (3)<br>17,800 (4)<br>- | (1) 1.7<br>(2) 3.3<br>(3) 4.6 |

(1) Refer to the raw data presented in the plots included in Appendix B.

(2) The transmitted flux was measured by a calorimeter located 0.400 inch behind fabric back face.

(3) Transmitted flux measured prior to onset of melting.

(4) Transmitted flux measured prior to ignition but after completion of melting.

Table A4. Ignition Time Test Results (Fabric Ignition After Partial Melting, Fabric No. 11).

| GIRCFF Fabric No. | Test No. (1) | Incident Heat Flux (2) $\frac{Btu}{hr - ft^2}$ | Transmitted Heat Flux (3) $\frac{Btu}{hr - ft^2}$ | Time to: (1) Onset of Melting (2) Completion of Melting (3) Ignition (seconds) |
|---|---|---|---|---|
| 11 | 4A | 23,900 | 4,450 (4) (5) | (1) 2.0<br>(2) indefinite<br>(3) no ignition (100 sec) |
| 11 | 28 | 34,000 | 7,690 (4)<br>20,200 (5) | (1) 1.5<br>(2) 43.0<br>(3) no ignition (60 sec) |
| 11 | 29 | 47,300 | 10,310 (4)<br>26,300 (5) | (1) 1.0<br>(2) 37.0<br>(3) 46.2 |
| 11 | 30 | 62,300 | 12,520 (4)<br>31.950 (5) | (1) 0.7<br>(2) 11.0<br>(3) 11.2 |
| 11 | 34 | 72,700 | 15,760 (4)<br>39,650 (5) | (1) 0.4<br>(2) 6.4<br>(3) 7.2 |

(1) Refer to the raw data presented in the plots included in Appendix B.

(2) Heat flux incident to fabric front face.

(3) The transmitted flux was measured by a calorimeter located 0.400 inch behind fabric back surface.

(4) Transmitted flux measured prior to melting.

(5) Transmitted flux measured after completion of melting but prior to flame.

Table A5. Ignition Time Test Results (Melting Fabric No. 12)

| GIRCFF Fabric No. | Test No. (1) | Incident Heat Flux (2) Btu / hr - ft$^2$ | Transmitted Heat Flux (3) Btu / hr - ft$^2$ | Time to: (1) Onset of Melting (2) Completion of Melting |
|---|---|---|---|---|
| 12 | 3A | 23,900 | 6,475 (4)<br>16,550 (5) | (1) 6.0<br>(2) 12.0 |
| 12 | 31 | 34,000 | 9,710 (4)<br>20,910 (5) | (1) 3.9<br>(2) 7.3 |
| 12 | 32 | 47,300 | 10,210 (4)<br>25,900 (5) | (1) 2.5<br>(2) 5.2 |
| 12 | 33 | 62,300 | 14,700 (4)<br>33,400 (5) | (1) 1.8<br>(2) 3.7 |
| 12 | 40 | 72,700 | 18,910 (4)<br>40,900 (5) | (1) 1.2<br>(2) 3.1 |

(1) Refer to the raw data presented in the plots included in Appendix B.

(2) Heat flux incident to fabric front face.

(3) The transmitted flux was measured by a calorimeter located 0.400 inch behind fabric back surface.

(4) Transmitted flux measured prior to onset of melting.

(5) Flux at calorimeter position after fabric destruction by complete melting.

Table A6. Ignition Time Test Results (Melting Fabric No. 13).

| CIRCFF Fabric No. | Test No. (1) | Incident Heat Flux (2) Btu / hr - ft$^2$ | Transmitted Heat Flux (3) Btu / hr - ft$^2$ | Time to: (1) Onset of Melting (2) Completion of Melting |
|---|---|---|---|---|
| 13 | 2A | 23,900 | 6,480 (7)<br>10,210 (8) | (1) 10.5<br>(2) indefinite (6) (4) |
| 13 | 19 | 34,000 | 9,350 (7)<br>13,700 (8) | (1) 7.0<br>(2) indefinite (6) (4) |
| 13 | 20 | 47,300 | 11,210 (7)<br>18,050 (8) | (1) 6.0<br>(2) indefinite (6) (4) |
| 13 | 21 | 62,300 | 17,420 (7)<br>25,000 (8) | (1) 5.0<br>(2) 13.2 (6) (5) |
| 13 | 39 | 72,700 | 19,910 (7)<br>28,400 (8) | (1) 4.0<br>(2) 9.4 (6) (5) |

(1) Refer to the raw data presented in the plots included in Appendix B.

(2) Heat flux incident to fabric front surface.

(3) The transmitted flux was measured by a calorimeter located 0.400 inch behind fabric back surface.

(4) Fabric degradation under heat exposure was a gradually increasing porosity. Individual fibers of material comprising the weave gradually diminished in diameter as molten material flowed away from the irradiated area or vaporized.

(5) At this time elapse after fabric exposure, no material remained in the irradiated area.

(6) At this time elapse after fabric exposure, rapid degradation had ceased and slow deterioration had begun.

(7) Transmitted heat flux measured prior to onset of melting.

(8) Transmitted heat flux measured at that time elapse when rapid degradation had ceased. The fabric had been significantly damaged at this time.

Table 8. Ignition Time Test Results (Fabric Ignition After Partial Melting, Fabric No. 17)

| GIROFF Fabric No. | Test No. (1) | Incident Heat Flux (5) Btu / hr - ft$^2$ | Transmitted Heat Flux (2) Btu / hr - ft$^2$ | Time to: (1) Onset of Melting (2) Completion of Melting (3) Ignition (seconds) |
|---|---|---|---|---|
| 17 | 1A | 23,900 | 4,850 (3)<br>8,290 (4) | (1) 3.0<br>(2) 25.0<br>(3) No flame (70 sec) |
| 17 | 22 | 34,000 | 7,480 (3)<br>12,320 (4) | (1) 3.0<br>(2) 17.0<br>(3) 41.0 |
| 17 | 23 | 47,300 | 9,910 (3)<br>13,740 (4) | (1) 2.0<br>(2) 7.0<br>(3) 11.4 |
| 17 | 24 | 62,300 | 13,320 (3)<br>17,590 (4) | (1) 1.6<br>(2) 3.2<br>(3) 5.8 |
| 17 | 36 | 72,700 | 14,550 (3)<br>20,200 (4) | (1) 1.2<br>(2) 2.8<br>(3) 4.8 |

(1) Refer to the raw data presented in the plots included in Appendix B.

(2) The transmitted flux was measured by a calorimeter located 0.400 inch behind fabric back face.

(3) Transmitted flux measured prior to melting.

(4) Transmitted flux measured after completion of melting but prior to flame.

(5) Heat flux incident to fabric sample front face.

Table A8. Ignition Time Test Results
(Fabric Ignition Without Destruction)

| GIRCFF Fabric No. | Test No. (2) | Incident Heat Flux $\frac{Btu}{hr - ft^2}$ | Transmitted Heat Flux (3) $\frac{Btu}{hr - ft^2}$ | Time to Ignition (sec) |
|---|---|---|---|---|
| 19 (1) | 5A | 23,900 | 3,840 | 8.2 |
| 19 | 5A | 23,900 | 6,470 (4) | - |
| 19 | 15 | 34,000 | 5,490 | 5.9 |
| 19 | 15 | 34,000 | 10,120 (4) | - |
| 19 | 16 | 47,300 | 7,090 | 4.5 |
| 19 | 16 | 47,300 | 11,920 (4) | - |
| 19 | 17 | 62,300 | 8,900 | 3.1 |
| 19 | 17 | 62,300 | 15,150 (4) | - |
| 19 | 38 | 72,700 | 9,710 | 2.4 |
| 19 | 38 | 72,700 | 15,360 (5) | - |
| 19 | 38 | 72,700 | 17,200 (5) | - |
| 19 | 38 | 72,700 | 18,400 (5) | - |
| 19 | 38 | 72,700 | 19,000 (5) | - |
| 19 | 38 | 72,700 | 20,000 (5) | - |

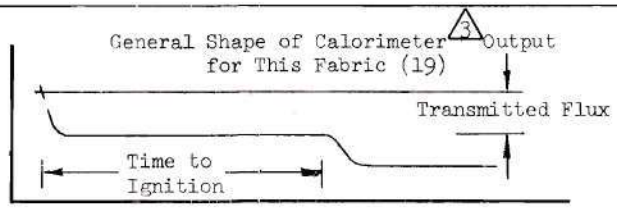


(1) Fabric 19 is 100 per cent cotton flannel treated to be fire retardant. Surface fuzz ignited, but flame extinguished without burning through the primary weave.

(2) Refer to the raw data presented by the plots included in Appendix B.

(3) The transmitted flux was measured by a calorimeter located 0.400 inch behind the fabric back face.

(4) Transmitted flux measured after flame extinction.

(5) Transmitted flux measured after flame extinction. At this high incident flux, fabric continued to degrade without burning.

Table A9. Composite of Data for Thermal Inertia of Various Materials.

| Material | $(k\rho C_p)$ $\frac{10^{-5}(cal)}{(cm)^4 - sec - (^oC)^2}$ | Reference | Comments |
|---|---|---|---|
| Masonite | 23.8 | 38 | |
| Masonite | 23.6 | 41 | |
| Birch (wood) | 10.9 | 38 | |
| Leather | 13.1 | 38 | Tanned with oak tree extracts |
| Human Bone | 50.0 | 38 | Obtained from autopsy |
| Human Fat | 26.0 | 38 | Obtained from autopsy |
| Human Muscle | 113.0 | 38 | Excised, moist |
| Human Muscle | 56.0 | 38 | Excised, dry |
| Human Skin | 75.0 | 38 | Excised, moist |
| Human Skin | 55.0 | 38 | Excised, dry |
| Human Skin | 90.0 | 38 | Living, vasoconstricted |
| Human Skin | 400.0 | 38 | Living, maximum vasodilation |
| Human Skin | 111.8 ± 3.44 | 41 | Vasodilated, long exposure, $q_i'' = 269$ mcal/sec-cm$^2$ |
| Human Skin | 90.0 - 400.0 | 43 | Depending on state of vasodilation |
| Human Skin | 96.0 | 42 | Vasodilated, long exposure, $q_i'' = 100$ mcal/sec-cm$^2$ |
| Human Skin | 159.0 | 42 | Vasodilated, long exposure, $q_i'' = 400$ mcal/sec-cm$^2$ |

Table A10. Skin Pain Thresholds - Comparison of Theory and Experiment.

| Radiant Flux Incident to the Skin. $\frac{\text{calories}}{(\text{cm})^2\ (\text{sec})}$ | Measured Skin Surface Temperature at the Time of Pain [1] °C | Time to Pain, Measured. [1] seconds | Time to Pain, Predicted [2] seconds |
|---|---|---|---|
| 0.10 | 45.1 | 13.5 | 7.7 |
| 0.20 | 46.5 | 5.5 | 3.2 |
| 0.30 | 47.1 | 2.9 | 1.8 |
| 0.40 | 48.3 | 2.2 | 1.1 |

[1] Value reported by Stoll and Greene [42]

[2] Value computed from equations developed in Chapter V.

Table A11. Intensities of Various Heat Sources.

| Radiant Energy Source | Intensity (1) | Reference |
|---|---|---|
| Aircraft Fuel Fire | 9,400 | 59 |
| Propane Fuel Laboratory Burner | 25,200 | 63 |
| Propane-Propylene Fuel Laboratory Burner | 21,400 | 61 |
| Household Gas Flame, maximum value | 30,500 | 51 |
| Electric Hot Plate, element at 480°F | 27,900 | 63 |
| Solar Radiation, clear day, near sea level | 210-300 | 43 |
| Solar Radiation, near space | 442 | 43 |
| Bunsen Burner, with flame temperature of 2300°F | 27,900 | 63 |
| JP-5 Aircraft Fuel Fire maximum value measured at a point internal to the flame boundary | 55,260 | 70 |
| JP-5 Aircraft Fuel Fire magnitude of heat flux near the top of the flame boundary | 16,800 | 70 |

(1) [Btu/hr - $ft^2$]

# APPENDIX B

## IGNITION TIME MEASUREMENTS

# APPENDIX B

## IGNITION TIME MEASUREMENTS

The following 10 pages present raw data from the Ignition Time Tests conducted during the period 1 - 6 July 1971 [5]. The individual curves were traced from photographic records of the tests taken from recording oscilloscope screens.

Details of the experimental equipment are included in Chapter II, and discussions of the experiments themselves are in Chapter III. The actual times to ignition (or melting) for the tested fabrics deduced from these records are tabulated in Appendix A.

# IGNITION TIME MEASUREMENTS

TESTED FABRIC: GIRCFF fabric no. 2, yellow textured woven blouse, 100 % polyester.

Test 9A (23,900 Btu/hr-ft$^2$)

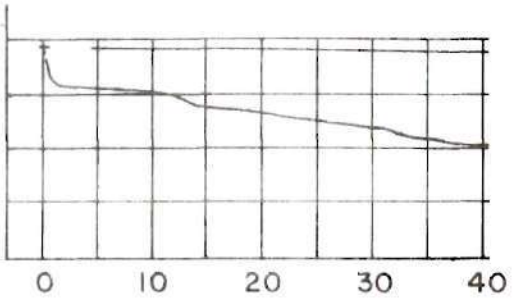


time, seconds

Test 6 (34,000 Btu/hr-ft$^2$)

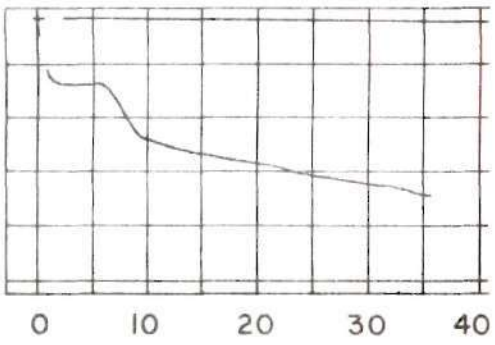


time, seconds

Test 7 (47,300 Btu/hr-ft$^2$)

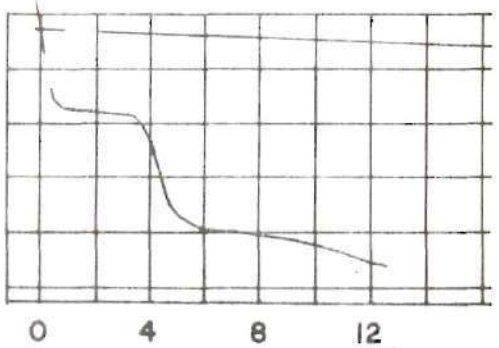


time, seconds

The heat fluxes reported were incident to fabric front face.

The plots present EMF output, from a calorimeter mounted 0·400 inch behind fabric back surface, versus time of exposure.

GIRCFF fabric no.2 melted without igniting.

Test 8 (62,300 Btu/hr-ft$^2$)

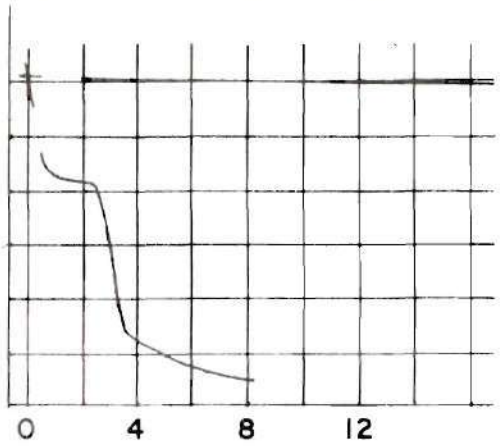


time, seconds

Test 41 (72,700 Btu/hr-ft$^2$)

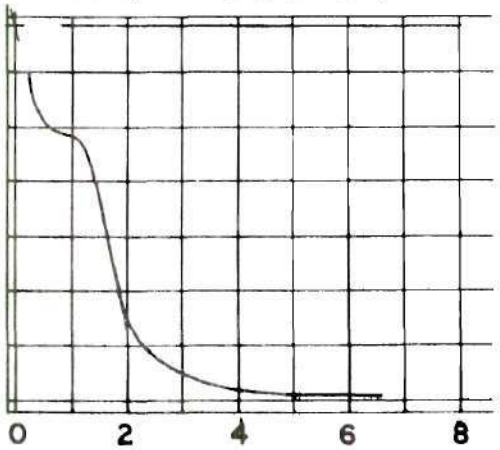


time, seconds

# IGNITION TIME MEASUREMENTS

TESTED FABRIC: GIRCFF fabric no. 5, white jersey T-shirt material, 100% cotton.

The heat fluxes reported were incident to fabric front face.

The plots present EMF output, from a calorimeter mounted 0·400 inch behind fabric back surface, versus time of exposure.

GIRCFF fabric no 5 ignited when irradiated.

Test 8A (23,900 Btu/hr-ft$^2$)

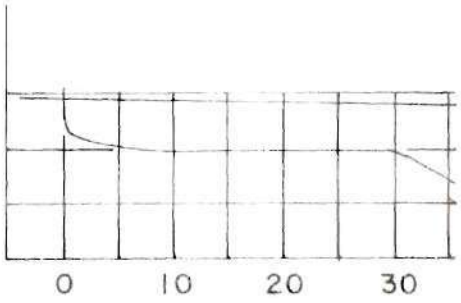


time, seconds

Test 9 (34,000 Btu/hr-ft$^2$)

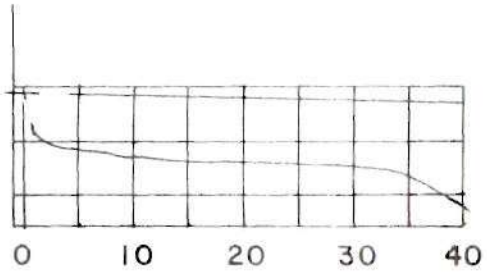


time, seconds

Test 10 (47,300 Btu/hr-ft$^2$)

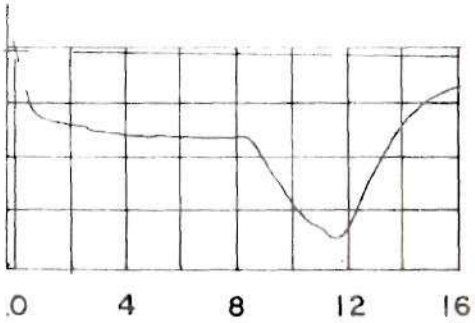


time, seconds

Test 11 (62,300 Btu/hr-ft$^2$)

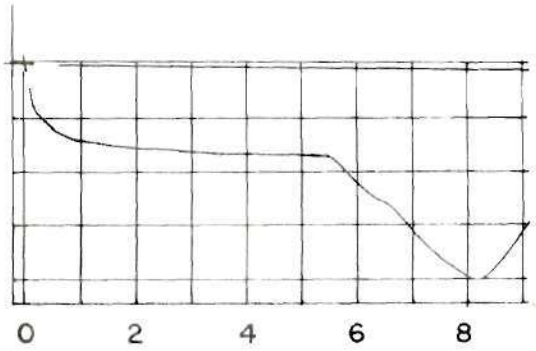


time, seconds

Test 42 (72,700 Btu/hr-ft$^2$)

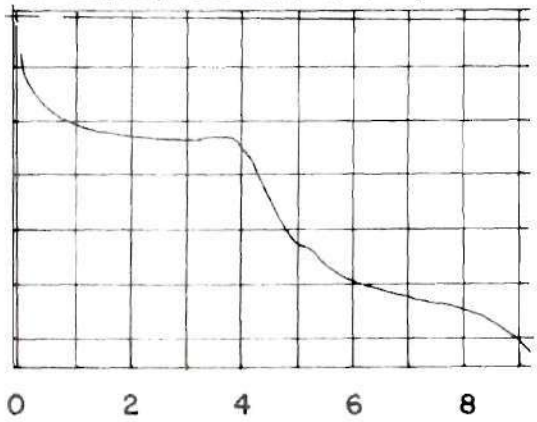


time, seconds

# IGNITION TIME MEASUREMENTS

TESTED FABRIC: GIRCFF fabric no.8, white jersey T-shirt material, 65% polyester, 35% cotton.

Test 10 A (23,900 Btu/hr-ft$^2$)

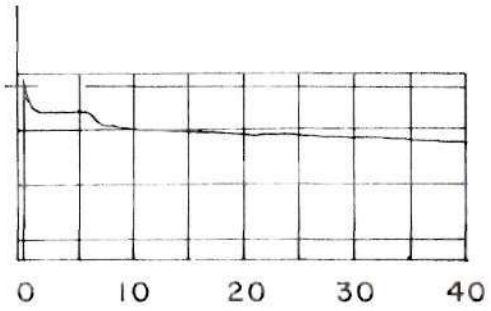


Test 25 (34,000 Btu/hr-ft$^2$)

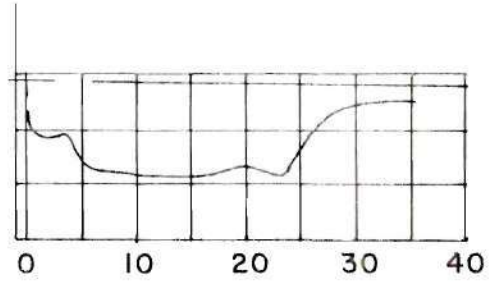


Test 26 (47,300 Btu/hr-ft$^2$)

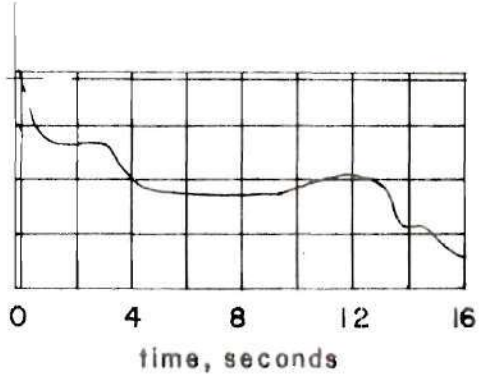


The heat fluxes reported were incident to fabric front face.

The plots present EMF output, from a calorimeter mounted 0·400 inch behind fabric back surface, versus time of exposure.

GIRCFF fabric no.8 partially melted and then ignited.

Test 27 (62,300 Btu/hr-ft$^2$)

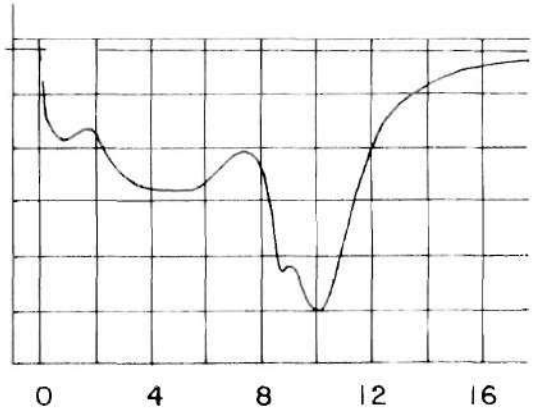


Test 35 (72,700 Btu/hr-ft$^2$)

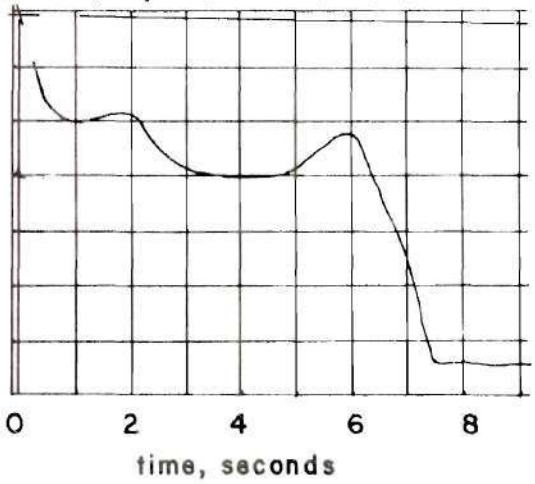

# IGNITION TIME MEASUREMENTS

TESTED FABRIC: GIRCFF fabric no.10, purple batiste, 100% cotton.

Test 7A (23,900 Btu/hr-ft$^2$)

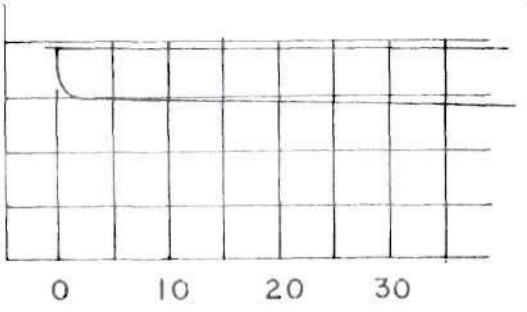


time, seconds

Test 2 (34,000 Btu/hr-ft$^2$)

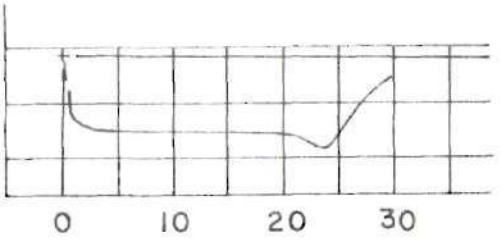


time, seconds

Test 4 (47,300 Btu/hr-ft$^2$)

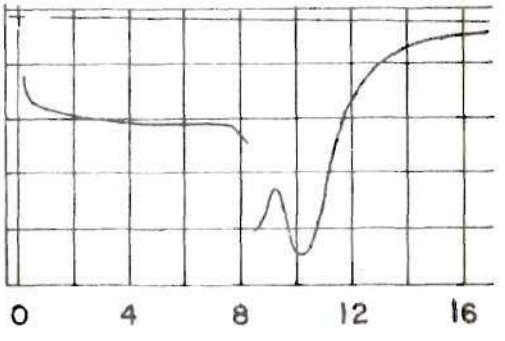


time, seconds

The heat fluxes reported were incident to fabric front face.

The plots present EMF output, from a calorimeter mounted 0·400 inch behind fabric back surface, versus time of exposure.

GIRCFF fabric no.10 ignited when irradiated.

Test 5 (62,300 Btu/hr-ft$^2$)

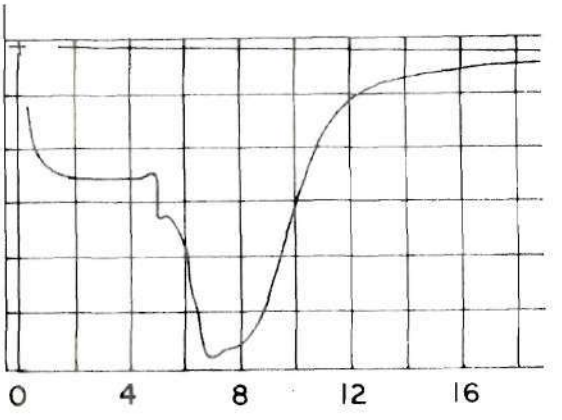


time, seconds

Test 43 (72,700 Btu/hr-ft$^2$)

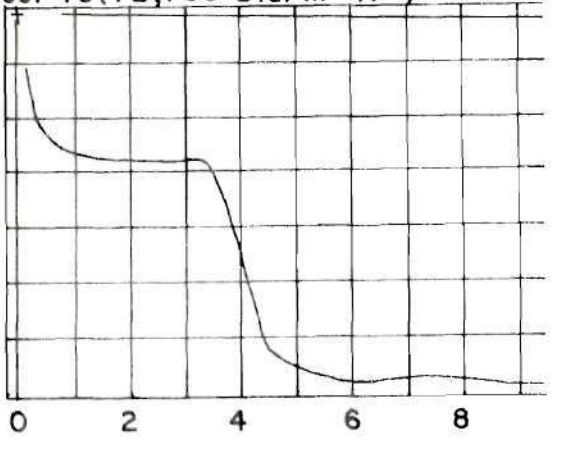


time, seconds

# IGNITION TIME MEASUREMENTS

TESTED FABRIC: GIRCFF fabric no.11, white tricot, 80% acetate, 20% nylon.

Test 4A (23,900 Btu/hr-ft$^2$)

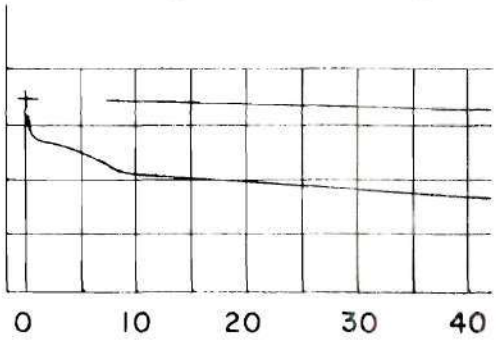


Test 28(34,000 Btu/hr-ft$^2$)

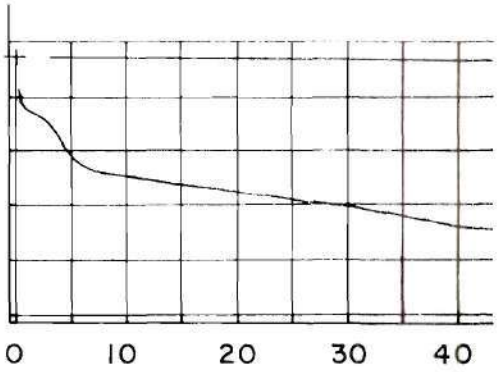


Test 29(47,300 Btu/hr-ft$^2$)

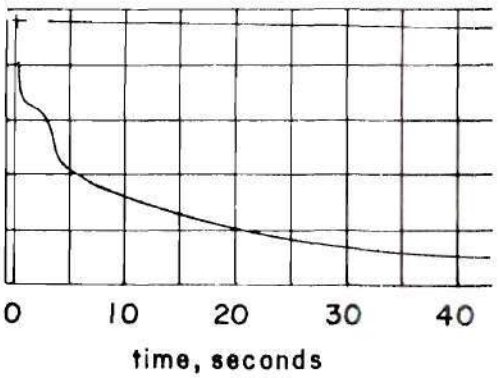


The heat fluxes reported were incident to fabric front face.

The plots present EMF output, from a calorimeter mounted 0·400inch behind fabric back surface, versus time of exposure.

GIRCFF fabric no.11 partially melted and then ignited.

Test 30(62,300 Btu/hr-ft$^2$)

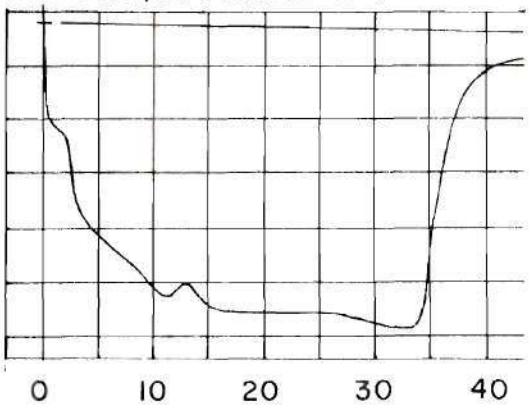


Test 34 (72,700 Btu/hr-ft$^2$)

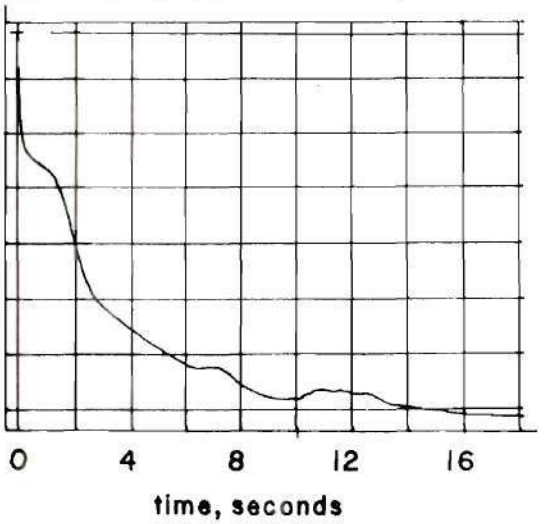

# IGNITION TIME MEASUREMENTS

TESTED FABRIC: GIRCFF fabric no.12, white tricot, 100% nylon.

Test 3A (23,900 Btu/hr-ft$^2$)

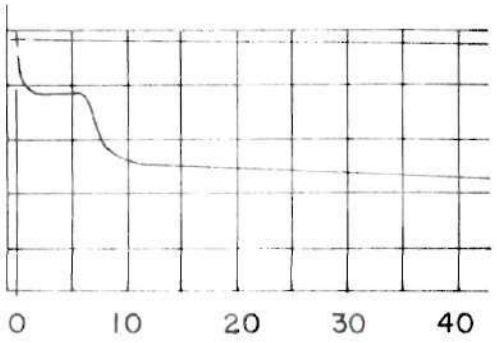


Test 31 (34,000 Btu/hr-ft$^2$)

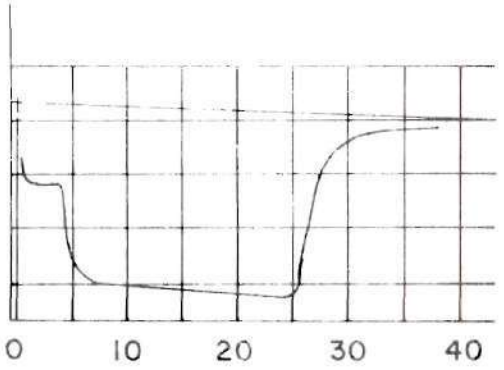


Test 32 (47,300 Btu/hr-ft$^2$)

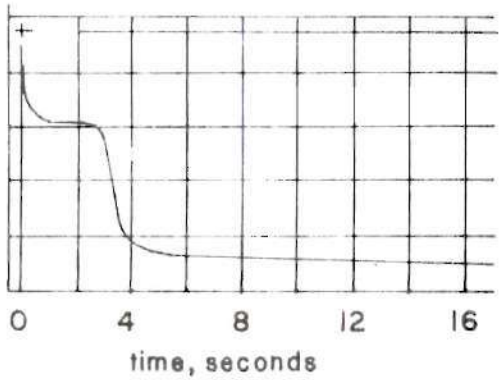


The heat fluxes reported were incident to fabric front face.

The plots present EMF output, from a calorimeter mounted 0·400 inch behind fabric back surface, versus time of exposure.

GIRCFF fabric no·12 melted without igniting.

Test 33 (62,300 Btu/hr-ft$^2$)

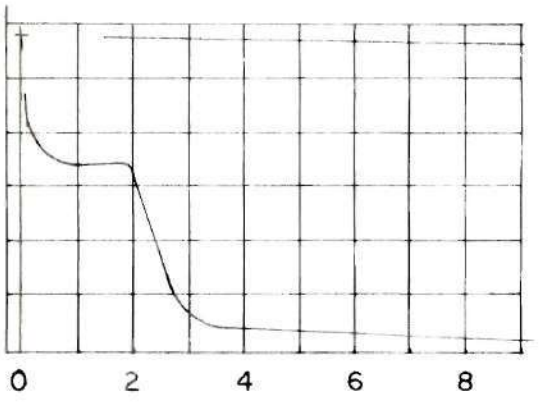


Test 40 (72,700 Btu/hr-ft$^2$)

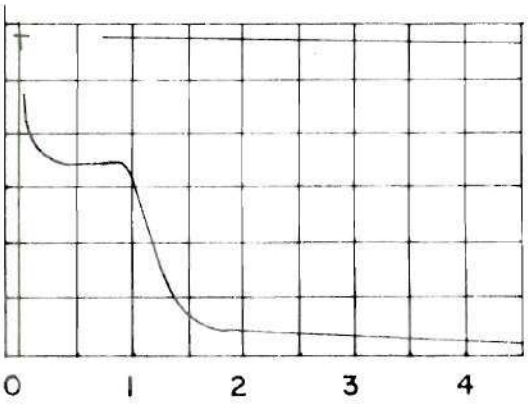

# IGNITION TIME MEASUREMENTS

TESTED FABRIC: GIRCFF fabric no.13, white tricot, 100 % acetate.

The heat fluxes reported were incident to fabric front face.

The plots present EMF output, from a calorimeter mounted 0·400 inch behind fabric back surface, versus time of exposure.

GIRCFF fabric no.13 melted without igniting.

Test 2A (23,900 Btu/hr.-ft.$^2$)

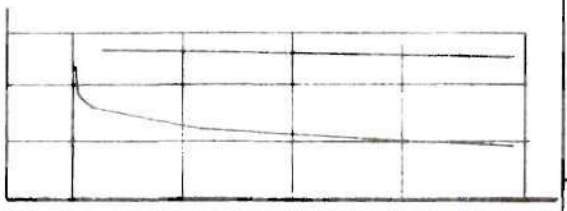


time, seconds

Test 19 (34,000 Btu/hr-ft$^2$)

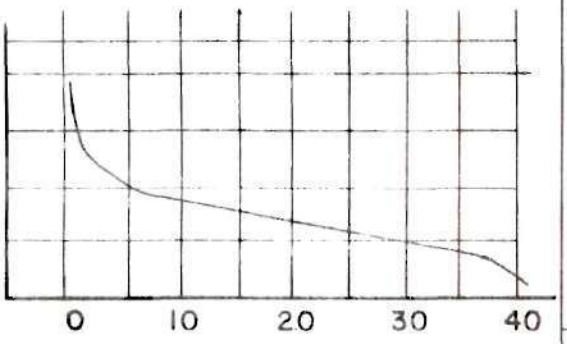


time, seconds

Test 20 (47,300 Btu/hr-ft$^2$)

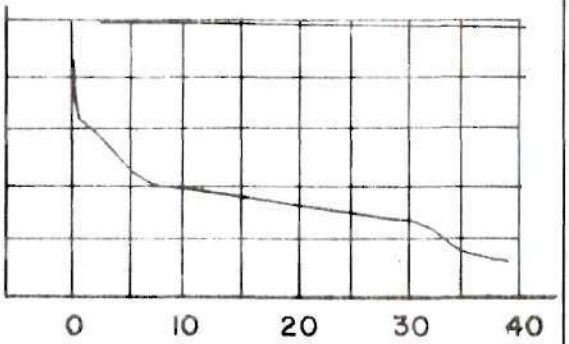


time, seconds

Test 21 (62,300 Btu/hr-ft$^2$)

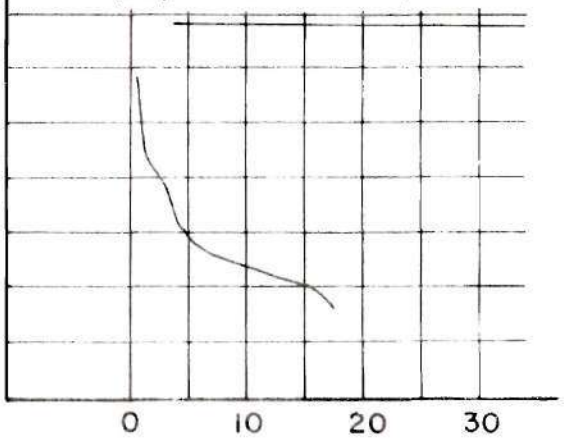


time, seconds

Test 39 (72,700 Btu/hr-ft$^2$)

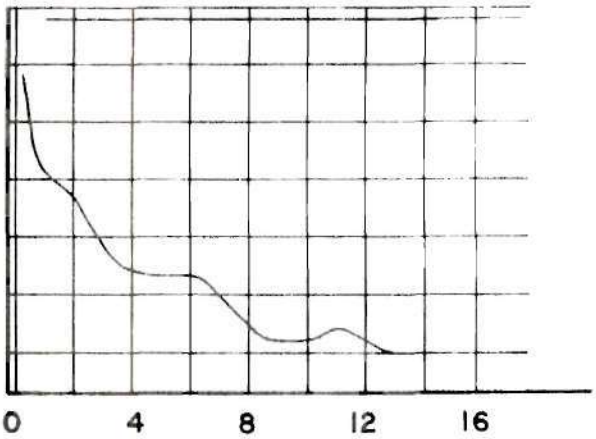


time, seconds

# IGNITION TIME MEASUREMENTS

TESTED FABRIC: GIRCFF fabric no.17, white batiste, 65% polyester, 35% cotton.

Test 1A (23,900 Btu/hr-ft$^2$)

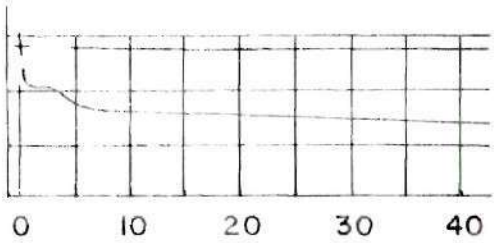


time, seconds

Test 22 (34,000 Btu/hr-ft$^2$)

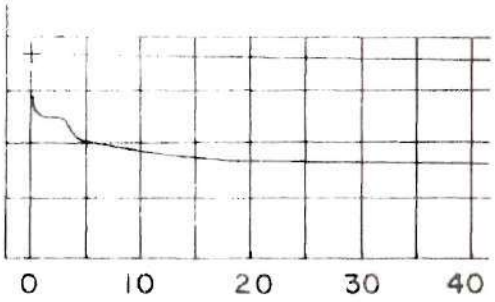


time, seconds

Test 23 (47,300 Btu/hr-ft$^2$)

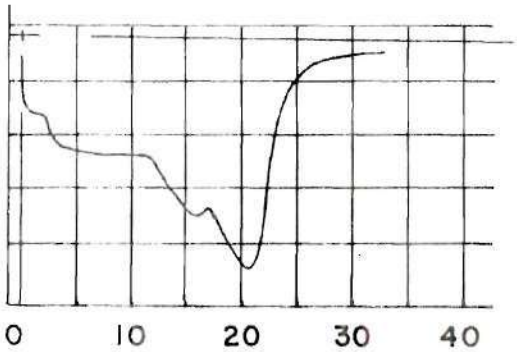


time, seconds

The heat fluxes reported were incident to fabric front face.

The plots present EMF output, from a calorimeter mounted 0·400 inch behind fabric back surface, versus time of exposure.

GIRCFF fabric no.17 partially melted and then ignited.

Test 24 (62,300 Btu/hr-ft$^2$)

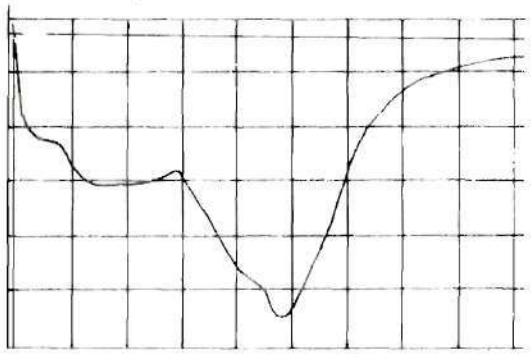


time, seconds

Test 36 (72,700 Btu/hr-ft$^2$)

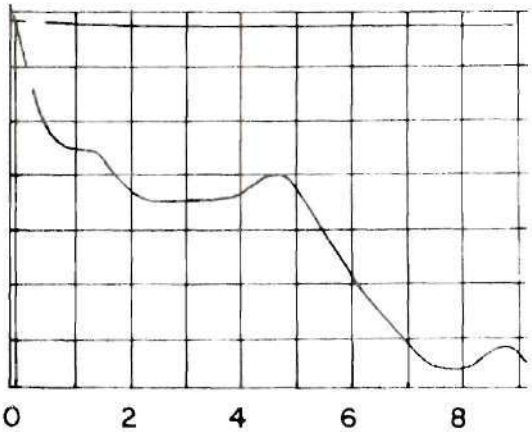


time, seconds

# IGNITION TIME MEASUREMENTS

TESTED FABRIC: GIRCFF fabric no.18, white flannel, 100% cotton.

Test 6A (23,900 Btu/hr-ft$^2$)

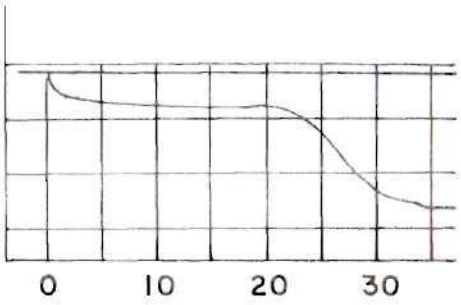


Test 12 (34,000 Btu/hr-ft$^2$)

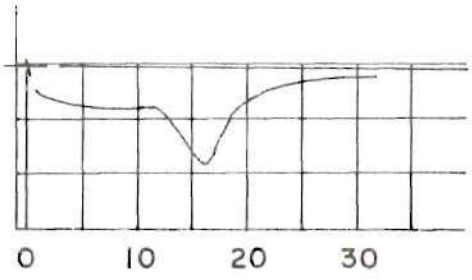


Test 13 (47,300 Btu/hr-ft$^2$)

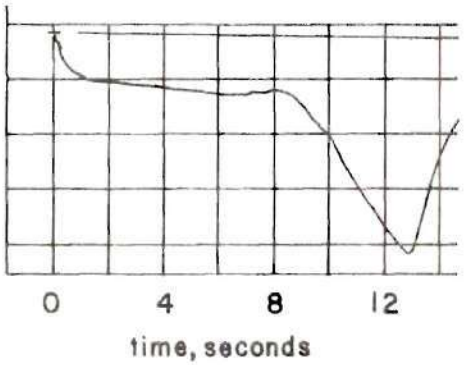


The heat fluxes reported were incident to fabric front face.

The plots present EMF output, from a calorimeter mounted 0·400inch behind fabric back surface, versus time of exposure.

GIRCFF fabric no.18 ignited when irradiated.

Test 14 (62,300 Btu/hr-ft$^2$)

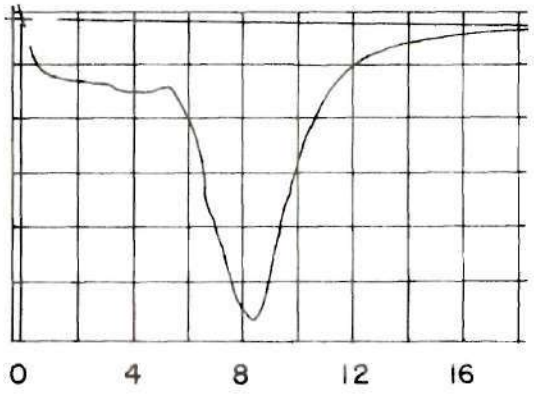


Test 37 (72,700 Btu/hr-ft$^2$)

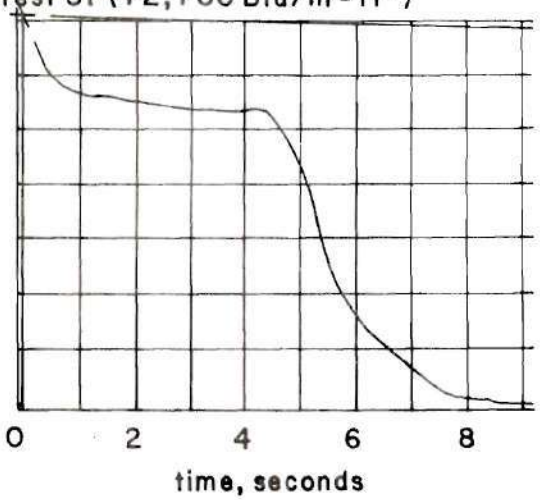

# IGNITION TIME MEASUREMENTS

TESTED FABRIC: GIRCFF fabric no.19, white flannel, 100% cotton, treated with fire retarding compound.

Test 5A (23,900 Btu/hr-ft$^2$)

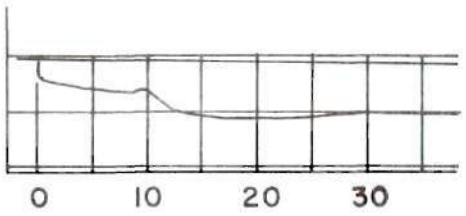


time, seconds

The heat fluxes reported were incident to fabric front face.

The plots present EMF output, from a calorimeter mounted 0·400 inch behind fabric back surface, versus time of exposure.

GIRCFF fabric no.19 ignited when irradiated, but only the surface burned. Flame extinguished without burning through the weave.

Test 15 (34,000 Btu/hr-ft$^2$)

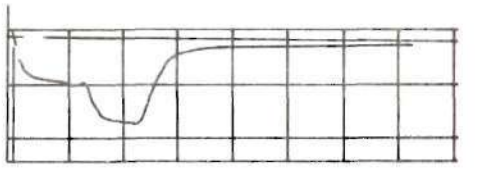


time, seconds

Test 17 (62,300 Btu/hr-ft$^2$)

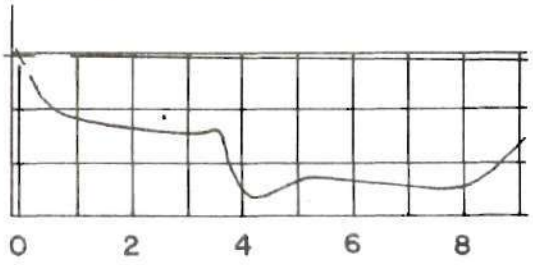


time, seconds

Test 16 (47,300 Btu/hr-ft$^2$)

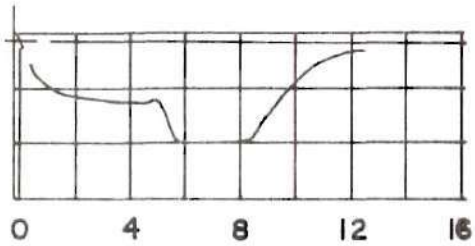


time, seconds

Test 38 (72,700 Btu/hr-ft$^2$)

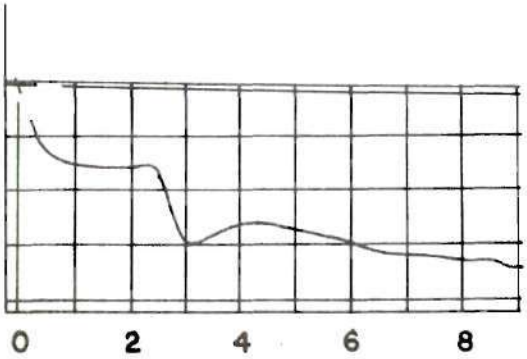


time, seconds

# APPENDIX C

## IGNITION TIME DEVICE - PRIMARY SPRING SIZE AND SHUTTER PLATE SPEED DETERMINATIONS

# APPENDIX C

## IGNITION TIME DEVICE - PRIMARY SPRING SIZE AND SHUTTER PLATE SPEED DETERMINATIONS

As discussed in Chapter II, fabric sample exposures with the ignition time device were rapid to comply with the traditional modelling assumption of a step heat input. The sudden exposures were accomplished by very rapid removal of the shielding shutter plate. That plate is attached to a heavy duty helical spring, termed primary spring, sized to cause exposure within a specified time interval. As discussed in Chapter II, exposure transients of less than 20 milliseconds were specified.

The system was designed with the shutter plate exposing edge at sample center when the spring is neutral. Spring motion was restricted to maximum displacements of 2.5 in. extension or compression.

The plate velocity originally was specified to be 500 in./sec. at spring neutral. Determination of the spring constant required for this velocity involved solution of a simple spring-mass system. The governing differential equation is:

$$m\left(\frac{d^2x}{dt^2}\right) + kx = -f$$

where:

f = friction force impeding shutter plate motion, lbf

k = spring constant, lbf/in.

x = 0 at spring neutral, x = -2.5 at maximum spring extension

x = + 2.5 for maximum spring compression

m = mass of moving system, slugs.

The general solution is given by:

$$x = A \sin wt + B \cos wt - (f/k)$$

where:

$$w^2 = (k/m)$$

The initial condition is

$$\text{at } t = 0,\ x = -2.5 \text{ in.}$$

While the boundary conditions are:

$$\text{at } x = 0,\ \left(\frac{dx}{dt}\right) = 500 \text{ in./sec.}$$

and at

$$x = -2.5 \text{ in.},\ \left(\frac{dx}{dt}\right) = 0$$

This displacement is then given by

$$x = [(f/k) - 2.5] \cos wt - (f/k)$$

To evaluate an initial estimate of the required spring stiffness, assume the spring to be massless and the friction to be negligible. Then

$$x = -2.5 \cos wt$$

$$w^2 = 40{,}000 \ (1/sec^2)$$

The parts attached to the spring were sized and found to weigh about 0.78 lbm, or

$$m = (0.78)/32.2 \cong 2.44 \times 10^{-2} \text{ slugs}$$

The required spring rate is then

$$k \cong 81 \ (lbf/in.)$$

A spring was ordered from Newcomb Springs of Atlanta, Georgia with the following characteristics:

Design Spring Rate = 100 lbf/in.

Actual Spring Rate = 115 lbf/in.

Mass = 1.20 lbm

Using these values and assuming a realistic friction force magnitude, shutter plate velocity and aperture opening time can be computed.

$$\text{Total mass} \cong 0.78 + (1/2)(1.20)$$

$$\cong 1.38 \text{ lbm}$$

Assume a friction force of 15 lbf. This assumption was based on a Coulomb friction coefficient of 0.20 between the operating rod and the catch assembly. Inserting this value into the displacement equation, the time required for the system to reach x = 0.5 in. is

$$t \cong 0.00079 \text{ sec.}$$

The time required for the system to reach x = +0.5 is

$$t \cong 0.0103 \text{ sec.}$$

The time required for the shutter to open is then

$$t \cong 0.0103 - 0.00079$$

$$\cong 0.0095 \text{ sec.}$$

Tests of the equipment have shown that shutter opening is somewhat slower than this estimate. Using two microswitches which

cammed on the shutter plate when $x = 0.5$ and $x = -0.5$, the opening time was measured to be approximately 0.015 seconds. Additional losses, including a dash-pot effect from air within the spring tube, would account for a longer computed opening time. The resulting shutter opening time was acceptable for the ignition time tests. None of the fabrics tested ignited or melted in less than 1.2 seconds, or almost 100 times the time required to uncover the fabric.

# BIBLIOGRAPHY

## Literature Cited


1. Alkidas, A., R. W. Hess, C. S. Kirkpatrick, M. J. Kirkpatrick, A. E. Bergles, W. Wulff, and N. Zuber, "Study of Hazards from Burning Apparel and the Relation of Hazards to Test Methods," Progress Report No. 1, Georgia Institute of Technology, April 1, 1971.

2. Alkidas, A., R. W. Hess, C. S. Kirkpatrick, A. E. Bergles, W. Wulff and N. Zuber, "Study of Hazards from Burning Apparel and the Relation of Hazards to Test Methods," Progress Report No. 2, Georgia Institute of Technology, July 1, 1971.

3. Alkidas, A., R. W. Hess, C. S. Kirkpatrick, R. L. Mays, W. Wulff, and N. Zuber, "Study of Hazards from Burning Apparel and the Relation of Hazards to Test Methods," Progress Report No. 3, Georgia Institute of Technology, October 1, 1971.

4. Alkidas, A., R. W. Hess, W. Wulff and N. Zuber, "Study of Hazards from Burning Apparel and the Relation of Hazards to Test Methods," Final Report, Georgia Institute of Technology, December 31, 1971.

5. Kirkpatrick, C. S. and A. E. Bergles, Memorandum to Dr. Kezios, Dr. Wulff and Dr. Zuber, "Ignition Time Tests," July 6, 1971.

6. Kalelkar, A. S. and H. C. Kung, "A Study of the Pre-Ignition Heat Transfer Through a Fabric-Skin System Subjected to a Heat Source," First Quarterly Report, Factory Mutual Research Corporation, March 31, 1971.

7. Kalelkar, A. S. and H. C. Kung, "A Study of the Pre-Ignition Heat Transfer Through a Fabric-Skin System Subjected to a Heat Source," Second Quarterly Report, Factory Mutual Research Corporation, July 1, 1971.

8. Kalelkar, A. S. and H. C. Kung, "A Study of the Pre-Ignition Heat Transfer Through a Fabric-Skin System Subjected to a Heat Source," Third Quarterly Report, Factory Mutual Research Corporation, October 1, 1971.

9. Sherrington, C. S., The Integrative Action of the Nervous System, second edition, Yale University Press, New Haven, Connecticut, 1948.

10. Fearing, F., Reflex Action, a Study in the History of Physiological Phychology, Hafner Publishing Company, Inc., New York, N. Y., 1964.

11. Swazey, J. P., Reflexes and Motor Integration: Sherrington's Concept of Integrative Action, Harvard University Press, 1969.

12. Basmajian, J. V., Primary Anatomy, sixth edition, The Williams and Wilkins Company, Baltimore, Maryland, 1970.

13. Johns, D. J., Thermal Stress Analysis, first edition, Pergamon Press, London, 1965.

14. Roark, Raymond J., Formulas for Stress and Strain, fourth edition, McGraw Hill Book Company, New York, 1965.

15. Alvares, N. J., "Measurement of the Temperature of the Thermally Irradiated Surface of Alpha Cellulose," U. S. Radiological Defense Laboratory Report No. TR-735, March 24, 1964.

16. Churchill, R. V., Operational Mathematics, second edition, McGraw Hill Book Company, New York, N. Y., 1958.

17. Storer, T. I. and R. L. Usinger, General Zoology, fourth edition, McGraw-Hill Book Company, New York, 1965.

18. Oppel, T. W. and J. D. Hardy, "Studies in Temperature Sensation I. A Comparison of the Sensation Produced by Infrared and Visible Radiation," The Journal of Clinical Investigation, Vol. 16, pp. 517-524, 1937.

19. Oppel, T. W. and J. D. Hardy, "Studies in Temperature Sensation II. The Temperature Changes Responsible for the Stimulation of the Heat End Organs," The Journal of Clinical Investigation, Vol. 16, pp. 525-532, 1937.

20. Hardy, J. D. and T. W. Oppel, "Studies in Temperature Sensation III. The Sensitivity of the Body to Heat and the Spatial Summation of the End Organ Responses," The Journal of Clinical Investigation, Vol. 16, pp. 533-540, 1937.

21. Hardy, J. D., "The Radiating Power of Human Skin in the Infrared," The American Journal of Physiology, Vol. 127, pp. 454-462, 1939.

22. Hardy, James D., "The Radiation of Heat from the Human Body II. A Comparison of Some Methods of Measurement," The Journal of Clinical Investigation, Vol. 13, pp. 605-614, 1934.

23. Hardy, James D., "The Radiation of Heat from the Human Body III.

The Human Skin as a Black Body Radiator," Journal of Clinical Investigation, Vol. 13, pp. 615-620, 1934.

24. Bigelow, N., I. Harrison, H. Goodell and H. G. Wolff, "Studies on Pain: Quantitative Measurements of Two Pain Sensations of the Skin, with Reference to the Nature of the 'Hyperalgesia of Peripheral Neuritis'," The Journal of Clinical Investigation, Vol. 24, pp. 503-512, 1945.

25. Schumacher, G. A., H. Goodell, J. D. Hardy and H. G. Wolff, "The Uniformity of Pain Threshold in Man," Science, Vol. 92, pp. 110-112, 1940.

26. Hardy, J. D., H. G. Wolff, and H. Goodell, "Studies on Pain: Discrimination of Differences in Intensity of Pain Stimulus as a Basis of a Scale of Pain Intensity," The Journal of Clinical Investigation, Vol. 26, pp. 1152-1158, 1947.

27. Henriques, F. C., Jr. and A. R. Moritz, "Studies of Thermal Injury I: The Conduction of Heat to and Through Skin and the Temperatures Attained Therein. A Theoretical and Experimental Investigation," The American Journal of Pathology, Vol. XXIII, pp. 531-549, 1947.

28. Moritz, A. F. and F. C. Henriques, Jr., "Studies of Thermal Injury II. The Relative Importance of Time and Surface Temperature in the Causation of Cutaneous Burns," The American Journal of Pathology, Vol. XXIII, pp. 695-720, 1947.

29. Moritz, A. R., "Studies of Thermal Injury III: The Pathology and Pathogenesis of Cutaneous Burns. An Experimental Study," The American Journal of Pathology, Vol. XXXIII, pp. 915-941, 1941.

30. Henriques, F. C., Jr., "Studies of Thermal Injury V. The Predictability and Significance of Thermally Induced Rate Processes Leading to Irreversible Epidermal Injury," Archives of Pathology, Vol. 43, pp. 489-502, 1947.

31. Buettner, Konrad, "Effects of Extreme Heat and Cold on Human Skin I. Analysis of Temperature Changes Caused by Different Kinds of Heat Application," Journal of Applied Physiology, Vol. 3, pp. 691-702, 1951.

32. Buettner, Konrad, "Effects of Extreme Heat and Cold on Human Skin II. Surface Temperature, Pain, and Heat Conductivity in Experiments with Radiant Heat," Journal of Applied Physiology, Vol. 3, pp. 703-713, 1951.

33. Buettner, Konrad, "Effects of Extreme Heat and Cold on Human Skin III. Numerical Analysis and Pilot Experiments on

Penetrating Flash Radiation Effects," Journal of Applied Physiology, Vol. 5, pp. 207-220, 1952.

34. Hardy, J. D., H. Goodell, and H. G. Wolff, "The Influence of Skin Temperature upon the Pain Threshold as Evolked by Thermal Radiation," Science, Vol. 114, pp. 149-150, 1951.

35. Wertheimer, M. and W. D. Ward, "The Influence of Skin Temperature Upon the Pain Threshold as Evolked by Thermal Radiation - A Confirmation," Science, Vol. 115, pp. 499-500, 1952.

36. Reader, S. R., and H. M. Whyte, "Tissue Temperature Gradients," Journal of Applied Physiology, pp. 396-402, 1951.

37. Gregg, E. C., Jr., "Physical Basis of Pain Threshold Measurements in Man," Journal of Applied Physiology, pp. 351-363, 1951.

38. Lipkin, M. and J. D. Hardy, "Measurement of Some Thermal Properties of Human Tissues," Journal of Applied Physiology, Vol. 7, pp. 212-217, 1954.

39. Hardy, J. D., H. G. Wolff, and H. Goodell, "Studies on Pain. A New Method for Measuring Pain Threshold: Observations on Spatial Summation of Pain," The Journal of Clinical Investigation, Vol. 19, pp. 649-657, 1940.

40. Lipkin, M., O. Bailey and J. D. Hardy, "Effect of Ultraviolet Irradiation Upon the Cutaneous Pain Threshold," Journal of Applied Physiology, Vol. 7, pp. 683-687, 1955.

41. Hendler, E., R. Crosbie and J. D. Hardy, "Measurement of Heating of the Skin During Exposure to Infrared Radiation," Journal of Applied Physiology, Vol. 12, pp. 177-185, 1958.

42. Stoll, A. M. and L. C. Greene, "Relationship Between Pain and Tissue Damage Due to Thermal Radiation," Journal of Applied Physiology, Vol. 14, pp. 373-382, 1959.

43. Stoll, A. M., "Heat Transfer in Biotechnology," Advances in Heat Transfer, Vol. 4, pp. 65-141, 1967.

44. Weaver, J. A. and A. M. Stoll, "Mathematical Model of Skin Exposed to Thermal Radiation," Aerospace Medicine, Vol. 40, pp. 24-30, 1969.

45. Hardy, J. D., I. Jacobs and M. D. Meixner, "Thresholds of Pain and Reflex Contraction as Related to Noxious Stimulation," Journal of Applied Physiology, Vol. 5, pp. 725-739, 1953.

46. Hardy, James D., "Method for the Rapid Measurement of Skin Temperature During Exposure to Intense Thermal Radiation," Journal of Applied Physiology, Vol. 5, pp. 559-566, 1953.

47. Stoll, A. M. and J. D. Hardy, "Direct Experimental Comparison of Several Temperature Measuring Devices," The Review of Scientific Instruments, Vol. 20, pp. 678-686, 1949.

48. Stoll, A. M., "A Wide Range Thermistor Radiometer for the Measurement of Skin Temperature and Environmental Radiant Temperature," The Review of Scientific Instruments, Vol. 25, pp. 184-187, 1954.

49. Hardy, James D., "The Radiation of Heat from the Human Body I. An Instrument for Measuring the Radiation and Surface Temperature of the Skin," The Journal of Clinical Investigation, Vol. 13, pp. 593-604, 1934.

50. Bates, J. J. and T. I. Monahan, "Research Report on Thermal Radiation Damage to Cloths as a Function of Time of Exposure, Rectangular Pulses," Final Report, Laboratory Project 5046-3, Materials Laboratory, New York Naval Shipyard, 1955.

51. Welker, J. R., H. R. Wesson and C. M. Sliepcevich, "Ignition of Alpha-Cellulose and Cotton Fabric by Flame Radiation," Fire Technology, pp. 59-66, 1969.

52. Stoll, A. M. and M. A. Chianta, "Method and Rating System for Evaluation of Thermal Protection," Aerospace Medicine, Vol. 40, pp. 1232-1238, 1969.

53. Stoll, A. M. and M. A. Chianta, "Burn Production and Prevention in Convective and Radiant Heat Transfer," Aerospace Medicine, Vol. 39, pp. 1097-1100, 1968.

54. Benjamin, F. B., "Pain Reaction to Locally Applied Heat," Journal of Applied Physiology, Vol. 4, pp. 907-910, 1952.

55. Alkidas, Alexandros, private communication, March 1972.

56. Carslaw, H. S. and J. C. Jaeger, Conduction of Heat in Solids, second edition, Oxford at the Clarendon Press, London, 1959.

57. Hensel, Harbert, "Physiologie der Thermorecption," Ergebnisse der Physiologie Biologischen Chemie und Experimentellen Pharmakologie, Vol. 47, pp. 166-368, 1952.

58. Brozek, J., E. Simonson, A. Keys and A. Snowden, "A Test of Speed of Arm and Lag Movements," Journal of Applied Physiology, Vol. 4, pp. 753-760, 1952.

59. Stoll, A. M., "Thermal Protection Capacity of Aviators Textiles," Aerospace Medicine, Vol. 33, pp. 846-850, 1962.

60. Chianta, M. A. and A. M. Stoll, "Heat Transfer in Protection from Flames," Aerospace Medicine, Vol. 35, pp. 7-11, 1964.

61. Stoll, A. M., M. A. Chianta and L. R. Munroe, "Flame Contact Studies," Journal of Heat Transfer, Vol. 86, pp. 449-456, 1964.

62. Stoll, A. M. and M. A. Chianta, "Thermal Injury by Radiation and Flame Contact," Abstract of paper presented to the 49th Annual Meeting of the Federation of American Societies for Experimental Biology.

63. Anon, "Learning How Fibers Protect Against High Temperature Hazards," Innovation, E. I. Dupont de Nemours and Company, Vol. 1, pp. 17-20, 1970.

64. Dunkle, R. V., F. Ehrenburg, and J. T. Gier, "Spectral Characteristics of Fabrics from 1 to 23 Microns," Journal of Heat Transfer, Vol. 82, pp. 64-70, 1960.

65. Alvares, N. J., P. L. Balckshear, Jr. and A. M. Kanury," The Influence of Free Convection on the Ignition of Vertical Cellulosic Panels by Thermal Radiation," Combustion Science and Technology, Vol. 1, pp. 407-413, 1970.

66. Patten, G. A., "Ignition Temperatures of Plastics," Modern Plastics, Vol. 38, pp. 119-120-122-180, July 1961.

67. Newman, A. B. and L. Green, "The Temperature History and Rate of Heat Loss of an Electrically Heated Slab," Transactions of the Electrochemical Society, Vol. 66, pp. 345-358, 1935.

68. Dussan, V., B. I. and R. I. Weiner, "A Study of Burn Hazard in Human Tissue and Its Implication on Consumer Product Design," ASME Publication No. 71-WA/HT-39, 7 pages, 1971.

69. Simms, D. L., "Experiments on the Ignition of Cellulostic Materials by Thermal Radiation," Combustion and Flame, Vol. 5, pp. 369-375, 1961.

70. Russell, L. H. and J. A. Cranfield, "Experimental Measurement of Heat Transfer to a Cylinder Immersed in a Large Aviation Fuel Fire," to be published in the Journal of Heat Transfer. 1972.

## Other References

Alpen, E. L., G. E. Sheline, P. R. Kuhl and A. J. Ahokus, "Effects of High Intensity Radiant Energy on Skin II. Quantitative Dependence of Tissue Injury on Duration of Exposure," A. M. A. Archives of Pathology, Vol. 55, pp. 280-285, 1953.

Chapman, W. P. and C. M. Jones, "Variations in Cutaneous and Visceral Pain Sensitivity in Normal Subjects," The Journal of Clinical Investigation, Vol. 23, pp. 81-91, 1944.

Davies, J. M., "Input Power Determined from Temperatures in Simulated Skin Portected Against Thermal Radiation," Journal of Heat Transfer, Vol. 88, pp. 154-160, May 1968.

Draper, J. W. and J. W. Boag, "Skin Temperature Distributions over Veins and Tumors," Physical Medical Biology, Vol. 16, No. 4, pp. 645-654, 1971.

Guibert, A. and C. L. Taylor, "Radiation Area of the Human Body," Journal of Applied Physiology, Vol. 5, pp. 24-37, 1952.

Hardee, H. C. and D. O. Lee, "A Simple Conduction Model for Skin Burns Resulting from an Incident Heat Flux of Short Duration," Sandia Laboratories Report, 1971.

Hardy, J. D. and T. W. Oppel, "Studies in Temperature Sensation IV. The Stimulation of Cold Sensation by Radiation," The Journal of Clinical Investigation, Vol. 17, pp. 771-778, 1938.

Hardy, J. D., H. G. Wolff and H. Goodell, "Experimental Evidence on the Nature of Cutaneous Hyperalgesia," The Journal of Clinical Investigation, Vol. 39, pp. 115-139, 1950.

Hardy, J. D., H. G. Wolff and H. Goodell, "Studies on Pain: Measurement of Aching Pain Threshold and Discrimination of Differences in Intensity of Aching Pain," Journal of Applied Physiology, Vol. 5, pp. 247-255, 1952.

Henriques, F. C., Jr., "Studies of Thermal Injury VIII. Automatic Recording Caloric Applicator and Skin Tissue and Skin Surface Thermocouples," The Review of Scientific Instruments, Vol. 18, pp. 673-680, 1947.

MacHattie, "Temperature Measurement of Textile Fabrics Under Intense Thermal Irradiation," Defense Research Medical Laboratories Report No. PB 197637, Toronto, Ontario, October 1961.

McLean, R., A. R. Moritz and A. Roos, "Studies of Thermal Injury VI. Hyperpotassemia Caused by Cutaneous Exposure to Excessive Heat," The Journal of Clinical Investigation, Vol. XXVI, pp. 497-504, 1947.

Moritz, A. R., F. C. Henriques, Jr., F. R. Dutra and J. R. Weisiger, "Studies of Thermal Injury IV. An Exploration of the Casualty-Producing Attributes of Conflagerations; Local and Systemic Effects of General Cutaneous Exposure to Excessive Circumbient (Air) and Circumradient Heat of Varying Duration and Intensity," Archives of Pathology, Vol. 43, pp. 466-488, 1947.

Roos, A., J. R. Weisiger and A. R. Moritz, "Studies of Thermal Injury VII: Physiological Mechanisms Responsible for Death During Cutaneous Exposure to Excessive Heat," The Journal of Clinical Investigation, Vol. XXVI, pp. 505-519, 1947.

Sheline, G. E., E. L. Alpen, P. R. Kuhl and A. J. Ahokas,"Effects of High Intensity Radiant Energy on Skin I. Type of Injury and its Relation to Energy Delivery Rate," A. M. A. Archives of Pathology, Vol. 55, pp. 265-279, 1953.

Simms, D. L., "Damage to Cellulostic Solids by Thermal Radiation," Combustion and Flame, Vol. 6, pp. 303-317, 1962.

Simms, D. L., "Ignition of Cellulostic Materials by Radiation," Combustion and Flame, Vol. 4, pp. 293-300, 1960.

Stoll, A. M. L. C. Greene and J. D. Hardy, "Pain and Thermal Burns in Skin Areas Previously Exposed to Ultraviolet Radiation," Journal of Applied Physiology, Vol. 15, pp. 489-492, 1960.

Stoll, A. M. and J. D. Hardy, "A Method for Measuring Radiant Temperatures of the Environment," Journal of Applied Physiology, Vol. 5, pp. 117-124, 1952.

Stoll, A. M. and J. D. Hardy, "Studies of Thermocouples as Skin Thermometers," Journal of Applied Physiology, Vol. 2, pp. 531-543, 1950.

Wolff, H. G., J. D. Hardy and H. Goodell, "Studies on Pain. Measurement of the Effect of Morphine, Codeine, and Other Opiates on the Pain Threshold and an Analysis of Their Relation to the Pain Experience," The Journal of Clinical Investigation, Vol. 19, pp. 659-680, 1940.

Zitowitz, L. and J. D. Hardy, "Influence of Cold Exposure on Thermal Burns in the Rat," Journal of Applied Physiology, Vol. 12, pp. 147-154, 1958.